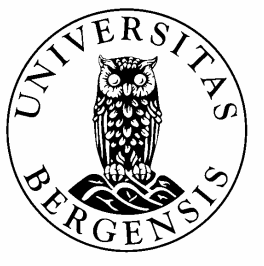

Electrophysiological and Hemodynamic Correlates of Expectancy in Target Processing

Tom Eichele

Dissertation for the degree philosophiae doctor (PhD)

2007

University of Bergen

To my family with sincere gratitude

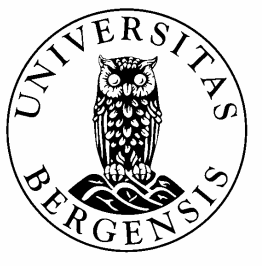

Electrophysiological and Hemodynamic Correlates of Expectancy in Target Processing

Tom Eichele

Dissertation for the degree philosophiae doctor (PhD)

Ψ

2007

Department of Biological and Medical Psychology

Faculty of Psychology

University of Bergen

ISBN 978-82-308-0452-0

Bergen, Norway, 2007

Printed by: Allkopi Bergen

CONTENTS

ABSTRACT

Identifying patterns of recurrent events is central to human perception, cognition and behavior. By extracting patterns from the environment, individuals can make efficient predictions about future events. By and large, the detection of these contingencies is the core faculty to respond to, interact with, and ultimately make sense of the world. The aim of this thesis was to investigate how the brain treats temporal patterns and generates expectancies from regular event sequences.

A variant of an auditory oddball paradigm was developed in which predictability was modulated with sequences of random and regular targets. In order to assess both the temporal and spatial implementation of these effects, single trial event related potentials and functional magnetic resonance imaging were employed.

In the first paper, the effect of predictability on brain activity was studied with single trial ERPs, yielding sigmoid-shaped learning curves on CNV, N2 and P3. The second paper described a method for integration of single-trial ERP with fMRI data, and reported three spatiotemporal activation patterns during the P2, N2, and P3 in addition to the generic activation elicited by target stimuli. An additional modulation beginning during the N1 was extracted in the third paper that employed a method for parallel unmixing of concurrent EEG-fMRI data.

The results of the thesis have implications for the understanding of ERP components, the concepts of how a standard representation is formed and how context is updated need to take into account the effects of predictability observed here. Furthermore, the thesis presents straightforward methods for single-trial ERP, and concurrent EEG-fMRI analysis that afford comprehensive spatio-temporal mapping of event-related processes in the brain.

ACKNOWLEDGMENT

Many people have made essential contributions to this work, and I am equally indebted to all of them –

My supervisors Kenneth Hugdahl and Helge Nordby provided complementary, inspiring, open-minded and open-hearted guidance in all aspects of PhD-Life.

Marijtje L.A. Jongsma and Rodrigo Quian Quiroga shared the idea for the pattern learning experiment used in this study.

Without the experience of Karsten Specht, Matthias Moosmann and Roger Barndon, the EEG-fMRI work would not have been possible.

Vince D. Calhoun generously shared his time and knowledge to discuss and develop our ideas about independent component analysis.

I would like to thank my colleagues at the IBMP for their friendship, particularly Kerstin von Plessen for comments on the thesis draft. Thanks also to the students that were involved in the project for their enthusiasm, and to the participants in the experiments for their patience.

Above all, I am deeply grateful for steadfast, loving support from my wife Heike, and for every bit of distraction from my daughters Emma and Ida.

GENERAL INTRODUCTION

> *'It is hardly surprising to find that the organism's response to "identical" stimuli is in flux. The nervous system is not a passive recipient of inputs that are obediently switched to outputs; rather it is a dynamic system that continuously generates hypotheses about the environment.' (Squires et al 1976)*

The brain is set to 'mining its sensory inputs' (Friston 2003), and is continuously attempting to identify patterns in the environment in order to generate accurate predictions about future events. In general, predictions are coded across all levels of processing, from the primary sensory, to high-level executive functions and may represent a major source of energy consumption in the brain (Fox et al 2005; Friston 2005a; Halgren & Marinkovic 1995; Llinas 2001; Raichle 2006).

When sequences of behaviourally relevant events contain non-random patterns, behavioural performance typically becomes more efficient with repetition. This happens regardless of whether participants are instructed to detect these patterns or not, and also independent of whether declarative (explicit) knowledge about patterns is made available a-priori, acquired by the participant during the experiment or not (Forkstam & Petersson 2005; Huettel et al 2002; Reber 1967; Seger 1994). People invariantly and implicitly adapt to patterns in their environment and this illustrates strong salience of patterns. However, research into pattern learning (see e.g. Janata & Grafton 2003) so far most directly probed the motor system, by studying adaptation to sequences with tasks requiring overt responses, such as the serial response time task (Reber 1967; Seger 1994). Motor sequence learning is, however, only one expression of pattern learning and

outcome prediction, there is a large variety of covert psychophysiological phenomena that are thought to rest upon generation and violation of expectancies. For these phenomena it is prudent to assume that detection and memory mechanisms that afford representations of stimuli and subsequent learning of *complex* relationships between events are implemented in a widespread fashion across the brain, both in sensory regions (Ulanovsky et al 2004; Ulanovsky et al 2003), as well as in heteromodal, higher-order brain areas (Friston 2005a; Huettel et al 2002).

The Orienting Response

The 'prototype' psychophysiological exemplar for prediction making in the brain is the change in the peripheral orienting response (OR) indexed by skin conductance and heart rate to stimulus repetition. The OR displays repetition suppression, habituation to regularly presented stimuli, dishabituation to deviations from patterns of preceding stimuli, and is elicited by omitted stimuli (Barry 1990; Loveless 1983; Rescorla & Wagner 1972; Sokolov 1963; Sokolov & Vinogradova 1976). It was already incorporated in Sokolov's original conception (Sokolov 1963) that the OR represents a change of prediction error in a learning system that adapts to regularly presented stimuli when the state of prediction is not changing and it dishabituates to deviations from a pattern of preceding stimuli when a prediction is not met: *'The "neuronal model of the stimulus" registers not only the elementary, but also the complex properties of the signal, such as coincidence or succession of several stimuli in time.'* (Sokolov & Vinogradova 1976, p. 218). However, similar to sequence learning effects in the motor system, OR effects lie 'downstream', i.e. on the output side in distal

effectors, such that these measures do not afford specific inferences about the earlier, perceptual and cognitive levels of processing in the brain.

The Oddball Paradigm

The perceptual and cognitive levels of information processing, i.e. the input side can be studied with the classic and widely applied 'oddball' paradigm. In the simplest version of this paradigm a repeated frequent 'standard' stimulus (Fig.1, dotted) is occasionally replaced at random intervals by an infrequently occurring deviant stimulus – the oddball or 'target' (Fig. 1, solid), which is different from the standard in some feature, such as pitch or duration.

Figure 1

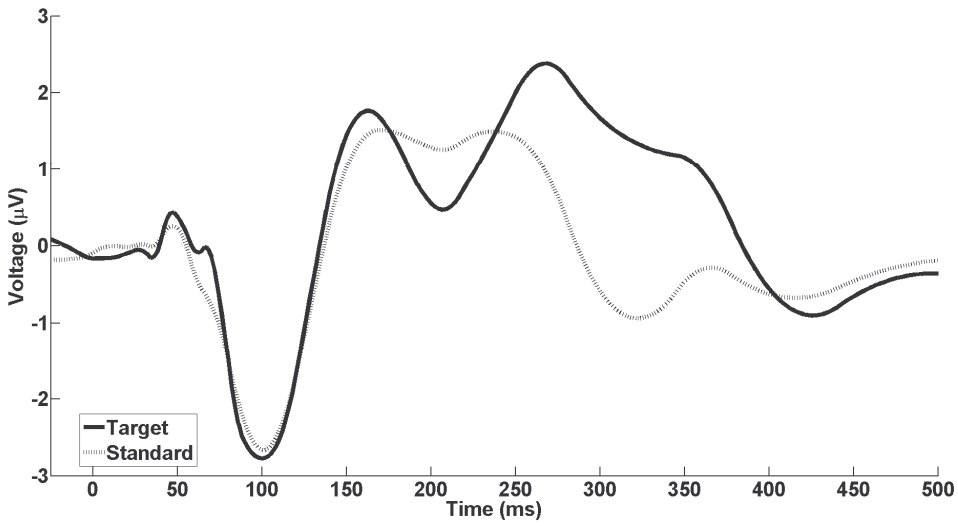

The mechanisms probed by this experiment are not confined to any particular sensory modality, such that they can be studied with auditory, visual, somatosensory, cross-modal stimulation, and stimulus omission alike, while ERP (fig.1) or fMRI (fig. 2) data are collected. When the stimulus material is to be *attended*, participants are typically instructed to respond to the deviants (button press, counting), while when the material is to be *ignored* in order to selectively

study the automatic, bottom-up effects, participants can be instructed to read a book, watch a video, or solve an unrelated task.

In broad terms, the stimulus-locked event-related potential (ERP) to oddball stimuli in the auditory modality represents the chronometry of processes leading to discrimination of the target stimuli and encompasses effects in a number of components: N1, P2, mismatch negativity (MMN), N2b, P3a, P3b, and slow waves (for overviews, see Coles & Rugg 1995; Fabiani et al 2000; Handy 2005; Luck 2005; Näätänen 1992; Polich 2003). In figure 1, the major difference between the standard and target ERPs is during the N2 and P3 latencies.

A variety of these deflections have been interpreted as cortical concomitants of the orienting response (Loveless 1983; Näätänen & Gaillard 1983; Roth 1983). The N1 and P2 typically are enhanced under 'attend' compared to 'ignore' conditions (Hillyard et al 1973; Näätänen & Picton 1987; Woods 1995). N1 subcomponents display adaptive effects to repetition and change, 'N1-enhancement' and particularly effects dependent on stimulus sequence such as (dis-/re-) habituation represent this type of function (Budd et al 1998; Haenschel et al 2005; Jaaskelainen et al 2004; Näätänen 1992; Näätänen et al 2005; Näätänen & Picton 1987; Sambeth et al 2004; Woods 1995). MMN represents an early, automatic response to violation of an auditory rule and reflects the comparison between the deviant input and a sensory memory trace (Näätänen 1992; Näätänen et al 1978; Näätänen et al 2001; Näätänen & Winkler 1999; Picton et al 2000a). The formation of the memory representation is likely instantiated via adaptation to the frequent, high-probability standard element(s), which corresponds to changes in the prediction of repetitive stimulus features (Baldeweg 2006; Haenschel et al 2005; Näätänen & Rinne 2002; Nordby et al

1988a; 1988b; Paavilainen et al 2001; Ritter et al 1992; Sussman et al 1998; Sussman et al 2003; Ulanovsky et al 2004; Ulanovsky et al 2003). When a task is associated with the deviant stimulus, MMN typically overlaps temporally, spatially, and functionally with the N2b. N2b is related to matching the incoming stimulus to an internally generated contextual template (Gehring et al 1992; Näätänen 1992; Näätänen et al 1982), that is usually followed by P3a, indicating a bottom-up shift of attention (Courchesne et al 1975; Friedman et al 2001; Polich 2003; Schroger 1997; Squires et al 1975).

The most prominent feature of the ERP waveform to auditory targets is a broad, parietal positivity from about 300 ms, the P3 (or P300, P3b), thought to reflect goal directed, effortful processing and working memory processes (Donchin 1981; Donchin & Coles 1988; Picton 1992; Polich 2003; Verleger 1988). This component and one of its major functions was first described in the seminal work of Samuel Sutton and colleagues (Sutton et al 1965; Sutton et al 1967). The experimental design and conception of the findings already then provided a perspective that was emphasizing expectancy vs. uncertainty as the critical determinant for the elicitation of the P3. The basic idea was that P3 corresponds to prediction error, meaning the difference between the stored representation of the environment and the current input. P3 thus reflects to the degree to which a 'surprise'-response to the sensory input was suppressed. This idea prevails in later theories about P3 (Donchin 1981; Donchin & Coles 1988; Verleger 1988), as well as in a generalized framework that assumes that the fundamental function of cortical responses is to generate predictions (Friston 2003; 2005a; Friston 2005b; see also, Llinas 2001). However, the P3 amplitude is sensitive to a wide array of experimental manipulations that interact with expectancy/surprise, such as target

probability (Duncan-Johnson & Donchin 1977; Tueting et al 1970), stimulus sequence (Jentzsch & Sommer 2001; Squires et al 1976), and inter-target interval (Croft et al 2003; Gonsalvez & Polich 2002).

A P3 compoenent is also elicited if a stimulus is omitted from a regular sequence (Hughes et al 2001; Jongsma et al 2005; Mustovic et al 2003; Ruchkin & Sutton 1978; Ruchkin et al 1975). These omission evoked potentials (OEPs) are elicited by the absence of an expected stimulus such that they are entirely endogenous by definition, which renders them a valuable tool for studying the cognitive, top-down dimension of ERP components. The existence of OEPs itself, and their parametric modulation by variables such as probability and predictability can be conceived as critical evidence for predictive coding.

Additionally, if a stimulus is expected, a negative shift in the ERP waveform may appear before the stimulus presentation, the 'Contingent Negative Variation' (CNV), which indicates response preparation for the target (Brunia 1999; Walter et al 1964).

The assembly of functions associated with information processing during the oddball task produces widespread brain activity, both temporally, as seen in the sequence of sensitive ERP components, as well as spatially: A number of functional magnetic resonance imaging (fMRI) studies have explored the oddball paradigm to examine the hemodynamic correlates of detecting changes and processing targets (Bledowski et al 2004; Clark et al 2000; Downar et al 2000; Horovitz et al 2002; Kiehl et al 2001; Kiehl et al 2005; Kirino et al 2000; Linden et al 1999). The most recent large sample study with 100 healthy participants showed that auditory target detection induces hemodynamic activation in about forty regional maxima including cortical, subcortical and cerebellar areas (Kiehl

et al 2005). Figure 2 shows three axial slices with typical fMRI results to oddball stimuli with extensive activation in the insula, basal ganglia, temporal lobes, lateral frontal, anterior cingulate, and sensorimotor regions.

Figure 2

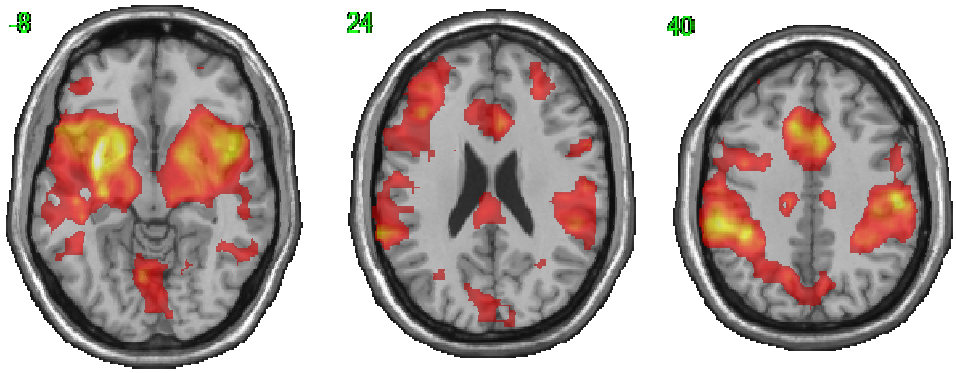

Such results support a view of widespread neuronal recruitment during simple target detection, which fits well with data from intracranial recordings (Baudena et al 1995; Halgren et al 1995a; Halgren et al 1995b; Halgren et al 1998). One interpretation is that in order to maximize the odds of learning potentially relevant information brain activation is global and principally unspecific, i.e. areas that are not necessarily relevant for the task at hand are nonetheless activated in a dynamic, adaptive fashion (Halgren & Marinkovic 1995; Kiehl et al 2005).

Research focusing on the hemodynamic correlates of the earlier evoked components N1, MMN, and P3a typically describes a more focused pattern localized mainly in the superior temporal gyri, lateral and medial frontal areas (Liebenthal et al 2003; Muller et al 2002; Opitz et al 1999; Rinne et al 2005; Sabri et al 2006). This pre-attentive deviance detection system signals to, and may in turn be top-down modulated by the later 'endogenous' components in the event related response that derive from higher levels of processing (Friston 2005a; Schroger 1997).

OBJECTIVES OF THE THESIS

The Learning Oddball

In this thesis, a variant of an oddball paradigm is used which allows tracking auditory temporal pattern learning (Jongsma et al 2004). The 'learning-oddball' paradigm is a simple two-stimulus paradigm with two alternating conditions: 1. The 'Random' condition in which a series of targets are presented with non-repetitive pseudo-random target-to-target intervals, and 2. The 'Regular' condition, in which targets appear repeatedly at the same target-to-target interval with the same number of standard sounds in between. In this paradigm, participants are not informed beforehand about the different patterns in the stimulus sequence and they are instructed to respond to the target stimuli with a synchronous delayed response in order to minimize confounding effects from speeding of response times on the stimulus-locked ERP. This paradigm affords to study selectively how brain activity changes with varying levels of predictability, while controlling for the confounding effects of target probability (Duncan-Johnson & Donchin 1977; Tueting et al 1970), sequence (Jentzsch & Sommer 2001; Squires et al 1976) and target-to-target interval (TTI, Croft et al 2003; Gonsalvez & Polich 2002). Probability, sequence, and interval are not changing during the regular periods of the experiment where predictability is increasing due to repetition of stimulus patterns. At the same time, expectancy-related effects in this paradigm are building up from the temporal and sequential relationships between *target* stimuli, and go beyond repetition effects related to the representation of the *standard* (cf. Baldeweg 2006; Näätänen et al 2001) or *context* (Donchin 1981; Donchin & Coles 1988).

Learning Model

A hypothesis about the shape of the effects can be deducted from the Rescorla-Wagner model (RW, Rescorla & Wagner 1972) assuming that targets are surprising and patterns are salient contingencies. The RW is a model for the explanation of learning through reinforcement, and changes in reinforcement expectancy with increasing experience. In this sense, the RW is based on surprise, i.e. prediction error (PE) as the reinforcement signal. PE refers to the difference between the actual (R_t) and the predicted outcome (V_{t-1}) at trial t. Updates of predicted outcomes (V_t) are the sum of the learning history and the current PE, and the learning rate (ε) determines the influence of the current trial on the future prediction

$$V_t = V_{t-1} + \varepsilon \cdot (R_t - V_{t-1})$$

It follows from the equation above that repetition of targets at regular intervals should yield a learning curve (Fig. 3, blue) that modulates activity according to an approximate exponential or sigmoid function whose shape is determined by the learning rate, and where prediction error would elicit transient responses between random and regular sequences (Fig. 3, orange).

Figure 3

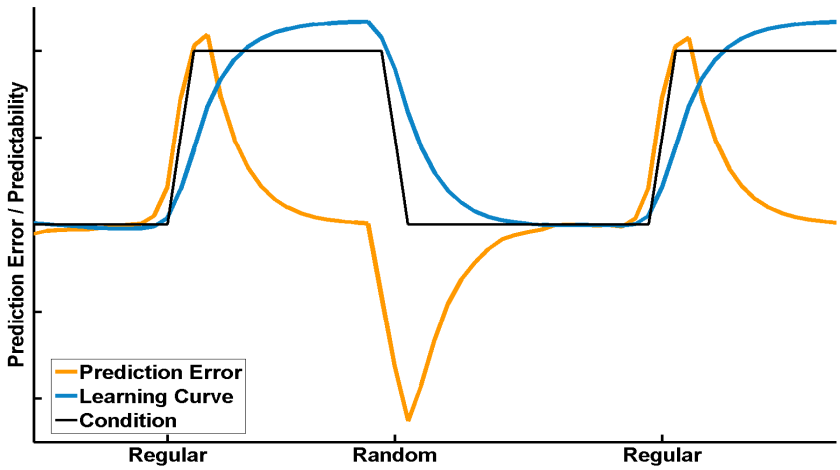

Adapting this relatively simple version of a predictive coding framework (Baldeweg 2006; Friston 2005a) to the auditory oddball is an attempt to address the similarities in the theories of Sokolov (Sokolov 1963), Sutton (Sutton et al 1965), Donchin (Donchin 1981; Donchin & Coles 1988) and Nataanen (Näätänen 1992). It also tries to add to Halgrens appealing proposal that *'the brain uses a full employment strategy'* and *'that activation is parallel and interdependent'* (Halgren & Marinkovic 1995; Halgren et al 1998) which was recently picked up by Kiehl (Kiehl et al 2005). The utility of such an integrative approach is obvious: in order to come to a conclusive interpretation of spatiotemporal information processing, it is necessary to acknowledge the tight coupling and common functions of temporally or spatially separable neuronal modules, such as in the sequence of responses elicited by the auditory oddball.

Single Trial Analysis

In order to study the dynamics of pattern learning, it is necessary to track responses on a single-trial basis and estimate individual event-related responses. The use of single trial evoked responses as markers of learning opens a range of novel applications and this type of information may prove invaluable in the understanding of cognitive processes (Debener et al 2006; Makeig et al 2004a; Spencer 2005). Moreover, such markers may yield more specific information about neuropsychiatric pathologies (Ford et al 1994).

A number of techniques for extraction of single-trial event-related activity with promising results are available to overcome the challenges of single-trial analysis due to the low signal-to-noise ratio of the responses. The analysis of the 'learning-oddball' experiments draws on these techniques using a combination of

independent component analysis (ICA) and wavelet denoising (Delorme & Makeig 2004; Quian Quiroga & Garcia 2003).

Localizing Generators

Apart from describing pattern learning effects at different latencies of the stimulus-locked scalp ERP, another objective of the study is to identify the locations of the underlying generators of these effects. To this end, concurrent EEG-fMRI is used, and the single-trial EEG data recorded inside the MR scanner serves as a predictor of hemodynamic activity over time. As outlined in the introduction, it can be assumed that pattern learning is such an elementary and pervasive effect that it is implemented in temporally and spatially distributed networks (Baudena et al 1995; Friston 2005a; Halgren et al 1995a; Halgren et al 1995b; Halgren & Marinkovic 1995; Halgren et al 1998; Kiehl et al 2005; Llinas 2001).

In summary, the aim of the thesis was to track dynamic markers of auditory pattern learning in trial-to-trial changes of ERP component amplitudes and fMRI regional activation:

Paper I (Jongsma et al 2006) presents the paradigm and a single trial EEG analysis with ICA and wavelet denoising. It describes pattern-learning effects in event-related potentials from the scalp with both pitch targets and stimulus omissions.

Paper II (Eichele et al 2005) develops a new method to predict regional activation in functional MRI data with single trial EEG to provide a spatiotemporal characterization of evoked responses associated with pattern learning. The idea is to find correspondences between EEG and fMRI by time-variant information in single trials, which permits inferences about fMRI responses with the temporal resolution provided by EEG/ERP.

Paper III (Eichele et al 2007) addresses the mixing problem of signals from latent neuronal sources that are spatially and temporally distributed across the brain. A parallel independent component analysis framework was developed to disentangle sources from the fMRI and EEG, in order to facilitate the identification of an additional pattern-learning effect in early, automatic auditory processing.

METHODS

> *'In all likelihood these fields of potential are epiphenomenal, probably equivalent to the sounds of internal combustion engines at work, or to antique computers in science fiction movies, or to the roars of crowds at football games.*
>
> *In fact, most neuroscientists reject EEG and MEG evidence, in the beliefs that the real work of brains is done by action potentials in neural networks, and that recording wave activity is equivalent to observing an engine with a stethoscope or a computer with a D'Arsonval galvanometer.*
>
> *However, one can learn a lot about a system by listening and watching, if one knows what to seek and find.' (Freeman 2000)*

The methods employed in this work were chosen to provide a comprehensive answer to the question when and where the brain adapts to predictability. While the implementation of single trial analysis for EEG and concurrent EEG-fMRI data add a momentum of technical complexity to an otherwise simple experiment, these methods in combination alleviate critical restrictions on the spatial and temporal inferences that can be drawn from the data (Debener et al 2006; Gratton 2000; Jennings & Stine 2000).

Electroencephalography

Electroencephalography (EEG) is one of the oldest and most widespread methods to study brain activity non-invasively. The presence of fluctuating electric fields in the brain was first described by Richard Caton in the late 19th century (Caton 1875). Caton's work was not widely recognized, and it was not until 1929 that Hans Berger demonstrated scalp recordings of electrical activity in humans (Berger 1929). In his initial experiments, Berger placed electrodes over the front

and the back of the head and observed rhythmic waves at a frequency of around 10 Hz. Since its discovery, EEG has become a routine tool to study neuronal activity non-invasively, and it is a valuable method for both clinicians and researchers. EEG has many advantages based on the fact that it is an instantaneous measure of brain function that can be used in several applications. The limitations of EEG are a limited spatial resolution as well as its inability to localize the source of activity with certainty.

As demonstrated in animal studies, scalp recorded EEG originates primarily from synchronized activity in pyramidal cells in the gray matter of the cerebral cortex. Pyramidal cells are oriented perpendicular to the cortical surface, and they generate post-synaptic potentials (PSPs). Ongoing EEG activity originates from summated PSPs in the dendrites of cortical neurons, and becomes measurable on the scalp only when larger patches (on the order of centimeters) of cortical tissue are synchronously active (see e.g. Tao et al 2007). It should be noted that EEG is thus not a direct product of action potentials (APs), PSPs are slower, graded potentials which are characterized by either a hyperpolarization or a depolarization of the cell membrane that eventually elicits an AP in receiving cells. A PSP is generated when an afferent excitatory signal at the synapse changes the resting membrane potential, with influx of positively charged ions into the cell and a negative charge in the extracellular space in the vicinity of the synapse. Although current circuits are induced by PSPs, only the extracellular currents flowing from the source to the sink can be detected in EEG recordings. The electrodes measure nearby field potentials of the tissue relative to a reference electrode as a positive deflection, because the potential at the site of the active electrode is decreased relative to the reference electrode. The situation is reversed

when a current flows toward the surface electrode, which results in the registration of a negative deflection. The EEG reflects the activity of many cortical neurons, the maximal dipole moment of single neurons is too weak to produce a measurable signal on the scalp. The spatial distribution of EEG signals is distorted, because the conducting layers of tissue and bone act like resistors and capacitors in an electric circuit. As a consequence, larger patches of cortical tissue with simultaneous activity are required to generate a detectable EEG signal (Davidson et al 2000; Hugdahl 1995; Kandel et al 2000; Nunez & Srinivasan 2006; Purves et al 2001).

Event Related Potentials

One commonly used tool in neuro- and psychophysiology are the evoked, or event related potentials (ERPs), that have characteristic waveform shapes that are reproducible under similar experimental conditions (Coles & Rugg 1995; Fabiani et al 2000; Gaillard 1988; Handy 2005; Hugdahl 1995; Luck 2005; Picton et al 2000b). By arranging stimuli in paradigms, it is possible to analyze the responses of the brain to different tasks, thus allowing the study of several sensitive cognitive functions and states. ERPs are defined as changes in the ongoing EEG due to stimulation (e.g. tones, light flashes), and are typically referred to as *averaged* time and phase-locked voltage fluctuations in the EEG, resulting from volume conducted neuronal responses to sensory, motor or cognitive events. One of the major advantages of the ERP technique is that aspects of information processing can be instantaneously measured, with excellent temporal resolution. ERP components are classically divided into two types of components based on their latency: Components with latencies of up to 100ms after stimulus onset are

assumed to be primarily determined by the physical characteristics of the stimulus, and are therefore labeled 'exogenous' components. The components later than about 100 ms after a stimulus onset are determined by cognitive aspects of information processing and are hence dubbed 'endogenous'.

Wavelet Denoising

Due to the low amplitude of event related changes in the EEG in the presence of unrelated background activity, responses to several stimuli are usually averaged together. Averaging yields data reduction and increases in the signal-to-noise ratio, however, it leads to a loss of the information about systematic variability between single trials. Preservation of single trial data affords a view into the spontaneous, adaptive dynamics of event related responses in the brain, and provides a rich source of information (Debener et al 2006; Quian Quiroga & Garcia 2003; Spencer 2005). We used a recenctly developed 'denoising' scheme for the estimation of single-trial ERPs in the ongoing EEG based on wavelet decomposition (Quian Quiroga & Garcia 2003). The method relies on the time-locking and morphological characteristics of the ERP and affords the recovery and visualization of event-related responses on single-trial level. The Wavelet Transform (WT) of a signal *x(t)* is defined as the inner product between the signal and the wavelet functions $\Psi_{a,b}(t)$

$$W_{\psi}x(a,b) = \left\langle x(t), \psi_{a,b}(t) \right\rangle$$

where $\Psi_{a,b}(t)$ are dilated (contracted) and shifted versions of a unique *wavelet function* $\Psi(t)$

$$\psi_{a,b}(t) = |a|^{-1/2} \psi\left(\frac{t-b}{a}\right)$$

The WT gives a time-frequency representation of a signal that has two main advantages: firstly, an optimal resolution both in the time and in the frequency domain; secondly, signals do not need to be stationary. In order to avoid redundancy and to increase the computational efficiency, it is usually defined at discrete scales *a* and discrete times *b* by choosing the dyadic set of parameters $a^j = 2^{-j}$, $b_{j,k} = 2^{-j}k$, for integers j and k. The discrete WT gives a decomposition of *x(t)* in different scales, tending to be maximum in those scales and times where the wavelet best resembles *x(t)*. Contracted versions of $\Psi_{a,b}(t)$ will match high frequency components of *x(t)* and on the other hand, dilated versions will match the low frequency ones.

The information given by the WT can be organized according to a hierarchical scheme called multiresolution analysis (Mallat 1989), which gives a decomposition of the signal in different levels of 'details', i.e. components in consecutive frequency bands, and a final approximation or 'residual' that is the difference between the original signal and the sum of all the details. Components corresponding to the different frequency bands can be reconstructed by applying an inverse transform. Quadratic bi-orthogonal B-Splines (Cohen et al 1992) are chosen as the basic wavelet functions due to their similarity with the ERP, thus providing a good localization of the ERP in the wavelet domain, and due to their optimal time-frequency resolution.

Briefly, the method consists of the following steps: firstly, the average ERP is decomposed in different scales and times by using the wavelet multiresolution decomposition. Then, the wavelet coefficients that constitute to the ERP are identified and the remaining ones are zeroed, such that the chosen coefficients cover a time range in which the single-trial ERPs are expected to occur. At this

step, one heuristically adjusts the selected coefficients by comparing the outcomes of the denoised single-trial ERP with the raw data. The criticial point is to ensure that the denoising implementation does not alter components with systematic latency variability, and that the method does not introduce spurious changes in the peaks of interest e.g. when the set of coefficients is too narrow and not sufficient for a proper reconstruction of the ERP. Once the coefficients are chosen, the method is parameter free and does not need to be adjusted further. Lastly, the inverse transform defined by the previous steps is applied to the single trials, thus recovering the single-trial variability.

Functional Magnetic Resonance Imaging

BOLD-fMRI

The most frequently used functional magnetic resonance imaging technique is based on changes in magnetic susceptibility of the blood during brain activation (Bandettini et al 2000; Frahm et al 1992; Huettel et al 2004; Kwong et al 1992; Ogawa et al 1992). Haemoglobin carries the oxygen necessary for aerobic metabolism in the brain. The blood-oxygenation-level-dependent (BOLD) contrast picks up the different magnetic properties of oxygenated and deoxygenated blood. Deoxygenated haemoglobin (deoxy-Hb) is a paramagnetic molecule, oxygenated haemoglobin (oxy-Hb) is diamagnetic. The presence of deoxy-Hb in a blood vessel causes dephasing of the local magnetization vectors, leading to a reduction in the transverse relaxation time T2*. T2* is a net property of the material being scanned, and specifies the signal decay which produces the contrast in a MRI scan that is set up to be sensitive to T2*. When neurons are activated, there is a localized change in blood flow and oxygenation that causes a

change in the magnetic resonance (MR) decay parameter T2*, thus, changes in oxygenation of the blood can be observed as signal changes in T2*-weighted images.

Neurovascular coupling

Electrical activity in neurons cannot be directly observed by any variant of the MRI procedure, BOLD-fMRI provides an indirect measure of brain activity based on the temporal and spatial coupling of neuronal activity, metabolic activity and blood flow parameters in the brain (Villringer & Dirnagl 1995). The mechanism that defines the relationship of deoxy-Hb and oxy-Hb among populations of neurons in a certain area of the brain during their activation is called neurovascular coupling. The ratio between deoxy-Hb and oxy-Hb depends on cerebral oxygen extraction rate, blood flow and blood volume. Neurovascular coupling can coarsely be characterized by two observations (Heeger & Ress 2002): firstly, the regional blood flow is coupled to the metabolic demand; secondly, the metabolic demand results mainly from synaptic activity, and therefore blood flow and synaptic activity are coupled. The transfer from neuronal to haemodynamic signals is complex and not yet fully understood (Buxton et al 2004; Lauritzen & Gold 2003; Logothetis 2003; Logothetis & Pfeuffer 2004). However, one robust effect of neuronal activation is haemodynamic overcompensation, i.e. a local increase of the concentration of oxygenated haemoglobine. The blood flow and oxygenation changes are temporally delayed relative to the neuronal activity, a factor known as hemodynamic lag. Since the amplitude and lag of the hemodynamic response are variable (Aguirre et al 1998; Fox et al 2006; McGonigle et al 2000), and because the exact transfer mechanism between the electrical and hemodynamic processes

is not known, it is usually not possible to recover the neurophysiological process from the hemodynamic process. Nevertheless, the hemodynamic signal remains an informative surrogate for neuronal activity.

Signal and Noise

Several types of signals are encoded within the hemodynamic signal measured by fMRI. Signals of interest include event/task-related, function-related, and transiently task-related signals. Some of these were identified by McKeown in the first application of independent component analysis to fMRI data (McKeown et al 2003; McKeown & Sejnowski 1998). The task-related signal is the easiest to model: a reference waveform based on the stimulation paradigm is convolved with a hemodynamic response and is correlated with the data.

However, the responses of the brain to a given task may not be translated in a fixed, linear fashion. For example, the signal may fade out before the stimulation is turned off or change over time as repeated stimuli are applied, leading to a transiently task-related signal. It is also conceivable that there are several different types of transiently task-related signals originate from different regions of the brain.

Function-related signals reflect temporal coherence between voxels within a particular domain, for example, the motor cortex on one side of the brain will correlate highly with voxels in the motor cortex on the opposite side of the brain (Biswal et al 1995).

Signals of no interest include physiological artefacts, motion-related, and scanner-related signals. Physiological signals such as breathing and heart rate tend to be strongest in the brain ventricles and large blood vessels and can produce artifactual activation in adjacent grey matter. Motion-related signals

produce offsets that tend to affect large regions of the volume, particularly at the cortical mantle and the base of the brain. Finally, there are scanner-related signals that can be varying in time such as scanner drift and system noise, or varying in space such as susceptibility and radio frequency artifacts. Other examples include slice dropout, and nyquist ghosting. Moreover, there are several types of (white) noise due to the magnetic resonance acquisition which can be conceived as object variability due to quantum thermodynamics and thermal noise.

Motion Correction

Head motion cannot be entirely avoided by immobilizing participants in the MR scanner, therefore realignment is performed as pre-processing step. The first image of the fMRI image series is used as a reference to which all subsequent scans are realigned using a least squares approach and a rigid body spatial transformation (Worsley & Friston 1995). The realignment parameters are subsequently used for reorienting and normalizing the image slices.

Normalization

Group studies require coregistration a number of individually shaped brains from several participants into a common space. Individual brains have the same gross anatomy, although differences remain due to shape, size and gyrification. A normalization procedure spatially transforms the MR images of different subjects into a reference space to allow for group comparisons of functional activations. SPM2 was used for the analysis of MR data in this study. The software employs a standard brain from the Montreal Neurological Institute (MNI) as template for normalization. The MNI defined a standard brain by using a large series of MRI scans on normal controls (Brett et al 2002; Collins 1994). The normalization procedure uses a two-step least squares approach to minimize variation from the

template to the actual subjects head. Firstly, affine transformations, and in a second step non-linear deformations are applied, whereby the non-linear deformations are defined by a linear combination of 3D discrete cosine basis functions (Ashburner & Friston 1999).

Smoothing

The rationale for spatial smoothing is to increase the signal-to-noise ratio of fMRI activations by the matched filter theorem (Tanaka & Iinuma 1975). Therefore, if an anticipated a signal has a Gaussian shape, and is of full width on half of the maximum (FWHM) of a certain size, then this signal will best be detected smoothing images with a Gaussian filter with that FWHM size. This is of particular relevance when comparing activations across subjects. The variability between subjects causes the signal to be rather widely distributed over the average cortical surface. Further, spatial smoothing is applied to ensure that the image data have the characteristics of a Random Gaussian Field, thereby safeguarding the validity of the assumptions underlying the statistical computations in SPM2.

fMRI Time-Series Analysis

Typically, fMRI studies rely on the detection of small intensity changes over time with relatively low image contrast-to-noise ratio (CNR) of the BOLD effect. A standard approach is to correlate the time-series data with a hypothetical reference signal (typically the stimulus sequence) that involves general linear modeling approaches and uses an estimate of the hemodynamic response (Bandettini et al 1993; Friston et al 1995; Worsley & Friston 1995). In the framework of the General Linear Model (GLM) it is assumed that the neuronal events $\vec{s}$ are

transformed linearly to a hemodynamic response by convolution with a kernel known as the hemodynamic response function (hrf, Boynton et al 1996):

$$\vec{x} = hrf \otimes \vec{s}$$

The events in $\vec{s}$ can be the timing of external stimulation, or, as in the context of this work, the modulation of an intrinsic brain signal such as the amplitude modulation of ERP components. The shape of the canonical transfer function is approximated by the summation of two gamma functions with a peak latency of about six seconds (Boynton et al 1996).

It is further assumed that the fMRI data $\vec{y}$ in any voxel consists of the hemodynamic response $\vec{x}$ and a normally distributed residual noise process $\vec{\varepsilon}$:

$$\vec{y} = \beta\, \vec{x} + \vec{\varepsilon} \quad \text{with} \quad \vec{y}, \vec{x}, \vec{\varepsilon} \in \mathbf{R}^n$$

where n is the number of fMRI scans. Assuming that the noise process is white$\left[N(0,\sigma^2)\right]$, the contribution β of a stimulus response to the fMRI BOLD signal $\vec{y}$ can be calculated via least squares estimates. If the errors are white, then the least squares estimates are also the maximum likelihood estimates, and are themselves normally distributed (Scheffe 1959).

The resulting β-maps from each participant are entered into a second level *t*-test for population inferences. In order to decide whether the modeled event $\vec{s}$ leads to a significant activation somewhere in the brain, every volume element (voxel) is tested under the null hypothesis of zero magnitude:

$$t = \frac{\beta}{\sqrt{\sum_{n=1}^{N} |\varepsilon_n|^2}}$$

This voxel-by-voxel test results in a spatial distribution of *t*-values. Since t-tests are performed for every voxel in the volume (typically about $3 \cdot 10^4$) one has to

deal with a severe multiple testing problem: The simplest, but overly conservative way to correct for multiple comparisons is to perform a Bonferroni correction, i.e. adjustment of the significance level by dividing it by the number of performed tests (Perneger 1998). Alternatively, spatial correlation between voxels can be used to estimate the number of independent voxel clusters, so-called resolution elements (resels). By calculating the Euler characteristics for a given resolution element in the framework of Gaussian random field theory, one can correct thresholds for significance tests in fMRI, referred to as family-wise-error correction (FWE) which is based on Gaussian random field theory, and does not require that all observations in a data set are independent of each other (Brett 1999; Friston et al 1994; Worsley & Friston 1995; Worsley et al 1996). Another way of controlling false positive tests is based on the shape of the distribution of p-values of the tested volume (Benjamini & Hochberg 1995).

Independent Component Analysis

Independent component analysis (ICA) is a method for extracting hidden factors from observed data. Unlike principal component analysis (PCA), which decomposes the data into uncorrelated factors, ICA algorithms work iteratively in higher-order statistics to achieve statistical independence. A typical ICA generative model assumes that the source signals are not observable, statistically independent, and non-Gaussian, and mixed together by an unknown linear process. Consider an observed M-dimensional random data vector denoted by $x = (x_1, x_2 \ldots x_M)^T$, which is generated by the ICA model:

$$x = As$$

where $s = (s_1, s_2, \ldots s_N)^T$ is an N-dimensional vector whose elements are assumed independent sources and $A_{M\times N}$ is an unknown mixing matrix. Typically M >= N, so A is usually of full rank. The goal of ICA is to estimate an unmixing matrix $W_{N\times M}$ such that y is a good approximation to the true sources s.

$$y = Wx$$

ICA is hence an approach to solve blind source separation (BSS) problems. For example, BSS techniques find solutions to the cocktail party problem in which several people are speaking simultaneously in the same room. The task is to separate the voices of the different speakers by using recordings of several microphones in the room (Bell & Sejnowski 1995; Stone 2002). Popular approaches for performing ICA include maximization of information transfer (Infomax), which is equivalent to maximum likelihood estimation, maximization of non-Gaussianity, mutual information minimization, and tensorial methods. The most commonly used ICA algorithms are Infomax (Bell & Sejnowski 1995; Lee et al 1999), FastICA (Hyvarinen & Oja 1997; 2000), and joint approximate diagonalization of eigenmatrices (JADE, Cardoso & Souloumiac 1993). The original Infomax algorithm is suited to estimation of supergaussian sources (Bell & Sejnowski 1995), and has been extended to simultaneously separate sub- and supergaussian sources (Lee et al 1999). Also, a flexible approach using a generalized gaussian density model method is available (Choi et al 2000). These algorithms typically work well for symmetric distributions but they are less accurate for skewed distributions. Recent extensions of ICA to overcome this limitation include kernel ICA (Bach & Jordan 2002) and adaptive nonlinear functions to better fit the underlying sources (Hong et al 2005; Vlassis & Motomura 2001).

ICA has general applicability to normally distributed two-dimensional data and is being applied to a variety of problems in e.g. biomedicine, communications, and astrophysics. Regarding psychophysiological and neuroimaging applications, ICA has been used for decomposition of averaged ERPs (Makeig et al 1997), single trial EEG (Jung et al 2001; Makeig et al 2004b; Onton et al 2006), structural MRI (Arfanakis et al 2002) and fMRI data (Biswal & Ulmer 1999; Calhoun & Adali 2006; McKeown et al 1998; McKeown & Sejnowski 1998), and EEG-fMRI integration (Calhoun et al 2006b; Debener et al 2005b; Eichele et al 2007; Feige et al 2005; Moosmann et al 2007).

EEG-fMRI

Simultaneous EEG-fMRI recordings are technically challenging since the recording devices for both measures strongly interfere with each other (Ives et al 1993). Several issues need attention when recording EEG in the MR-scanner: Safety, MR-related artifacts in the EEG, as well as signal distortions of the MR signal due to the EEG setup.

Safety

MR imaging may induce currents in EEG electrodes and wires by movement in the static magnetic field, rapid gradient-switching that is needed for spatial coding of the MR image, or radio frequency (RF) pulses emitted by the MR coils. These currents can heat up the EEG equipment and bear the potential of harming the participant. In order to minimize these hazards, conductive loops of electrode cables should minimized and current-limiting resistors should be introduced (Krakow et al 2000). RF-induced electromotive forces were identified as the most

important hazard (Lemieux et al 1997), but the recent development of MR-compatible amplifier systems largely eliminate these hazards.

Artifacts

An EEG measured in the static magnetic field of a MR scanner shows large cardio-ballistic artefacts (Ives et al 1993). It is believed that the cardio-ballistic artefact arises mainly from pulsation induced movements of the electrodes in the B_0-field (Anami et al 2003), and to a lesser degree from electromotive force of blood ions (Bonmassar et al 2002). The pulsatile movements of the subjects' skin are picked up by the electrodes and wires and lead to an inductive voltage that is recorded by the EEG. The cardio-ballistic artefact can be minimized by immobilizing the patients head, the electrodes and the wiring between electrode cap and EEG amplifier (Anami et al 2002; Benar et al 2002). The residual cardio-ballistic artefact can be corrected by adaptive artifact filtering methods based on template matching (Allen et al 1998; Bonmassar et al 2002) or multivariate decomposition (Debener et al 2007; Niazy et al 2005).

The strongest influence of the MR-environment on the EEG system results from the switching MR gradients and high frequency (HF) pulses from echo-planar sequences (EPI) that are used to measure the BOLD contrast. Both HF pulses as well as the MR-gradients are registered in the EEG by inducing a voltage in the electrode cables. EEG amplifiers with a broad dynamic range can record both low voltage physiological EEG and high voltage MR gradients. Typical filter algorithms are based on estimating an artifact template in the frequency or time domain, which is subtracted from the contaminated EEG signal (Allen et al 2000). Anami et al. (Anami et al 2003) modified the imaging sequence to reduce

MR-gradient specific artifacts in the EEG system by synchronizing EEG and fMRI systems on a sub-millisecond scale.

The quality of the MR images can also be affected by the EEG system. Echo planar imaging (EPI) pulse sequences are highly sensitive to changes of susceptibility that can be induced by the EEG electrodes. However, at 1.5T, local signal dropouts with appropriate electrodes are reported to be minor and limited to subcutaneous fat (Krakow et al 2000; Lazeyras et al 2001). At 3T, the signal to noise ratio of MR images is significantly reduced with 128 electrodes, whereas the use of 64 electrodes provides a good ratio between spatial EEG resolution and MR signal drop-out (Scarff et al 2004). Further sources of imaging artifacts can be the electromagnetic noise due to the EEG digitizing circuit, which can be avoided with the appropriate shielding of the EEG amplifier (Krakow et al 2000).

Integration

The integration of multiple neuroimaging modalities aims at developing a better understanding of where and when cognitive processes take place in the brain. Both EEG and fMRI provide complementary advantages with regard to the temporal and spatial resolution for mapping of brain activity. Developing approaches for analysis which draw upon the strengths of each method can afford a spatiotemporally and functionally comprehensive characterization of regional brain responses (Debener et al 2006; Hopfinger et al 2005; Horwitz & Poeppel 2002; Makeig 2002). The rationale to implement concurrent recordings instead of separate sessions or studies is simple: when used separately, the major neuroimaging methods EEG/ERP and fMRI are limited to spatially or temporally restricted inferences regarding brain activity. This means that the interpretation of data from either method alone will only yield partial and not necessarily

comprehensive conclusions about brain function. FMRI measures local changes in brain hemodynamics associated with cognitive processing with high spatial precision, however, the BOLD contrast is an indirect and delayed metabolic correlate of these processes after a complex set of reactions that constitute the neurovascular coupling (Lauritzen & Gold 2003; Logothetis 2003; Villringer & Dirnagl 1995). In contradistinction to BOLD-fMRI, EEG and ERP record the electrical potentials induced by synchronized synaptic activity directly, and typically allow an effective temporal resolution of cognitive processes on the order of tens of milliseconds. However, the scalp EEG picks up a volume conducted and blurred mixture of the underlying activity and spatial inferences are critically limited by the inverse problem.

One approach to analyze concurrent EEG-fMRI is to predict the fMRI timecourse as a parametric modulation of a select EEG/ERP feature. This feature can be convolved with a hemodynamic response function under the assumption of approximate linear coupling relationships between local field potentials, the scalp EEG and the hemodynamic response (Arthurs & Boniface 2002; Heeger & Ress 2002; Lauritzen & Gold 2003; Logothetis 2003; Logothetis et al 2001; Mukamel et al 2005). Integration by prediction was utilized to localize sources of epileptic activity based on the timing of EEG-recorded spikes (Benar et al 2002; Gotman et al 2004; Krakow et al 1999; Salek-Haddadi et al 2003; Warach et al 1996). Another application was the study of regional activations predicted by amplitude modulation in the power spectrum of EEG rhythms, so far with the largest interest in the 8-12Hz (alpha) band (Feige et al 2005; Goldman et al 2002; Goncalves et al 2006; Laufs et al 2003a; Laufs et al 2003b; Moosmann et al 2003). The general pattern of results in these studies agrees well with the brain structures that are

assumed to be directly or indirectly involved with the generation or modulation of EEG alpha activity on the scalp. The main finding in these studies is that BOLD activity in the occipital cortex is negatively correlated with EEG alpha power, consistent with the idea that synchronized activity in the alpha band represents an idling rhythm with relative cortical deactivation.

The feasibility of EEG-fMRI integration through correlation between timecourses of both modalities in resting state data suggested that the trial-to-trial amplitude (and latency) variability of event related brain activity induced by external stimulation also could be utilized for integration. The extension of this method to single trial event-related time-domain data affords quantification of induced or spontaneous modulation of regional responses in the fMRI with the effective temporal resolution of the ERP (Debener et al 2006; Debener et al 2005b; Eichele et al 2005). Studies that implement single-trial EEG-fMRI methodology have so far described regional BOLD correlates for a number of ERP components: Contingent Negative Variation (CNV, Hinterberger et al 2005; Nagai et al 2004), P2 and N2 (Eichele et al 2005), P3 (Benar et al 2007; Eichele et al 2005) and Error Related Negativity (ERN, Debener et al 2005b).

LIST OF PAPERS

I. Jongsma ML, Eichele T, Van Rijn CM, Coenen AM, Hugdahl K, Nordby H, Quiroga RQ. (2006) Tracking pattern learning with single-trial event-related potentials. *Clinical Neurophysiology*. 117(9):1957-73.

II. Eichele T, Specht K, Moosmann M, Jongsma ML, Quiroga RQ, Nordby H, Hugdahl K. (2005) Assessing the spatiotemporal evolution of neuronal activation with single-trial event-related potentials and functional MRI. *Proceedings of the National Academy of Sciences of America*. 102(49):17798-803.

I. Jongsma ML, Eichele T, Van Rijn CM, Coenen AM, Hugdahl K, Nordby H, Quiroga RQ. (2006) Tracking pattern

III. Eichele T, Calhoun VD, Specht K, Moosmann M, Jongsma ML, Quiroga RQ, Nordby H, Hugdahl K. (2007) Unmixing concurrent EEG-fMRI with parallel independent component analysis. *International Journal of Psychophysiology,* epub Aug 2

SUMMARY OF PAPERS

Paper I (Jongsma et al 2006) presents the paradigm and a single trial EEG analysis with ICA and wavelet denoising. The results describe pattern-learning effects in scalp event-related potentials with both infrequent pitch targets, as well as stimulus omissions. The main objective in this paper was to track the dynamics of pattern-learning using single-trial ERPs. A new variant of an oddball paradigm was tested in 24 participants: in this pattern-learning paradigm eight randomly occurring targets were followed by eight regularly appearing targets interspersed among standard tones and single-trial responses to all targets were extracted. Following random targets, ERPs showed a marked P3-N2 component that significantly decreased in amplitude to regular targets, where also a contingent negative variation (CNV) appeared. The ERP amplitude variability across random-regular sequences was best accounted for by sigmoid learning-curves. Single-trial analyses showed that learning occurred more rapidly with time-on-trial and suggested that the CNV developed prior to the decay of the N2-P3 component.

Paper II (Eichele et al 2005) develops a novel method to predict functional MRI with single trial EEG to provide a spatiotemporal characterization of evoked responses. The idea was to find matches between EEG and fMRI by time-variant information in single trials, which permits inferences about regional responses with the temporal resolution provided by EEG/ERP. The method was used to study the spatial correlates of the predictability effects in the pattern learning oddball. In addition to electrophysiologic and hemodynamic evoked responses to

auditory targets per se, single-trial modulations were expressed during the latencies of the P2 (170 ms), N2 (200 ms), and P3 (320 ms) components and predicted spatially separate regional responses, involving areas in the precuneus, perihippocampal, medial and lateral frontal, temporal, and parietal regions.

Paper III (Eichele et al 2007) addresses the mixing problem for signals from latent neural sources that are spatially and temporally distributed across the brain. Concurrent event-related EEG-fMRI recordings pick up volume-conducted and hemodynamically convoluted signals from latent neural sources that are spatially and temporally mixed across the brain, i.e. the observed data in both modalities represent multiple, simultaneously active, regionally overlapping neuronal mass responses. This mixing process decreases the sensitivity of voxel-by-voxel prediction of hemodynamic activation by the EEG when multiple sources contribute to the predictor and response variables. To this end, a novel parallel independent component analysis framework was developed to unmix sources from the fMRI and EEG, in order to facilitate the search for additional pattern-learning effects in early, automatic auditory processing. We used parallel ICA to recover maps from the fMRI and timecourses from the EEG, and matched these components across the modalities by correlating their trial-to-trial modulation. The method extracted a previously undetected EEG-fMRI component from the concurrent pattern-learning data, colocalizing with the N1-ERP and fronto-temporal fMRI activation.

DISCUSSION

> *'Although this experiment did not deal specifically with the related question of whether enhanced attentiveness increases the amplitude of the evoked potential, results obtained by Davis in an auditory discrimination situation indicate that this may be the case.' (Haider et al 1964)*

> *'We encounter many differences in the slow evoked responses, both across subjects and across trials. So far, the task described above has been our most consistent way of enhancing the response. We believe that this effect of making a rather difficult sensory discrimination is a counterpart of the relation of the amplitude of the evoked response to vigilance, recently demonstrated by Haider.' (Davis 1964)*

The dynamic and spatiotemporally extensive activations observed in this thesis constitute essential loci of orienting, memory formation and allocation of cognitive resources (Donchin & Coles 1988; Halgren & Marinkovic 1995; Huettel et al 2002; Kiehl et al 2005; Loveless 1983). Being able to perceive regular patterns in the environment and maintaining a mental representation of these means to extract contingency rules with highly salient predictive value (Huettel et al 2002; Llinas 2001). The findings in this work provide a novel, but foreseeable perspective on event related responses and the basic notion about generation of predictions/expectancies permeates the models that account for aspects of event related processes in the brain (Donchin & Coles 1988; Friston 2005a; Näätänen 1992; Sokolov 1963). The current results provide evidence that basic models are also operational for higher levels of complexity in the relationship between stimuli. The paradigm used in this work modulates the predictability of upcoming targets and induce systematic trial-to-trial variations in

ERP and fMRI responses. The signal processing and statistical methods that were employed for analysis of the data provide a clearer view onto the spatial and temporal dimensions of single trial modulations associated with pattern learning. The difference between previous studies and the design used here is that inferences are drawn from single trial modulations across successive targets rather than the averaged ERP waveforms or fMRI contrast images, which affords inferences about the ongoing dynamics of cognitive processing (Debener et al 2006; Makeig et al 2004a; Onton et al 2006; Quian Quiroga & Garcia 2003; Spencer 2005).

Expectancy Modulation

The common observation in the results of papers I and II (Eichele et al 2005; Jongsma et al 2006) were sigmoid-shaped amplitude modulations with turning points between the 2^{nd}-3^{rd} repetition of the target-to-target interval. These learning curves in response to patterns in the sequence were spanning the random and regular targets and occurred in the latency-ranges for various components in the auditory ERP waveform, namely the N2, P3 and CNV to pitch targets and omissions in paper I (Jongsma et al 2006); P2, N2, and P3 to pitch targets in paper II (Eichele et al 2005). Learning curves remained at a stable upper plateau during random target presentations, before decreasing to a lower plateau after three to four regularly presented targets. Detecting patterns in discrete event sequences requires spanning of the temporal interval between the events. The neural systems involved must create a representation of the event that can be retained for a certain interval of time (Hughes et al 2001; Näätänen 1992; Winkler et al 2001). In this case, at least two consecutive targets with the same interval or

number of preceding background tones are necessary in order to perceive the pattern, which means that the window of temporal integration for detection of the regularity ranged between 12-16 seconds in the current experiments.

A different modulation was seen in the spatiotemporal independent component reported in paper III (Eichele et al 2007) that did show a smooth gamma-shaped response with the peak at the 1st random target after a sequence of regular ones, suggesting a selective response to increases in prediction error (surprise).

Long-Term Predictions

In paper I (Jongsma et al 2006), an additional higher order dynamic of learning was observed, complementing the learning curves at the transition between random and regular targets. Within the first presentation cycle the N2-P3 complex decreased between the 5th and 6th regularly presented target, however, with each repetition of the presentation cycle the N2b-P3 effect occurred earlier. This meant that learning curves during later phases of the experiment had unexpectedly early turning points occurring before the target regularity could be perceived. This was not reported in detail in paper II (Eichele et al 2005) and paper III (Eichele et al 2007), however, the group averaged amplitude modulations in both reports show that the effects start to develop one trial earlier than what one would expect from a 'local' response to changes in predictability. This means that there is an indication of an additional 'global' predictability effect occurring across repetitions of the target sequences, however, with considerable inter-subject variability, and thus not verifiable statistically. Nevertheless, this global predictability effect provides some support for the idea that transitions between random and regular contexts were predicted by the participants. Unfortunately,

formal learning models such as Rescorla-Wagner do not include these anticipatory effects, i.e. represent an anticipated change in prediction error. Usually, these models employ a single learning curve and would have to be extended, in our case to represent local (immediate) and emergent global (long-term) learning curves and prediction error (cf. Gläscher & Büchel 2005) simultaneously.

Regional Activation

The observation that a simple cognitive task such as target detection in an auditory oddball experiment induces spatially and temporally widespread neuronal responses (Baudena et al 1995; Calhoun et al 2006b; Eichele et al 2005; Halgren et al 1995a; Halgren et al 1995b; Kiehl et al 2005) relates to distributed network responses more than to localized sources (Fox et al 2005; Halgren & Marinkovic 1995; Nunez 2000). Activation associated with target processing, but insensitive to pattern learning was seen in areas commonly associated with auditory or visual target detection (Bledowski et al 2004; Kiehl et al 2005; Linden et al 1999). In addition, a total of four temporally and spatially separated activation stages were identified in papers II and III, where amplitude modulations of single trial ERP sequences selectively predicted fMRI activation patterns. The correlation between the modalities was interpreted as a reflection of the common neuronal function probed by the stimulation paradigm. Note, however, that in addition to the induced modulation it is plausible that unspecific, task-unrelated physiological fluctuations are also captured, and may influence the covariation between EEG and fMRI components. Such spontaneous fluctuations, however, are specific with respect to their spatial origin and temporal occurrence.

Bypassing the Inverse Problem

Another aspect of this work is that papers II and III provide methods that bypass the electromagnetic inverse problem, in that spatial inferences are made from the trial-to-trial modulations, and not by means of inverse modelling. In the methods presented here, brain sources are not necessarily conceived as regional maxima in fMRI activation (derived from standard GLM analysis), topographies or equivalent dipoles, but rather concurrent spatially fixed electromagnetic activity that is spatially and temporally independent of activity arising in other sources.

Thus, a source is conceived more as the common electrophysiologic and hemodynamic correlate of the information processing expressed in the across-trial modulation than an actual location of the fMRI activation and the spatial projection and match with a dipolar/distributed model. This means that networks representing such concurrent activity are not per se defined as spatially or temporally fixed distributions in the brain. In addition, the analysis schemes make no assumptions about, or distinctions between open-field superficial electrical sources that would actually propagate to the scalp and other sources corresponding to deeper, closed-field sources that are coupled with the former, but which likely are not directly detected on the scalp. While there is an implicit assumption that some parts of an fMRI map would have a predisposition to host dipolar sources as soon as we find a correspondence in the scalp EEG/ERP, it remains unspecified where in the map they are located.

Component Effects

CNV

In paper I (Jongsma et al 2006), a frontally distributed contingent negative variation (CNV) was observed in the pre-stimulus period of regularly presented targets, but not in ERPs to random targets. This component was not reported in papers II and III (Eichele et al 2007; Eichele et al 2005), due to optimization of ICA and wavelet denoising preprocessing steps for the faster (higher frequency) post-stimulus components. CNV is commonly elicited in paradigms in which a 'warning' stimulus precedes and predicts a subsequent 'imperative' target stimulus (Brunia 1999; Walter et al 1964). In this experiment, it is conceivable that regularly presented stimuli started to function as warning stimuli, although conventionally the CNV develops before the motor response, it also develops before an expected stimulus that does not require a motor response (Hohnsbein et al 1998). Here, CNV is assumed to reflect the preparation and facilitation of relevant brain areas for the upcoming trial. It is likely that a representation of the regular target-to-target interval affords a temporal anticipation (Nobre 2001; Nobre & O'Reilly 2004). With respect to higher order learning dynamics, we observed that CNV started to develop between the third to fourth regular target within the first cycle, which was prior to the decrease of N2b and P3 (from fifth to sixth regular target). With each repetition of the presentation cycle the effects occurred earlier. It is possible that the CNV early in the regular sequence follows from a prediction that some regularity is present. The continuing N2b and P3 would reflect evaluation of the situation to confirm the hypothesis, while later, when the prediction has been confirmed, the stimulus evaluation decreases, which

would be in accordance with generic models of ERP generation (Friston 2003; 2005a; Kotchoubey 2006).

N1-P2

In paper III (Eichele et al 2007) the development of a parallel independent component analysis scheme for the EEG and fMRI data afforded the extraction of a central N1 at 100ms which was followed by smaller P2, N2 and P3 (270ms) deflections. The difference between standard and target yielded a biphasic pattern with a sustained negativity from 100-200ms, followed by the P3, which altogether suggested that this component reflected N1-enhancement and a subsequent N2b-P3a (Näätänen 1992; Näätänen & Picton 1987) as one coherent process. Given the experimental parameters, the 'N1-enhancement' may have contained contributions from genuine sources of mismatch negativity (MMN), attentive processing negativity (PN/Nd) and so-called ‘fresh afferents’ of the N1 alike (Näätänen 1992; Näätänen & Picton 1987). The N2b-P3a portion of the waveform following the N1/MMN is seen with attention-switching at large or task-relevant stimulus contrasts (Näätänen 1992; Schroger 1997). Single trial EEG amplitudes selectively covaried with an fMRI component with local maxima in the superior temporal gyri (R>L), the temporal poles, the anterior cingulate gyrus, and inverse correlations in the brainstem. This partition of the map encompasses the assumed sources of the scalp N1/MMN (Näätänen & Picton 1987; Picton et al 2000a; Picton et al 1999; Woods 1995), and the brain areas that previous imaging experiments have described for automatic auditory deviance detection, stimulus discrimination, sensory memory, as well as novelty (surprise) related functions (Downar et al 2000; Liebenthal et al 2003; Molholm et al 2005;

Muller et al 2002; Opitz et al 1999; Rinne et al 2005; Sabri et al 2006). The slow linear decrement on the trial-to-trial amplitudes is in line with reports describing long term habituation for N1, MMN as well as P3a across the observation time (Debener et al 2005a; Friedman et al 2001; Loveless 1983; McGee et al 2001; Sambeth et al 2004; Woods & Elmasian 1986), and may reflect a slow adaptive process related to repetitions of stimulus sequences (Jongsma et al 2006; Ulanovsky et al 2004), or an unspecific correlate of a decline in arousal and vigilance. The local amplitude modulation saw an increment at the transition from regular to random intervals, the corresponding transition from random to regular did, however, not elicit an equal or inverse response. Hence, instead of cyclical or sigmoid learning curves that characterized the behaviour of the other components (Eichele et al 2005; Jongsma et al 2006), a gamma-shaped function provided the best fit. An explanation for this result can be deducted from a selective, valued learning model, i.e. the process responds only to positive-signed changes in prediction error, such that the weight change elicited by the comparison between actual input and the learning history would only reflect increments of surprise with the appearance of a target at an unpredicted interval, but not a constant error within one context or decrements at the onset of the regular pattern. Further, the time-span for which the process accumulates information into the learning history may be limited to 10 seconds or less (Winkler et al 2001), such that it would be plausible that the component does retain enough interval repetitions to recognize the emergence of a pattern. For both accounts it is plausible to assume that the modulation is not self-sustaining but that it receives backward input from higher levels of cortical processing represented in later components. These may exert an inhibitory influence when intervals are predictable, while the response to the

more surprising transition from predictable to unpredictable intervals represents a salient bottom-up signal (Friston 2005a; Schroger 1997).

Sustained N1 subcomponents are also existing during the latency of the P2 (Näätänen & Picton 1987), and the earliest spatiotemporal stage seen in paper II (Eichele et al 2005) reached maximum intensity during P2 at about 170 ms post-stimulus. P2 is modulated by processing negativities that reflect matching processes between the sensory input and a neuronal representation of relevant stimuli for further processing, and are markers of selective attention (Näätänen 1992; Näätänen & Picton 1987). The main sources of these subcomponents are found in the temporal and frontal lobes (Näätänen 1992) as seen in the N1-related independent component above. However, the predicted fMRI activation was located in the precuneus, supramarginal gyri, posterior cingulate gyri, superior and inferior parietal lobule. The areas that covaried with the P2 effect on the scalp include many of the regions commonly associated with the 'default mode' of brain activation (Greicius et al 2003; Raichle et al 2001). It is conceivable that these brain regions either represent a previously unrecognized, likely modality-independent source of the N1/P2, or, alternatively have modulatory effects on the N1 subcomponents (or later components, respectively). The interpretation that this component mediates (in part) allocation of resources when target occurrence is predictable would also be consistent with the functional role of the 'default mode' (Greicius et al 2003; Laufs et al 2003b; Raichle 2006; Raichle et al 2001; Sonuga-Barke & Castellanos 2007). The locations also fit well with the onset latency of a widespread waveform that has been reported from intracranial recordings at about 170ms (Halgren et al 1995a). FMRI/PET studies of temporal

attention, and sequencing are also overlapping with these regions (Cabeza & Nyberg 2000; Janata & Grafton 2003).

N2b-P3

We observed that ERPs in response to randomly presented target stimuli contained marked N2b and P3 components. N2b is thought to reflect detection of a mismatch between stimulus features and an actively generated memory template (Gehring et al 1992; Näätänen 1992; Näätänen et al 1982), while P3 has been suggested to index a mechanism that is elicited when a memory representation of the recent stimulus context is updated upon detection of deviance from it (Donchin 1981; Donchin & Coles 1988). N2b and P3 were smaller in response to regularly presented targets as compared to randomly presented targets in both the pitch target and omission sessions. Compared to the current experiment, Eimer and colleagues (Eimer et al 1996) described similar N2 effects due to implicit pattern learning, others have reported decreased P3 in associative learning (Rose et al 2001). Correspondingly, in a previous study we found that the N2 and P3 diminished when omitted target stimuli were expected (Jongsma et al 2005). FMRI correlates of the N2b were found in frontomedian and parahippocampal cortex, in line with other fMRI studies of this iconic memory process (Cabeza & Nyberg 2000) and the reduced N2b to auditory targets in patients with bilateral hippocampal damage (Kiehl et al 2005; Knight 1996). The locations were also in accord with intracranial N2's in the same latency range found in intra-operative recordings in the vicinity of these regions (Baudena et al 1995; Halgren et al 1995b). FMRI-correlates of the P3 were found in right hemisphere frontal, temporal and parietal regions. The activation in these

regions is consistent with a variety of related functions, including target detection (Bledowski et al 2004; Horovitz et al 2002; Linden et al 1999), attention and working memory (Cabeza & Nyberg 2000) as well as sequencing and pattern recognition (Huettel et al 2002; Janata & Grafton 2003). Also, intracranial recordings have reported depth-P3's from the same sites (Baudena et al 1995; Halgren et al 1995a; Halgren et al 1995b).

SUGGESTIONS FOR FUTURE RESEARCH

> *'While the dictum that the brain is the organ of thought is little questioned in scientific circles, it is only in the last few years that specific information has been obtained on the relation between complex psychological variables and the activity of the brain.' (Sutton et al 1965)*

There are many questions for future research that can be deducted from the paradigm, methods, and results presented in this work.

Exploration of Adaptive Effects in Audition

One application of the pattern-learning paradigm that we have developed is to study the effect of expectancy on single trial level when stimuli are not attended. The major phenomenon in both studies so far was the sigmoid-shaped amplitude modulation coherently expressed in the ERP and fMRI, as intervals became predictable. As noted in the introduction, models that can account for these effects go back to Sokolov's original account of the orienting response (Huettel et al 2002; Loveless 1983; Sokolov 1963). This principal functionality is overlapping with that of the mismatch negativity (MMN) process, although the MMN has so far been understood as a more low-level automatic response (Näätänen 1992; Näätänen & Winkler 1999) that would typically not code some of the features that e.g. the P3 process is sensitive to, such as predictability of stimulus sequence (cf. Sussman et al 1998).

However, Ulanovsky et al. (Ulanovsky et al 2004; Ulanovsky et al 2003) have recently shown that the firing patterns of neurons in *primary* auditory cortex adapt to repetition and sequence on multiple timescales, also exceeding

sensory/short-term memory (approx. 10-12s, from Winkler et al 2001). Haenschel et al. (Haenschel et al 2005) found that the MMN, the negativity in the *difference wave* between standard and deviant stimulus ERP received contribution from enhancement of a slow positive wave in the *standard* ERP with stimulus repetition. This positivity may represent a human correlate of stimulus-specific adaptation, a plausible neuronal mechanism underlying memory formation in the auditory cortex (Baldeweg 2006; Haenschel et al 2005; cf. Näätänen & Rinne 2002; Ulanovsky et al 2004; Ulanovsky et al 2003). Since current views on MMN (and P3 alike) can not fully account for these findings is plausible to attempt a revision of these models within a predictive coding framework that defines reciprocally connected hierarchical models that construct context-dependent expectancies (Baldeweg 2006; Friston 2005a; Llinas 2001). We are currently exploring how temporal patterns are extracted from auditory event sequences when the stimuli are not attended, probing the proposed adaptation effects in the event-related response during automatic deviance detection, and the ERP to adjacent standard stimuli. So far, 32 participants were enrolled in this study and were reading a text while infrequent duration deviants interspersed with frequent standards were presented at an SOA of 350 ms. Twenty additional participants participated in a control experiment where stimulus omissions were used as deviants. Predictability was introduced by alternating stimulus sequences with randomly varying or regular inter-deviant intervals. EEGs were collected from 64 channels and were treated with individual ICA (Delorme & Makeig 2004), wavelet-denoising (Quian Quiroga & Garcia 2003) and subsequent group temporal ICA. The results provide evidence for modulation of ERP components induced by trial-to-trial learning of interval associations with multiple

simultaneous learning rates. The temporal windows of integration of the learning rates span ~ 1/2 – 6 minutes thus covering a range where both local patterns and global rules of repetition can be encoded. The sensitivity of ERP components to stimulus sequence in the absence of a related task indicates that a principle function at early automatic stages of processing is to mine events for higher-order patterns/contexts (Friston 2005a; Ulanovsky et al 2004).

The improvement of multimodal imaging technology in terms of recording and analysis are necessary first steps in order to study the adaptive dynamics of human cognitive processing. The current experiment is easily adapted for joint recordings and data fusion. We expect that bilateral middle temporal and middle frontal gyri would show interval adaptation effects, possibly supplemented by inversely related medial frontal and precuneus activity representing default mode. We will employ a MR sequence that collects data only with slices crossing through a restricted fronto-temporal region of interest. This allows for a much faster MR sampling rate, and together with joint EEG/ERP this sampling procedure will assess adaptive effects on the regional BOLD responses.

EEG-fMRI Fusion

The coherence between scalp electrophysiologic and hemodynamic correlates of neuronal activity should be detected by a symmetric common fusion model that simultaneously assesses all available data (Debener et al 2006; Hopfinger et al 2005; Horwitz & Poeppel 2002; Makeig 2002). Currently, three different frameworks have been suggested for such multimodal fusion: *Dynamic Causal Modelling* (Friston 2005a; Kiebel & Friston 2004a; 2004b), an approach based on a hierarchical Bayesian framework (see also Daunizeau et al 2007), *Partial Least*

Squares (Martinez-Montes et al 2004), and *Joint Independent Components Analysis* (Calhoun et al 2006a; Calhoun et al 2006b), however, none of these have been implemented for single trial EEG-fMRI. The simpler solution that has been used so far is integration by prediction, where we assume a fixed hemodynamic response and a linear neurovascular coupling relationship between local field potentials and the hemodynamic response and test for a correlation between the modalities in order to draw spatio-temporal inferences. The validity of these inferences is, however, critically dependent upon the parameters of neurovascular coupling and hemodynamic response function that are used in the model. In paper II, we have predicted the fMRI signal as a function of the denoised single trial EEG, convolved with a canonical hemodynamic response, and thus proposed EEG-fMRI integration by means of induced amplitude modulations on single trial level, yielding a functionally specific temporal expansion of the fMRI activity (Eichele et al 2005). Independently, Debener et al. (Debener et al 2005b) developed a similar approach that is based on decomposition of the scalp EEG into independent components via ICA prior to integration. Paper III (Eichele et al 2007) employed parallel spatial and temporal ICA of EEG-fMRI recordings in order to address the mixing problem in both modalities. All three solutions rest on prediction of data in one modality through data in the other modality meaning meaning that symmetrical fusion was not realized in either report.

One natural extrapolation is to adapt joint ICA to concurrent EEG and fMRI single trial data to provide a novel, widely applicable data-driven analysis framework which combines and advances the methodology presented in recent reports (Calhoun et al 2006b; Debener et al 2005b; Eichele et al 2007; Eichele et al 2005). The idea is to pre-process the data separately with filtering,

normalization, and single subject ICA for artefact removal, using the appropriate tools in the academic freeware toolboxes SPM, EEGLAB, and GIFT. A joint data space is then created by adding for each trial hrf-convolved single-trial EEG into the MR image time-series as additional 'slices', that is submitted to a group ICA. We have begun evaluating the performance of joint ICA across a number of decomposition details with variable preprocessing and data reduction steps, number of sources and estimated ICs. Our preliminary results at this point (Eichele et al 2006; Moosmann et al 2007) suggest that joint ICA provides a promising framework for data-driven multimodal fusion that can more completely characterize evoked responses in the human brain.

Ground Truth

The single trial EEG-fMRI methods presented so far in papers II and III (Eichele et al 2007; Eichele et al 2005), as well as the complementary work of Debener (Debener et al 2006; Debener et al 2005b) make way for unprecedented precision in non-invasive spatiotemporal mapping of brain responses. However, one should be careful to keep in mind and acknowledge that it is to date not determined for any of the available analysis frameworks, such as integration by constraints, integration by prediction and common generative models, in which conditions they are fully appropriate and ultimately can reveal the 'true' spatiotemporal maps. This is because a study design for assessment of neurovascular coupling and spatiotemporal mixing with a conclusive chain of evidence requires concurrent direct measurements of intracranial EEG (or LFP/MUA, respectively) from the cortical surface during collection of scalp EEG and fMRI data. Data from such a design would be necessary to establish a ground truth about the

coupling between the modalities and would be adequate for validation of non-invasive EEG-fMRI, but one should consider that this study would be extremely challenging to technically realize. So far, none of the studies we are aware of in humans (usually epileptic patients) or in subhuman species (monkeys, cats) has achieved this (for example, see Logothetis et al 2001; Mukamel et al 2005). The development of feasible study protocols should be a major effort for future work.

Connectivity

Large-sample studies, meta-analyses and databases demonstrate that hemodynamic brain activation can be dissociated into a limited number of large-scale regional systems/networks. This view is complementary to the conception of electrophysiological phenomena during information processing such as the ERP, induced oscillations and phase resetting as being correlates of widespread network activity, rather than selective point sources (Makeig 2002; Makeig et al 2004a). Apart from delineating the spatiotemporal structure of these evoked response systems, it is important to address the question in which fashion they relate to an external stimulation paradigm, and, crucially, how they relate to each other, i.e. coupling (Engel et al 2001; Friston 2005a; Friston 2005b; Varela et al 2001). In our previous work, hierarchical relationships were inferred solely by means of the timing of peak activation in the ERP with respect to stimulus onset (Eichele et al 2007; Eichele et al 2005). In the jICA framework, we can assess the relationships between a selected set of independent sources with techniques such as tree clustering, structural equation models (SEM) and dynamic causal models (DCM, Friston 2005a), respectively, or with paradigm-specific generative models based on e.g. formal learning theory. These techniques derive the levels of

hierarchical organization from the data and the utility for multimodal data is that this allows for generation of more specific hypothesis regarding the functional coupling between components.

Coherence

The event related response reflects only a small portion of the EEG variability, and there are a variety of task related, functionally relevant effects such as spectral perturbations, phase resetting and coherency whose hemodynamic correlates deserve exploration in fused data (Makeig et al 2004a; Makeig et al 2004b; Rodriguez et al 1999; Varela et al 2001). While ERP information most likely yields the most robust temporal processing information, the other sources of variance are likely to elucidate processes such as feature binding (Fries et al 2001; Gray et al 1989), predictive coding (Engel et al 2001) and efferent/afferent functional coupling (Schoffelen et al 2005). These phenomena are expressed less in the transient response and more in amplitude/phase coherency between cortical sites, and also between the cortex and peripheral effectors.

One application would be an investigation of the hemodynamic correlates of cortico-cortical, and cortico-muscular coherence in the EEG spectrum. For example, we can estimate event related coherence between central EEG sites and distal EMG to compare changes in efferent coupling between predictable and unpredictable conditions as follows: For *n* epochs, $F_k(f,t)$ is the spectral estimate of epoch *k* at frequency *f* and time *t*. For two channels *a* and *b* event related phase cross coherence (Delorme & Makeig 2004; Tallon-Baudry et al 1996) is then defined by

$$coh^{a,b}(f,t) = \frac{1}{n}\sum_{k=1}^{n}\frac{F_k^a(f,t)\,F_k^b(f,t)^*}{\left|F_k^a(f,t)\,F_k^b(f,t)\right|}$$

where $|\ |$ is the complex norm and $F_k^b(f,t)$ is the complex conjugate of $F_k^b(f,t)$.

It is prudent to assume that cortico-muscular synchronization should display differences between expected and unexpected targets, and this study would be important for addressing questions about the interaction between perceptual and cognitive levels and the coding/efficacy in the motor system (Kilner et al 2003; Mima et al 2001; Schoffelen et al 2005).

Replication

Another important promise with concurrent single trial EEG -fMRI studies is that it allows to re-examine in detail the seminal psychophysiological experiments and concepts (for examples, Hillyard et al 1973; Näätänen et al 1978; Sutton et al 1965). Such replication/reassessment studies would combine different methods and ideally also include peripheral psychophysiological measures such as electrodermal and cardio-respiratory activity. This allows to assess and to localize many of the basic model elements and theoretical foundations of modern cognitive neuroscience and neuroimaging. Multimodal imaging can update these models and thus improve our concepts and understanding of the brain-behavior relationship.

CONCLUSION

This thesis makes two contributions to cognitive neuroscience and neuroimaging: Firstly, the salient pattern learning effects during the oddball paradigm extend the putative functions of a variety of ERP components from the basic standard vs. deviant contrast to more complex rules in the stimulus material.

Secondly, the methods for single-trial analysis and EEG-fMRI integration that were developed for the purpose of extracting the pattern-learning effects have general applicability in multimodal imaging experiments in cognitive neuroscience.

Future studies should investigate these predictability effects in detail across varying pattern complexity and sensory modalities, and attempt to develop a comprehensive learning model that integrates effects on multiple levels and timescales.

Also, method development should spur further progress in multimodal integration, in particular single-trial data fusion with independent component analysis or other suitable data-driven algorithms promises to open new avenues for exploration of human brain function.

REFERENCES

Aguirre GK, Zarahn E, D'Esposito M. 1998. The variability of human, BOLD hemodynamic responses. *Neuroimage* 8:360-9

Allen PJ, Josephs O, Turner R. 2000. A method for removing imaging artifact from continuous EEG recorded during functional MRI. *Neuroimage* 12:230-9

Allen PJ, Polizzi G, Krakow K, Fish DR, Lemieux L. 1998. Identification of EEG events in the MR scanner: the problem of pulse artifact and a method for its subtraction. *Neuroimage* 8:229-39

Anami K, Mori T, Tanaka F, Kawagoe Y, Okamoto J, et al. 2003. Stepping stone sampling for retrieving artifact-free electroencephalogram during functional magnetic resonance imaging. *Neuroimage* 19:281-95

Anami K, Saitoh O, Yumoto M. 2002. Reduction of ballistocardiogramwith a vacuum head-fixating system during simultaneous fMRI and multi-channel monopolar EEG recording. *Recent Adv Hum Brain Mapp* 1232:427–31

Arfanakis K, Cordes D, Haughton VM, Carew JD, Meyerand ME. 2002. Independent component analysis applied to diffusion tensor MRI. *Magn Reson Med* 47:354-63

Arthurs OJ, Boniface S. 2002. How well do we understand the neural origins of the fMRI BOLD signal? *Trends Neurosci* 25:27-31

Ashburner J, Friston KJ. 1999. Nonlinear spatial normalization using basis functions. *Hum Brain Mapp* 7:254-66

Bach F, Jordan M. 2002. Kernel independent component analysis. *Journal of Machine Learning Research* 3:1-48

Baldeweg T. 2006. Repetition effects to sounds: evidence for predictive coding in the auditory system. *Trends Cogn Sci* 10:93-4

Bandettini PA, Birn RM, Donahue KM. 2000. Functional MRI. Background, Methodology, Limits and Implementation. In *Handbook of Psychophysiology*, ed. JT Cacioppo, LG Tassinary, GG Berntson. Cambridge, UK: Cambridge University Press

Bandettini PA, Jesmanowicz A, Wong EC, Hyde JS. 1993. Processing strategies for time-course data sets in functional MRI of the human brain. *Magn.Res.Med.* 30:161-73

Barry RJ. 1990. The orienting response: stimulus factors and response measures. *Pavlov J Biol Sci* 25:93-9; discussion 9-103

Baudena P, Halgren E, Heit G, Clarke JM. 1995. Intracerebral potentials to rare target and distractor auditory and visual stimuli. III. Frontal cortex. *Electroencephalogr Clin Neurophysiol* 94:251-64

Bell AJ, Sejnowski TJ. 1995. An information-maximization approach to blind separation and blind deconvolution. *Neural Comput* 7:1129-59

Benar CG, Gross DW, Wang Y, Petre V, Pike B, et al. 2002. The BOLD response to interictal epileptiform discharges. *Neuroimage* 17:1182-92

Benar CG, Schon D, Grimault S, Nazarian B, Burle B, et al. 2007. Single-trial analysis of oddball event-related potentials in simultaneous EEG-fMRI. *Hum Brain Mapp*

Benjamini Y, Hochberg Y. 1995. Controlling the false discovery rate: a practical and powerful approach to multiple testing. *Journal of the Royal Statistical Society. Series B. Methodological* 57:289-300

Berger H. 1929. Über das Elektroenkephalogramm des Menschen. *Arch Psychiat Nervenkr* 87:527-70
Biswal B, Yetkin FZ, Haughton VM, Hyde JS. 1995. Functional connectivity in the motor cortex of resting human brain using echo-planar MRI. *Magn Reson Med* 34:537-41
Biswal BB, Ulmer JL. 1999. Blind source separation of multiple signal sources of fMRI data sets using independent component analysis. *J Comput Assist Tomogr* 23:265-71
Bledowski C, Prvulovic D, Hoechstetter K, Scherg M, Wibral M, et al. 2004. Localizing P300 generators in visual target and distractor processing: a combined event-related potential and functional magnetic resonance imaging study. *J Neurosci* 24:9353-60
Bonmassar G, Purdon PL, Jaaskelainen IP, Chiappa K, Solo V, et al. 2002. Motion and ballistocardiogram artifact removal for interleaved recording of EEG and EPs during MRI. *Neuroimage* 16:1127-41
Boynton GM, Engel SA, Glover GH, Heeger DJ. 1996. Linear systems analysis of functional magnetic resonance imaging in human V1. *J Neurosci* 16:4207-21
Brett M. 1999. Thresholding with Random Field Theory: http://imaging.mrc-cbu.cam.ac.uk/imaging/PrinciplesMultipleComparisons.
Brett M, Johnsrude IS, Owen AM. 2002. The problem of functional localization in the human brain. *Nat Rev Neurosci* 3:243-9
Brunia CH. 1999. Neural aspects of anticipatory behavior. *Acta Psychol (Amst)* 101:213-42
Budd TW, Barry RJ, Gordon E, Rennie C, Michie PT. 1998. Decrement of the N1 auditory event-related potential with stimulus repetition: habituation vs. refractoriness. *Int J Psychophysiol* 31:51-68
Buxton RB, Uludag K, Dubowitz DJ, Liu TT. 2004. Modeling the hemodynamic response to brain activation. *Neuroimage* 23 Suppl 1:S220-33
Cabeza R, Nyberg L. 2000. Imaging cognition II: An empirical review of 275 PET and fMRI studies. *J Cogn Neurosci* 12:1-47
Calhoun V, Adali T. 2006. Unmixing fMRI with independent component analysis. *IEEE Engineering in Medicine and Biology Magazine* 25:79-90
Calhoun V, Adali T, Liu J. 2006a. A Feature-Based Approach to Combine Functional MRI, Structural MRI, and EEG Brain Imaging Data. *EMBS*. New York, NY
Calhoun VD, Adali T, Pearlson GD, Kiehl KA. 2006b. Neuronal chronometry of target detection: fusion of hemodynamic and event-related potential data. *Neuroimage* 30:544-53
Cardoso JF, Souloumiac A. 1993. Blind Beamforming for Non Gaussian Signals. *IEE-Proceeding-F* 140:362-70
Caton R. 1875. The electrical currents of the brain. *British Medical Journal* 2:278
Choi S, Cichocki A, Amari SI. 2000. Flexible independent component analysis. *Journal of VLSI Signal Processing* 26:25-38
Clark VP, Fannon S, Lai S, Benson R, Bauer L. 2000. Responses to rare visual target and distractor stimuli using event-related fMRI. *J Neurophysiol* 83:3133-9
Cohen A, Daubechies I, Feauveau J. 1992. Bi-orthogonal bases of compactly supported wavelets. *Comm. Pure Appl. Math* 45:485-560

Coles MG, Rugg MD. 1995. *Electrophysiology of Mind*. Oxford: Oxford University Press

Collins DL. 1994. *3D Model-Based Segmentation of Individual Brain Structures from Magnetic Resonance Imaging*. Mc Gill University

Courchesne E, Hillyard SA, Galambos R. 1975. Stimulus novelty, task relevance and the visual evoked potential in man. *Electroencephalogr Clin Neurophysiol* 39:131-43

Croft RJ, Gonsalvez CJ, Gabriel C, Barry RJ. 2003. Target-to-target interval versus probability effects on P300 in one- and two-tone tasks. *Psychophysiology* 40:322-8

Daunizeau J, Grova C, Marrelec G, Mattout J, Jbabdi S, et al. 2007. Symmetrical event-related EEG/fMRI information fusion in a variational Bayesian framework. *Neuroimage* 36:69-87

Davidson RJ, Jackson DC, Larson CL. 2000. Human Electroencephalography. In *Handbook of Psychophysiology*, ed. JT Cacioppo, LG Tassinary, GG Berntson. Cambridge: Cambridge University Press

Davis H. 1964. Enhancement of Evoked Cortical Potentials in Humans Related to a Task Requiring a Decision. *Science* 145:182-3

Debener S, Makeig S, Delorme A, Engel AK. 2005a. What is novel in the novelty oddball paradigm? Functional significance of the novelty P3 event-related potential as revealed by independent component analysis. *Brain Res Cogn Brain Res* 22:309-21

Debener S, Strobel A, Sorger B, Peters J, Kranczioch C, et al. 2007. Improved quality of auditory event-related potentials recorded simultaneously with 3-T fMRI: removal of the ballistocardiogram artefact. *Neuroimage* 34:587-97

Debener S, Ullsperger M, Siegel M, Engel AK. 2006. Single-trial EEG-fMRI reveals the dynamics of cognitive function. *Trends Cogn Sci* 10:558-63

Debener S, Ullsperger M, Siegel M, Fiehler K, von Cramon DY, Engel AK. 2005b. Trial-by-trial coupling of concurrent electroencephalogram and functional magnetic resonance imaging identifies the dynamics of performance monitoring. *J Neurosci* 25:11730-7

Delorme A, Makeig S. 2004. EEGLAB: an open source toolbox for analysis of single-trial EEG dynamics including independent component analysis. *J Neurosci Methods* 134:9-21

Donchin E. 1981. Presidential address, 1980. Surprise!...Surprise? *Psychophysiology* 18:493-513

Donchin E, Coles MGH. 1988. Is the P300 component a manifestation of context updating? *Behavioral and Brain Sciences* 11:357-74

Downar J, Crawley AP, Mikulis DJ, Davis KD. 2000. A multimodal cortical network for the detection of changes in the sensory environment. *Nat Neurosci* 3:277-83

Duncan-Johnson CC, Donchin E. 1977. On quantifying surprise: the variation of event-related potentials with subjective probability. *Psychophysiology* 14:456-67

Eichele T, Calhoun V, Moosmann M, Specht K, Jongsma M, et al. 2007. Unmixing concurrent EEG-fMRI with parallel independent component analysis. *Int J Psychophysiol*

Eichele T, Moosmann M, Calhoun VD, Specht K, Nordby H, Hugdahl K. 2006. Joint ICA of simultaneous single trial ERP-fMRI. *Neuroimage* 32 Suppl 1:S92

Eichele T, Specht K, Moosmann M, Jongsma ML, Quiroga RQ, et al. 2005. Assessing the spatiotemporal evolution of neuronal activation with single-trial event-related potentials and functional MRI. *Proc Natl Acad Sci U S A* 102:17798-803

Eimer M, Goschke T, Schlaghecken F, Sturmer B. 1996. Explicit and implicit learning of event sequences: evidence from event-related brain potentials. *J Exp Psychol Learn Mem Cogn* 22:970-87

Engel AK, Fries P, Singer W. 2001. Dynamic predictions: oscillations and synchrony in top-down processing. *Nat Rev Neurosci* 2:704-16

Fabiani M, Gratton G, Coles MG. 2000. Event-Related Brain Potentials. In *Handbook of Psychophysiology*, ed. JT Cacioppo, LG Tassinary, GG Berntson. Cambridge, UK: Cambridge University Press

Feige B, Scheffler K, Esposito F, Di Salle F, Hennig J, Seifritz E. 2005. Cortical and subcortical correlates of electroencephalographic alpha rhythm modulation. *J Neurophysiol* 93:2864-72

Ford JM, White P, Lim KO, Pfefferbaum A. 1994. Schizophrenics have fewer and smaller P300s: a single-trial analysis. *Biol Psychiatry* 35:96-103

Forkstam C, Petersson KM. 2005. Towards an explicit account of implicit learning. *Curr Opin Neurol* 18:435-41

Fox MD, Snyder AZ, Vincent JL, Corbetta M, Van Essen DC, Raichle ME. 2005. The human brain is intrinsically organized into dynamic, anticorrelated functional networks. *Proc Natl Acad Sci U S A* 102:9673-8

Fox MD, Snyder AZ, Zacks JM, Raichle ME. 2006. Coherent spontaneous activity accounts for trial-to-trial variability in human evoked brain responses. *Nat Neurosci* 9:23-5

Frahm J, Bruhn H, Merboldt KD, Hanicke W. 1992. Dynamic MR imaging of human brain oxygenation during rest and photic stimulation. *J Magn Reson Imaging* 2:501-5

Freeman WJ. 2000. A proposed name for aperiodic brain activity: stochastic chaos. *Neural Netw* 13:11-3

Friedman D, Cycowicz YM, Gaeta H. 2001. The novelty P3: an event-related brain potential (ERP) sign of the brain's evaluation of novelty. *Neurosci Biobehav Rev* 25:355-73

Fries P, Neuenschwander S, Engel AK, Goebel R, Singer W. 2001. Rapid feature selective neuronal synchronization through correlated latency shifting. *Nat Neurosci* 4:194-200

Friston K. 2003. Learning and inference in the brain. *Neural Netw* 16:1325-52

Friston K. 2005a. A theory of cortical responses. *Philos Trans R Soc Lond B Biol Sci* 360:815-36

Friston KJ. 2005b. Models of brain function in neuroimaging. *Annu Rev Psychol* 56:57-87

Friston KJ, Holmes AP, Poline JB, Grasby PJ, Williams SC, et al. 1995. Analysis of fMRI time-series revisited. *Neuroimage* 2:45-53

Friston KJ, Worsley KJ, Frackowiak RS, Mazziotta JC, Evans AC. 1994. Assessing the significance of focal activations using their spatial extent. *Human Brain Mapping* 1:210-20

Gaillard AW. 1988. Problems and paradigms in ERP research. *Biol Psychol* 26:91-109
Gehring WJ, Gratton G, Coles MG, Donchin E. 1992. Probability effects on stimulus evaluation and response processes. *J Exp Psychol Hum Percept Perform* 18:198-216
Gläscher J, Büchel C. 2005. Formal learning theory dissociates brain regions with different temporal integration. *Neuron* 47:295-306
Goldman RI, Stern JM, Engel J, Jr., Cohen MS. 2002. Simultaneous EEG and fMRI of the alpha rhythm. *Neuroreport* 13:2487-92
Goncalves SI, de Munck JC, Pouwels PJ, Schoonhoven R, Kuijer JP, et al. 2006. Correlating the alpha rhythm to BOLD using simultaneous EEG/fMRI: inter-subject variability. *Neuroimage* 30:203-13
Gonsalvez CL, Polich J. 2002. P300 amplitude is determined by target-to-target interval. *Psychophysiology* 39:388-96
Gotman J, Benar CG, Dubeau F. 2004. Combining EEG and FMRI in epilepsy: methodological challenges and clinical results. *J Clin Neurophysiol* 21:229-40
Gratton G. 2000. Biosignal Processing. In *Handbook of Psychophysiology*, ed. JT Cacioppo, LG Tassinary, GG Berntson. Cambridge: Cambridge University Press
Gray CM, Konig P, Engel AK, Singer W. 1989. Oscillatory responses in cat visual cortex exhibit inter-columnar synchronization which reflects global stimulus properties. *Nature* 338:334-7
Greicius MD, Krasnow B, Reiss AL, Menon V. 2003. Functional connectivity in the resting brain: a network analysis of the default mode hypothesis. *Proc Natl Acad Sci U S A* 100:253-8
Haenschel C, Vernon DJ, Dwivedi P, Gruzelier JH, Baldeweg T. 2005. Event-related brain potential correlates of human auditory sensory memory-trace formation. *J Neurosci* 25:10494-501
Haider M, Spong P, Lindsley DB. 1964. Attention, Vigilance, and Cortical Evoked-Potentials in Humans. *Science* 145:180-2
Halgren E, Baudena P, Clarke JM, Heit G, Liegeois C, et al. 1995a. Intracerebral potentials to rare target and distractor auditory and visual stimuli. I. Superior temporal plane and parietal lobe. *Electroencephalogr Clin Neurophysiol* 94:191-220
Halgren E, Baudena P, Clarke JM, Heit G, Marinkovic K, et al. 1995b. Intracerebral potentials to rare target and distractor auditory and visual stimuli. II. Medial, lateral and posterior temporal lobe. *Electroencephalogr Clin Neurophysiol* 94:229-50
Halgren E, Marinkovic K. 1995. General principles for the physiology of cognition as suggested by intracranial ERPs. In *Recent Advances in Event-Related Brain Potential Research*, ed. C Ogura, Y Koga, M Shimokochi, pp. 1072-84. Amsterdam: Elsevier
Halgren E, Marinkovic K, Chauvel P. 1998. Generators of the late cognitive potentials in auditory and visual oddball tasks. *Electroencephalogr Clin Neurophysiol* 106:156-64
Handy TC. 2005. *Event-Related Potentials. A Methods Handbook*. Cambridge, MA: The MIT Press
Heeger DJ, Ress D. 2002. What does fMRI tell us about neuronal activity? *Nat Rev Neurosci* 3:142-51

Hillyard SA, Hink RF, Schwent VL, Picton TW. 1973. Electrical signs of selective attention in the human brain. *Science* 182:177-80

Hinterberger T, Veit R, Wilhelm B, Weiskopf N, Vatine JJ, Birbaumer N. 2005. Neuronal mechanisms underlying control of a brain-computer interface. *Eur J Neurosci* 21:3169-81

Hohnsbein J, Falkenstein M, Hoormann J. 1998. Performance differences in reaction tasks are reflected in event-related brain potentials (ERPs). *Ergonomics* 41:622-33

Hong B, Pearlson GD, Calhoun VD. 2005. Source density-driven independent component analysis approach for fMRI data. *Hum Brain Mapp* 25:297-307

Hopfinger JB, Khoe W, Song AW. 2005. Combining Electrophysiology with Structural and Functional Neuroimaging: ERPs, PET, MRI, and fMRI. In *Event Related Potentials. A Methods Handbook.*, ed. TC Handy, pp. 345-80. Cambridge: The MIT Press

Horovitz SG, Skudlarski P, Gore JC. 2002. Correlations and dissociations between BOLD signal and P300 amplitude in an auditory oddball task: a parametric approach to combining fMRI and ERP. *Magn Reson Imaging* 20:319-25

Horwitz B, Poeppel D. 2002. How can EEG/MEG and fMRI/PET data be combined? *Hum Brain Mapp* 17:1-3

Huettel SA, Mack PB, McCarthy G. 2002. Perceiving patterns in random series: dynamic processing of sequence in prefrontal cortex. *Nat Neurosci* 5:485-90

Huettel SA, Song AW, McCarthy G. 2004. *Functional Magnetic Resonance Imaging*. Sunderland, MA: Sinauer

Hugdahl K. 1995. *Psychophysiology. The Mind-Body Perspective*. Cambridge, MA: Harvard University Press

Hughes HC, Darcey TM, Barkan HI, Williamson PD, Roberts DW, Aslin CH. 2001. Responses of human auditory association cortex to the omission of an expected acoustic event. *Neuroimage* 13:1073-89

Hyvarinen A, Oja E. 1997. A fast fixed-point algorithm for independent component analysis. *Neural Comput.* 9:1483-92

Hyvarinen A, Oja E. 2000. Independent component analysis: algorithms and applications. *Neural Netw* 13:411-30

Ives JR, Warach S, Schmitt F, Edelman RR, Schomer DL. 1993. Monitoring the patient's EEG during echo planar MRI. *Electroencephalogr Clin Neurophysiol* 87:417-20

Jaaskelainen IP, Ahveninen J, Bonmassar G, Dale AM, Ilmoniemi RJ, et al. 2004. Human posterior auditory cortex gates novel sounds to consciousness. *Proc Natl Acad Sci U S A* 101:6809-14

Janata P, Grafton ST. 2003. Swinging in the brain: shared neural substrates for behaviors related to sequencing and music. *Nat Neurosci* 6:682-7

Jennings JR, Stine LA. 2000. Salient Method, Design, and Analysis Concerns. In *Handbook of Psychophysiology*, ed. JT Cacioppo, LG Tassinary, GG Berntson. Cambridge, UK: Cambridge University Press

Jentzsch I, Sommer W. 2001. Sequence-sensitive subcomponents of P300: topographical analyses and dipole source localization. *Psychophysiology* 38:607-21

Jongsma M, Eichele T, Coenen, AML, Hugdahl K, Nordby H, et al. 2004. The Auditory evoked P3 and the omission evoked potential decrease with predictability: a single-trial analyses with wavelet denoising reveals individual learning curves. *Evoked Potentials International Conference XIV*, p. 190. Leipzig

Jongsma ML, Eichele T, Quian Quiroga R, Jenks KM, Desain P, et al. 2005. Expectancy effects on omission evoked potentials in musicians and non-musicians. *Psychophysiology* 42:191-201

Jongsma ML, Eichele T, Van Rijn CM, Coenen AM, Hugdahl K, et al. 2006. Tracking pattern learning with single-trial event-related potentials. *Clin Neurophysiol* 117:1957-73

Jung TP, Makeig S, Westerfield M, Townsend J, Courchesne E, Sejnowski TJ. 2001. Analysis and visualization of single-trial event-related potentials. *Hum Brain Mapp* 14:166-85

Kandel ER, Schwartz JH, Jessell TM. 2000. *Principles of neural science*. New York: McGraw-Hill Publishing Co

Kiebel SJ, Friston KJ. 2004a. Statistical parametric mapping for event-related potentials (II): a hierarchical temporal model. *Neuroimage* 22:503-20

Kiebel SJ, Friston KJ. 2004b. Statistical parametric mapping for event-related potentials: I. Generic considerations. *Neuroimage* 22:492-502

Kiehl KA, Laurens KR, Duty TL, Forster BB, Liddle PF. 2001. Neural sources involved in auditory target detection and novelty processing: an event-related fMRI study. *Psychophysiology* 38:133-42

Kiehl KA, Stevens MC, Laurens KR, Pearlson G, Calhoun VD, Liddle PF. 2005. An adaptive reflexive processing model of neurocognitive function: supporting evidence from a large scale (n = 100) fMRI study of an auditory oddball task. *Neuroimage* 25:899-915

Kilner JM, Salenius S, Baker SN, Jackson A, Hari R, Lemon RN. 2003. Task-dependent modulations of cortical oscillatory activity in human subjects during a bimanual precision grip task. *Neuroimage* 18:67-73

Kirino E, Belger A, Goldman-Rakic P, McCarthy G. 2000. Prefrontal activation evoked by infrequent target and novel stimuli in a visual target detection task: an event-related functional magnetic resonance imaging study. *J Neurosci* 20:6612-8

Knight R. 1996. Contribution of human hippocampal region to novelty detection. *Nature* 383:256-9

Kotchoubey B. 2006. Event-related potentials, cognition, and behavior: a biological approach. *Neurosci Biobehav Rev* 30:42-65

Krakow K, Allen PJ, Lemieux L, Symms MR, Fish DR. 2000. Methodology: EEG-correlated fMRI. *Adv Neurol* 83:187-201

Krakow K, Woermann FG, Symms MR, Allen PJ, Lemieux L, et al. 1999. EEG-triggered functional MRI of interictal epileptiform activity in patients with partial seizures. *Brain* 122:1679-88

Kwong KK, Belliveau JW, Chesler DA, Goldberg IE, Weisskoff RM, et al. 1992. Dynamic magnetic resonance imaging of human brain activity during primary sensory stimulation. *Proc Natl Acad Sci U S A* 89:5675-9

Laufs H, Kleinschmidt A, Beyerle A, Eger E, Salek-Haddadi A, et al. 2003a. EEG-correlated fMRI of human alpha activity. *Neuroimage* 19:1463-76

Laufs H, Krakow K, Sterzer P, Eger E, Beyerle A, et al. 2003b. Electroencephalographic signatures of attentional and cognitive default

modes in spontaneous brain activity fluctuations at rest. *Proc Natl Acad Sci U S A* 100:11053-8
Lauritzen M, Gold L. 2003. Brain function and neurophysiological correlates of signals used in functional neuroimaging. *J Neurosci* 23:3972-80
Lazeyras F, Zimine I, Blanke O, Perrig SH, Seeck M. 2001. Functional MRI with simultaneous EEG recording: feasibility and application to motor and visual activation. *J Magn Reson Imaging* 13:943-8
Lee T, Girolami M, Sejnowski T. 1999. Independent Component Analysis Using an Extended Infomax Algorithm for Mixed Subgaussian and Supergaussian Sources. *Neural Comput* 11:417-41
Lemieux L, Allen PJ, Franconi F, Symms MR, Fish DR. 1997. Recording of EEG during fMRI experiments: patient safety. *Magn Reson Med* 38:943-52
Liebenthal E, Ellingson ML, Spanaki MV, Prieto TE, Ropella KM, Binder JR. 2003. Simultaneous ERP and fMRI of the auditory cortex in a passive oddball paradigm. *Neuroimage* 19:1395-404
Linden DE, Prvulovic D, Formisano E, Vollinger M, Zanella FE, et al. 1999. The functional neuroanatomy of target detection: an fMRI study of visual and auditory oddball tasks. *Cereb Cortex* 9:815-23
Llinas RR. 2001. *i of the vortex: from neurons to self*. Cambridge: The MIT Press
Logothetis NK. 2003. The underpinnings of the BOLD functional magnetic resonance imaging signal. *J Neurosci* 23:3963-71
Logothetis NK, Pauls J, Augath M, Trinath T, Oeltermann A. 2001. Neurophysiological investigation of the basis of the fMRI signal. *Nature* 412:150-7
Logothetis NK, Pfeuffer J. 2004. On the nature of the BOLD fMRI contrast mechanism. *Magn Reson Imaging* 22:1517-31
Loveless N. 1983. The Orienting Response and Evoked Potentials in Man. In *Orienting and Habituation: Perspectives in Human Research*, ed. D Siddle, pp. 71-108. Chichester: Wiley
Luck SJ. 2005. *An Introduction to the Event-Related Potential Technique*. Cambridge, MA: The MIT Press
Makeig S, Debener S, Onton J, Delorme A. 2004a. Mining event-related brain dynamics. *Trends Cogn Sci* 8:204-10
Makeig S, Delorme A, Westerfield M, Jung TP, Townsend J, et al. 2004b. Electroencephalographic brain dynamics following manually responded visual targets. *PLoS Biol* 2:e176
Makeig S, Jung TP, Bell AJ, Ghahremani D, Sejnowski TJ. 1997. Blind separation of auditory event-related brain responses into independent components. *Proc Natl Acad Sci U S A* 94:10979-84
Makeig S, Jung, T-P-, Sejnowski, TJ. 2002. Having your voxels and timing them too? In *Exploratory Analysis and Data Modeling in Functional Neuroimaging*, ed. F Sommer, Wichert, A. Cambridge: The MIT Press
Mallat S. 1989. A theory for multiresolution signal decomposition: the wavelet representation. . *IEEE Trans. Pattern Analysis and Machine Intell.* 2:674-93
Martinez-Montes E, Valdes-Sosa PA, Miwakeichi F, Goldman RI, Cohen MS. 2004. Concurrent EEG/fMRI analysis by multiway Partial Least Squares. *Neuroimage* 22:1023-34

McGee TJ, King C, Tremblay K, Nicol TG, Cunningham J, Kraus N. 2001. Long-term habituation of the speech-elicited mismatch negativity. *Psychophysiology* 38:653-8

McGonigle DJ, Howseman AM, Athwal BS, Friston KJ, Frackowiak RS, Holmes AP. 2000. Variability in fMRI: an examination of intersession differences. *Neuroimage* 11:708-34

McKeown MJ, Hansen LK, Sejnowski TJ. 2003. Independent component analysis of functional MRI: what is signal and what is noise? *Curr Opin Neurobiol* 13:620-9

McKeown MJ, Makeig S, Brown GG, Jung TP, Kindermann SS, et al. 1998. Analysis of fMRI data by blind separation into independent spatial components. *Hum Brain Mapp* 6:160-88

McKeown MJ, Sejnowski TJ. 1998. Independent component analysis of fMRI data: examining the assumptions. *Hum Brain Mapp* 6:368-72

Mima T, Matsuoka T, Hallett M. 2001. Information flow from the sensorimotor cortex to muscle in humans. *Clin Neurophysiol* 112:122-6

Molholm S, Martinez A, Ritter W, Javitt DC, Foxe JJ. 2005. The neural circuitry of pre-attentive auditory change-detection: an fMRI study of pitch and duration mismatch negativity generators. *Cereb Cortex* 15:545-51

Moosmann M, Eichele T, Nordby H, Hugdahl K, Calhoun V. 2007. Joint independent component analysis for simultaneous EEG-fMRI: Principle and Simulation. *Int J Psychophysiol*

Moosmann M, Ritter P, Krastel I, Brink A, Thees S, et al. 2003. Correlates of alpha rhythm in functional magnetic resonance imaging and near infrared spectroscopy. *Neuroimage* 20:145-58

Mukamel R, Gelbard H, Arieli A, Hasson U, Fried I, Malach R. 2005. Coupling between neuronal firing, field potentials, and FMRI in human auditory cortex. *Science* 309:951-4

Muller BW, Juptner M, Jentzen W, Muller SP. 2002. Cortical activation to auditory mismatch elicited by frequency deviant and complex novel sounds: a PET study. *Neuroimage* 17:231-9

Mustovic H, Scheffler K, Di Salle F, Esposito F, Neuhoff JG, et al. 2003. Temporal integration of sequential auditory events: silent period in sound pattern activates human planum temporale. *Neuroimage* 20:429-34

Näätänen R. 1992. *Attention and Brain Function*. Hillsdale: Lawrence Erlbaum Associates. 494 pp.

Näätänen R, Gaillard AW. 1983. The orienting reflex and the N2 deflection of the ERP. In *Tutorials in Event Related Potentials Research: Endogenous Components*, ed. AW Gaillard, W Ritter, pp. 119-41. Amsterdam, North Holland: Elsevier

Näätänen R, Gaillard AW, Mantysalo S. 1978. Early selective-attention effect on evoked potential reinterpreted. *Acta Psychol* 42:313-29

Näätänen R, Jacobsen T, Winkler I. 2005. Memory-based or afferent processes in mismatch negativity (MMN): a review of the evidence. *Psychophysiology* 42:25-32

Näätänen R, Picton T. 1987. The N1 wave of the human electric and magnetic response to sound: a review and an analysis of the component structure. *Psychophysiology* 24:375-425

Näätänen R, Rinne T. 2002. Electric brain response to sound repetition in humans: an index of long-term-memory - trace formation? *Neurosci Lett* 318:49-51
Näätänen R, Simpson M, Loveless NE. 1982. Stimulus deviance and evoked potentials. *Biol Psychol* 14:53-98
Näätänen R, Tervaniemi M, Sussman E, Paavilainen P, Winkler I. 2001. "Primitive intelligence" in the auditory cortex. *Trends Neurosci* 24:283-8
Näätänen R, Winkler I. 1999. The concept of auditory stimulus representation in cognitive neuroscience. *Psychol Bull* 125:826-59
Nagai Y, Critchley HD, Featherstone E, Fenwick PB, Trimble MR, Dolan RJ. 2004. Brain activity relating to the contingent negative variation: an fMRI investigation. *Neuroimage* 21:1232-41
Niazy RK, Beckmann CF, Iannetti GD, Brady JM, Smith SM. 2005. Removal of FMRI environment artifacts from EEG data using optimal basis sets. *Neuroimage* 28:720-37
Nobre AC. 2001. Orienting attention to instants in time. *Neuropsychologia* 39:1317-28
Nobre AC, O'Reilly J. 2004. Time is of the essence. *Trends Cogn Sci* 8:387-9
Nordby H, Roth WT, Pfefferbaum A. 1988a. Event-related potentials to breaks in sequences of alternating pitches or interstimulus intervals. *Psychophysiology* 25:262-8
Nordby H, Roth WT, Pfefferbaum A. 1988b. Event-related potentials to time-deviant and pitch-deviant tones. *Psychophysiology* 25:249-61
Nunez PL. 2000. Toward a quantitative description of large-scale dynamic neocortical dynamic function and EEG. *Behavioral and Brain Sciences* 23:371-437
Nunez PL, Srinivasan R. 2006. *Electric Fields of the Brain. The Neurophysics of EEG*. New York: Oxford University Press
Ogawa S, Tank DW, Menon RS, Ellermann JM, Kim SG, et al. 1992. Intrinsic signal changes accompanying sensory stimulation: functional brain mapping with magnetic resonance imaging. *Proc Natl Acad Sci USA* 89:5951-5
Onton J, Westerfield M, Townsend J, Makeig S. 2006. Imaging human EEG dynamics using independent component analysis. *Neurosci Biobehav Rev* 30:808-22
Opitz B, Mecklinger A, Von Cramon DY, Kruggel F. 1999. Combining electrophysiological and hemodynamic measures of the auditory oddball. *Psychophysiology* 36:142-7
Paavilainen P, Simola J, Jaramillo M, Näätänen R, Winkler I. 2001. Preattentive extraction of abstract feature conjunctions from auditory stimulation as reflected by the mismatch negativity (MMN). *Psychophysiology* 38:359-65
Perneger TV. 1998. What's wrong with Bonferroni adjustments. *BMJ* 316:1236-8
Picton TW. 1992. The P300 wave of the human event-related potential. *J Clin Neurophysiol* 9:456-79
Picton TW, Alain C, Otten L, Ritter W, Achim A. 2000a. Mismatch negativity: different water in the same river. *Audiol Neurootol* 5:111-39
Picton TW, Alain C, Woods DL, John MS, Scherg M, et al. 1999. Intracerebral sources of human auditory-evoked potentials. *Audiol Neurootol* 4:64-79

Picton TW, Bentin S, Berg P, Donchin E, Hillyard SA, et al. 2000b. Guidelines for using human event-related potentials to study cognition: recording standards and publication criteria. *Psychophysiology* 37:127-52
Polich J. 2003. *Detection of Change: Event-Related Potential and fMRI findings*. Norwell, MA: Kluwer Academic Publishers
Purves D, Augustine GJ, Fitzpatrick D, Katz LC, LaMantia A-S, et al. 2001. *Neuroscience*. Sunderland: Sinauer
Quian Quiroga R, Garcia H. 2003. Single-trial event-related potentials with wavelet denoising. *Clin Neurophysiol* 114:376-90
Raichle ME. 2006. Neuroscience. The brain's dark energy. *Science* 314:1249-50
Raichle ME, MacLeod AM, Snyder AZ, Powers WJ, Gusnard DA, Shulman GL. 2001. A default mode of brain function. *Proc Natl Acad Sci U S A* 98:676-82
Reber PJ. 1967. Implicit learning of artificial grammars. *J. Verbal Learn. Verbal Behav.*:855-63
Rescorla RA, Wagner AR. 1972. A Theory of Pavlovian Conditioning: Variations in the Effectiveness of Reinforcement and Nonreinforcement. In *Classical Conditioning II*, ed. AH Black, WF Prokasy. New York: Appleton-Century-Crofts
Rinne T, Degerman A, Alho K. 2005. Superior temporal and inferior frontal cortices are activated by infrequent sound duration decrements: an fMRI study. *Neuroimage* 26:66-72
Ritter W, Paavilainen P, Lavikainen J, Reinikainen K, Alho K, et al. 1992. Event-related potentials to repetition and change of auditory stimuli. *Electroencephalogr Clin Neurophysiol* 83:306-21
Rodriguez E, George N, Lachaux JP, Martinerie J, Renault B, Varela FJ. 1999. Perception's shadow: long-distance synchronization of human brain activity. *Nature* 397:430-3
Rose M, Verleger R, Wascher E. 2001. ERP correlates of associative learning. *Psychophysiology* 38:440-50
Roth WT. 1983. A comparison of P300 and skin conductance response. In *Tutorials in Event Related Potential Research: Endogenous Components*, ed. AW Gaillard, W Ritter, pp. 177-99. Amsterdam, North Holland: Elsevier
Ruchkin DS, Sutton S. 1978. Emmitted P300 potentials and temporal uncertainty. *Electroencephalogr Clin Neurophysiol* 45:268-77
Ruchkin DS, Sutton S, Tueting P. 1975. Emitted and evoked P300 potentials and variation in stimulus probability. *Psychophysiology* 12:591-5
Sabri M, Liebenthal E, Waldron EJ, Medler DA, Binder JR. 2006. Attentional modulation in the detection of irrelevant deviance: a simultaneous ERP/fMRI study. *J Cogn Neurosci* 18:689-700
Salek-Haddadi A, Friston KJ, Lemieux L, Fish DR. 2003. Studying spontaneous EEG activity with fMRI. *Brain Res Brain Res Rev* 43:110-33
Sambeth A, Maes JH, Quian Quiroga R, Van Rijn CM, Coenen AM. 2004. Enhanced re-habituation of the orienting response of the human event-related potential. *Neurosci Lett* 356:103-6
Scarff CJ, Reynolds A, Goodyear BG, Ponton CW, Dort JC, Eggermont JJ. 2004. Simultaneous 3-T fMRI and high-density recording of human auditory evoked potentials. *Neuroimage* 23:1129-42
Scheffe H. 1959. *The Analysis of Variance*. New York: Wiley

Schoffelen JM, Oostenveld R, Fries P. 2005. Neuronal coherence as a mechanism of effective corticospinal interaction. *Science* 308:111-3
Schroger E. 1997. On the detection of auditory deviations: a pre-attentive activation model. *Psychophysiology* 34:245-57
Seger CA. 1994. Implicit learning. *Psychol Bull* 115:163-96
Sokolov EN. 1963. *Perception and the Conditioned Reflex*. Oxford: Pergamon Press
Sokolov EN, Vinogradova OS. 1976. *Neuronal Mechansims of the Orienting Reflex*. Hillsdale, NJ: Lawrence Erlbaum Associates
Sonuga-Barke EJ, Castellanos FX. 2007. Spontaneous attentional fluctuations in impaired states and pathological conditions: A neurobiological hypothesis. *Neurosci Biobehav Rev*
Spencer KM. 2005. Averaging, Detection, and Classification of single-trial ERPs. In *Event Related Potentials. A Methods Handbook*, ed. TC Handy, pp. 209-28. Cambridge: The MIT Press
Squires KC, Wickens C, Squires NK, Donchin E. 1976. The effect of stimulus sequence on the waveform of the cortical event-related potential. *Science* 193:1142-6
Squires NK, Squires KC, Hillyard SA. 1975. Two varieties of long-latency positive waves evoked by unpredictable auditory stimuli in man. *Electroencephalogr Clin Neurophysiol* 38:387-401
Stone JV. 2002. Independent component analysis: an introduction. *Trends Cogn Sci* 6:59-64
Sussman E, Ritter W, Vaughan HG, Jr. 1998. Predictability of stimulus deviance and the mismatch negativity. *Neuroreport* 9:4167-70
Sussman E, Sheridan K, Kreuzer J, Winkler I. 2003. Representation of the standard: stimulus context effects on the process generating the mismatch negativity component of event-related brain potentials. *Psychophysiology* 40:465-71
Sutton S, Braren M, Zubin J, John ER. 1965. Evoked-potential correlates of stimulus uncertainty. *Science* 150:1187-8
Sutton S, Tueting P, Zubin J, John ER. 1967. Information delivery and the sensory evoked potential. *Science* 155:1436-9
Tallon-Baudry C, Bertrand O, Delpuech C, Pernier J. 1996. Stimulus specificity of phase-locked and non-phase-locked 40 Hz visual responses in human. *J Neurosci* 16:4240-9
Tanaka E, Iinuma TA. 1975. Correction functions for optimizing the reconstructed image in transverse section scan. *Phys Med Biol* 20:789-98
Tao JX, Baldwin M, Hawes-Ebersole S, Ebersole JS. 2007. Cortical substrates of scalp EEG epileptiform discharges. *J Clin Neurophysiol* 24:96-100
Tueting P, Sutton S, Zubin J. 1970. Quantitative evoked potential correlates of the probability of events. *Psychophysiology* 7:385-94
Ulanovsky N, Las L, Farkas D, Nelken I. 2004. Multiple time scales of adaptation in auditory cortex neurons. *J Neurosci* 24:10440-53
Ulanovsky N, Las L, Nelken I. 2003. Processing of low-probability sounds by cortical neurons. *Nat Neurosci* 6:391-8
Varela F, Lachaux JP, Rodriguez E, Martinerie J. 2001. The brainweb: phase synchronization and large-scale integration. *Nat Rev Neurosci* 2:229-39

Verleger R. 1988. Event–related potentials and cognition: A critique of the context updating hypothesis and an alternative interpretation of P3. *Behavioural and Brain Sciences* 11:343–56

Villringer A, Dirnagl U. 1995. Coupling of brain activity and cerebral blood flow: basis of functional neuroimaging. *Cerebrovasc Brain Metab Rev* 7:240-76

Vlassis N, Motomura Y. 2001. Efficient source adaptivity in independent in independent component analysis. *IEEE Trans.Neural Networks* 12:559-66

Walter WG, Cooper R, Aldridge VJ, McCallum WC, Winter AL. 1964. Contingent Negative Variation: an Electric Sign of Sensorimotor Association and Expectancy in the Human Brain. *Nature* 203:380-4

Warach S, Ives JR, Schlaug G, Patel MR, Darby DG, et al. 1996. EEG-triggered echo-planar functional MRI in epilepsy. *Neurology* 47:89-93

Winkler I, Schroger E, Cowan N. 2001. The role of large-scale memory organization in the mismatch negativity event-related brain potential. *J Cogn Neurosci* 13:59-71

Woods DL. 1995. The component structure of the N1 wave of the human auditory evoked potential. *Electroencephalogr Clin Neurophysiol Suppl* 44:102-9

Woods DL, Elmasian R. 1986. The habituation of event-related potentials to speech sounds and tones. *Electroencephalogr Clin Neurophysiol* 65:447-59

Worsley KJ, Friston KJ. 1995. Analysis of fMRI time-series revisited--again. *NeuroImage* 2:173-81

Worsley KJ, Marrett S, Neelin P, Vandal AC, Friston KJ, Evans AC. 1996. A unified statistical approach for determining significant signals in images of cerebral activation. *Human Brain Mapping* 4:58-73

ABBREVIATIONS

AP – Action Potential

BOLD – Blood Oxygenation Level Dependent Response

BSS – Blind Source Separation

CNV – Contingent Negative Variation

EEG – Electroencephalography

EPI – Echo Planar Imaging

ERP – Event Related Potential

FMRI – Functional Magnetic Resonance Imaging

FWHM – Full Width at Half Maximum

GLM – General Linear Model

HRF – Hemodynamic Response Function

ICA – Independent Component Analysis

LFP – Local Field Potential

MUA – Multi Unit Activity

OEP – Omission Evoked Potential

OR – Orienting Response

PCA – Principal Component Analysis

PSP – Post-Synaptic Potential

RW – Rescorla-Wagner Model

SPM – Statistical Parametric Mapping

TTI – Target to Target Interval

WT – Wavelet Transform

Paper I

Jongsma ML, Eichele T, Van Rijn CM, Coenen AM, Hugdahl K, Nordby H, Quiroga RQ. (2006) Tracking pattern learning with single-trial event-related potentials. *Clinical Neurophysiology*. 117(9):1957-73.

ELSEVIER

Clinical Neurophysiology 117 (2006) 1957–1973

www.elsevier.com/locate/clinph

Tracking pattern learning with single-trial event-related potentials

Marijtje L.A. Jongsma [a,*], Tom Eichele [b], Clementina M. Van Rijn [a], Anton M.L. Coenen [a], Kenneth Hugdahl [b,d], Helge Nordby [b], Rodrigo Quian Quiroga [c]

[a] *NICI – Department of Biological Psychology, Radboud University, Nijmegen, The Netherlands*
[b] *Department of Biological and Medical Psychology, Division of Cognitive Neuroscience, University of Bergen, Norway*
[c] *Department of Engineering, University of Leicester, Leicester, UK*
[d] *Division of Psychiatry, Haukeland University Hospital, University of Bergen, Norway*

Accepted 21 May 2006
Available online 18 July 2006

Abstract

Objective: The main aim was to track the dynamics of pattern-learning using single-trial event-related potentials (ERPs). A new 'learning-oddball' paradigm was employed presenting eight random targets (the 'no-pattern') followed by eight regular targets (the 'pattern'). In total, six repetitions of the 'no-pattern' followed by the 'pattern' were presented.
Methods: We traced the dynamics of learning by measuring responses to 16 (eight random–eight regular) targets. Since this alternation of the 'no-pattern' followed by the 'pattern' was repeated six times, we extracted single-trial responses to all 96 targets to determine if learning occurred more rapidly with each repetition of the 'pattern.'
Results: Following random targets, ERPs contained a marked P3–N2 component that decreased to regular targets, whereas a contingent negative variation (CNV) appeared. ERP changes could be best described by sigmoid 'learning' curves. Single-trial analyses showed that learning occurred more rapidly over repetitions and suggested that the CNV developed prior to the decay of the N2-P3 component.
Conclusions: We show a new paradigm-analysis methodology to track learning processes directly from brain signals.
Significance: Single-trial ERPs analyses open a wide range of applications. Tracking the dynamic structure of cognitive functions may prove crucial in the understanding of learning and in the study of different pathologies.

Keywords: Learning; P3; N2; CNV; Single-trial; Wavelet analyses; Auditory ERPs; Oddball; Omitted stimuli

1. Introduction

1.1. Studies on pattern learning

Extracting patterns from the environment is central to human cognition. By identifying patterns, individuals are able to form predictions about upcoming events, helping them to function more efficiently within their environment (Friston, 2005; Huettel et al., 2002; Llinas, 2001). Behavioral research has revealed that recognition of patterns in event sequences occurs for the most part automatically and seems to rely on memory formation (Reber, 1967, 1989; Seger, 1994). When a sequence follows a repeating pattern, performance typically improves (i.e., becomes more efficient) (Eimer et al., 1996; Honda et al., 1998; Jentzsch and Sommer, 2001; Rüsseler et al., 2003; Salamon, 2002; Seger, 1994), often without conscious awareness (Honda et al., 1998; Reber, 1967, 1989; Schendan et al., 2003; Schlaghecken et al., 2000; Seger, 1994). This suggests that people acquire knowledge about patterns incidentally. Pattern learning is most often observed through changes in reaction times of overt motor responses (Reber, 1967, 1989; Seger, 1994). However, an important issue raised in incidental learning literature is the separate roles played by motor and perceptual processes (Eimer et al., 1996;

* Corresponding author. Tel.: +31 24 3616278; fax: +31 24 3616066.
E-mail address: jongsma@nici.ru.nl (M.L.A. Jongsma).

1388-2457/$32.00
doi:10.1016/j.clinph.2006.05.012

Rüsseler et al., 2003). It is therefore preferable to employ a measure that allows to study pattern learning directly from neural responses, independent of motoric aspects that can hamper the interpretation of observed changes.

1.2. ERPs and pattern learning

Event-related potentials (ERPs) are time-locked voltage fluctuations in the EEG, resulting from neuronal responses to sensory, motor or cognitive events (Rugg and Coles, 1995). One of the major advantages of employing ERP measurements is that aspects of information processing can be instantaneously measured, without interference from e.g., motor skills, (Gaillard, 1988). Previous ERP (Baldwin and Kutas, 1997; Eimer et al., 1996; Lang and Kotchoubey, 2000; Rose et al., 2001; Rüsseler et al., 2003; Rüsseler and Rösler, 2000; Schlaghecken et al., 2000), PET (Berns et al., 1997; Honda et al., 1998) and fMRI (Aizenstein et al., 2004; Schendan et al., 2003) studies have focused on the study of learning patterned sequences by comparing performance before and after training (Schlaghecken et al., 2000). However, a caveat with these studies has been that the before and after comparison does not account for the instantaneous dynamics of the learning process. Though some of these studies have also attempted to track these dynamic processes by constructing consecutive sub-averages during a learning session (Honda et al., 1998), to our knowledge, this is the first study to track the dynamics of learning processes on a continuous trial-to-trial basis. The use of single trial evoked responses as markers of learning opens a wide range of new applications of ERPs. In particular, this information may prove crucial in understanding cognitive processes, and even in the study of different pathologies.

1.3. The "learning oddball" paradigm

In order to study the dynamics of pattern learning, it is necessary to track neuronal responses (using ERPs, PET or fMRI) on a single-trial basis throughout the experimental session, whereby the evoked neuronal response to every target tone is determined individually. This is a challenging task, owing to the low signal-to-noise ratio of the single-trial responses. A number of techniques for extraction of single-trial ERPs with optimum results have recently been proposed (Quian Quiroga and Garcia, 2003; Spencer, 2005). In particular, a de-noising procedure based on the Wavelet Transform (wavelet de-noising) has led to new insights concerning trial-to-trial changes in ERPs due to factors such as habituation (Quian Quiroga and van Luijtelaar, 2002; Sambeth et al., 2003), learning (Jongsma et al., 2004) and skill training (Atienza et al., 2005; Talnov et al., 2003).

In this study we present a new paradigm, the 'learning-oddball' paradigm, which exploits the possibility of obtaining single-trial responses using wavelet de-noising. Such analysis allows us to track the dynamic process of auditory pattern learning. The 'learning-oddball' paradigm has been developed as a variant on an auditory oddball paradigm. In a typical oddball experiment, frequent background stimuli are occasionally replaced (at random intervals) by infrequently occurring deviant stimuli – the 'oddball' or target stimuli. The most striking feature of ERPs elicited by these unexpected target stimuli is the appearance of a 'P3' component (also referred to as the 'P300' or 'P3b' component), a positive wave appearing between 300 and 600 ms after target presentation, and with a maximum amplitude over the central posterior region of the brain (Katayama and Polich, 1999; Picton, 1992, 1996; Pritchard, 1981). The P3 appears to have multiple underlying generators with involvement of the temporal and parietal lobes (Bledowski et al., 2004; Kiss et al., 1989). In addition, the thalamus (Horovitz et al., 2002) and hippocampus (Halgren et al., 1998; McCarthy et al., 1989; Tarkka et al., 1995) have also been found to contribute to P3 generation.

Though less studied, unexpected target stimuli give also rise to a 'N2' component (also referred to as the 'N2b'), a centrally distributed negative wave appearing before the P3 (ca. 200 ms after target presentation). The N2 is considered to be intimately linked to the P3 (Daffner et al., 2000; Nuchpongsai et al., 1999; Naatanen et al., 1981). Though it has been hypothesized that there also exist non-identical generators for the N2 and P3, at least activity in the supramarginal gyrus has been found to contribute to both the N2 and P3 component (Smith et al., 1990). In addition, (Karakas et al., 2000) found that an interplay of theta- and delta oscillations produced the morphology of both the P3 and N2(b) component (Karakas et al., 2000).

With the 'learning-oddball' paradigm, we studied responses to eight targets presented in a random oddball sequence, followed by responses to eight targets presented in a fixed oddball sequence (see also Fig. 1). This alternation of random targets and regular, or patterned, targets was repeated several times ($n = 6$).

The P3 amplitude has long been known to be sensitive to a wide array of manipulations, such as target probability, the inter-stimulus intervals and inter-target intervals (Croft et al., 2003; Fitzgerald and Picton, 1981; Gonsalvez et al., 1995; Gonsalvez and Polich, 2002). In addition, the P3 amplitude is also sensitive to sequence effects, independent of probability effects, which appears to be caused by confirmation or disconfirmation of expectancies (Jentzsch and Sommer, 2001; Squires et al., 1976). Despite the theoretical and empirical implications of these findings, systematic assessment of increased predictability due to learning has not been investigated. However, the P3 and N2 can be expected to increase as the unexpectedness of a target increases. Accordingly, when learning a regular sequence, the expectation of regular targets increases, resulting in the decreased P3 - and N2 - amplitude (Donchin, 1981; Jentzsch and Sommer, 2001; Jongsma et al., 2005; Polich and Kok, 1995).

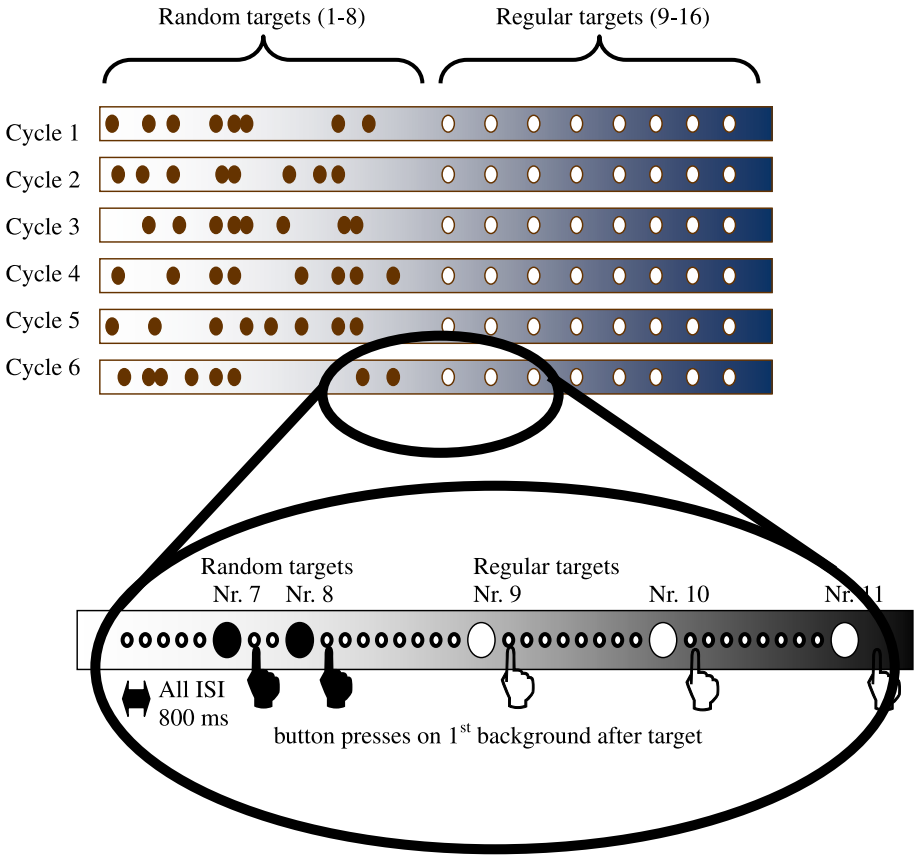

Fig. 1. This figure shows a diagram of the 'learning-oddball' paradigm. In this study eight targets were randomly (i.e., with 2–6 and 8–12 background tones in between to consecutive target tones) presented (depicted as black dots) within an ongoing steady sequence of auditory background tones (proportion targets:backgrounds, 1:8). Next, eight targets were presented at a regular position within the train of background tones (depicted as white dots). This alternation of random and regular target presentation was presented six times (cycles 1–6). Each cycle lasted 102.4 s, the total session lasted about 10 min. Part of the sequence has been magnified at the bottom. Targets were interspersed in an ongoing regular train of auditory background stimuli (small dots) with an 800 ms stimulus onset asynchrony (SOA). After eight targets, targets were presented regularly with seven background tones presented in between making the inter-target interval (ITI) 6.4 s. Participants had to give a mouse click after the first background stimulus following a target stimulus (depicted in pointing hands).

1.4. Hypotheses

Thus, in the current experiment we hypothesize that N2 and P3 responses to all random targets should be equal in case the target regularity is not perceived (i.e., the pattern is not learned). However, if pattern learning occurs, decreased single-trial N2 and P3 responses should be observed.

Additionally, if a target is expected, a slow negative shift in the ERP waveform should appear, starting about 300 ms before target stimulus onset – the 'Contingent Negative Variation,' or 'CNV' (Birbaumer et al., 1990; Walter et al., 1964), that is proposed to be generated by a network of cortical and subcortical structures (Bennett et al., 2004) including the basal ganglia (Zappoli, 2003). Although the CNV is ordinarily elicited in other paradigms than the oddball paradigm, the CNV appears to be sensitive to the expectancy of the target stimulus, and – like the P3 – has also been found to be sensitive to probability effects (Bauer et al., 1992; Korunka et al., 1993). We thus hypothesize that no CNV should be elicited in case the pattern is not learned. However, if pattern learning occurs, the elicitation of a CNV should be observed when target presentation becomes regularly spaced.

In this study, we first determined the conventional product of pattern learning, measuring the difference between the average performance to all random targets, compared to the average performance to all regular targets (see Fig. 2a). Second, we traced the dynamics of the learning process by measuring responses to all 16 consecutive targets (i.e., eight random targets, followed by eight regular targets; see Fig. 2b). Third, since the alternation of random and regular target presentation was repeated six times, we extracted single-trial responses to all 96 target stimuli individually. This allowed us to study whether pattern learning occurred more rapidly with consecutive repetitions (see Fig. 2c).

1.5. Main aim

Summarizing, we aimed to track the single trial-to-trial changes in the ERP CNV, N2, and P3 component

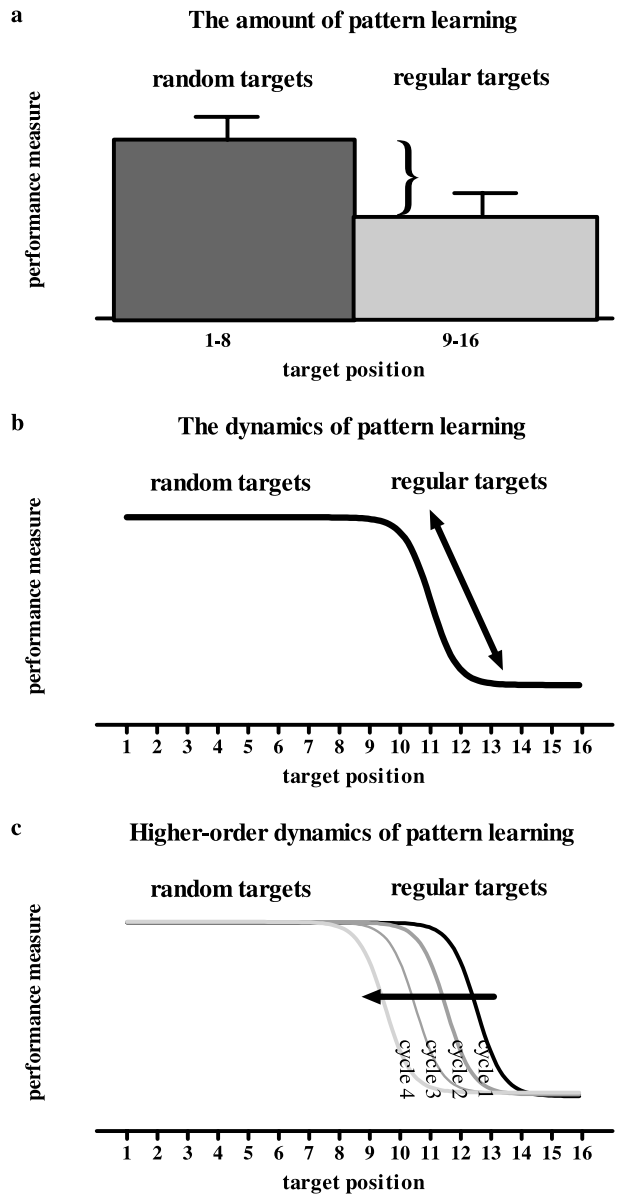

Fig. 2. This figure depicts the a priori defined hypotheses. The *x*-axes depicts target position (1–8 for random targets, 9–16 for regular targets) and the *y*-axes depicts the efficiency of performance (arbitrary units – lower values means better performance). (a) Depicts the alternative hypothesis regarding the average performance. (b) depicts the alternative hypotheses regarding the dynamics of pattern learning. (c) depicts the alternative hypotheses regarding higher-order dynamics of pattern learning. The H_0 hypotheses, namely, no difference between performances on random targets compared to regular targets are not depicted.

amplitudes, and to use them as dynamic markers of auditory pattern learning induced by switching from a pseudo-random to a fixed sequence of target stimuli. Though the N2, P3 and the CNV components have been under investigation for over 40 years, this is the first study – as far as we are aware – to investigate how the ERP components change from trial-to-trial during pattern learning.

2. Methods

2.1. Participants

Twenty-four participants (13 females, 11 males) took part in the experiment. Only right-handed healthy adults, not using medication and without a neurological or psychiatric history, were accepted. All participants signed a written statement of informed consent. They had a mean age of 27.4 ± 4.9 (mean $\pm$ SD) years. The participants sat comfortably in a recliner during the experiment and were instructed to keep their eyes closed and to sit as still as possible. This to avoid motor artifacts, in particular eye blinks. Both eye movements and blinking produce electric fields that overlap in time with the ERP of interest. Commonly, trials containing eye blinks are excluded from further analyses. However, since our aim was to track the trial-to-trial changes of ERP components due to pattern learning, no trials could be excluded. In addition, instructions to suppress eye blinking have also been found to affect the P3 amplitude (Ochoa and Polich, 2000). Thus – although this might have led to a general increase in ongoing alpha activity in the EEG – we measured ERPs during an eyes closed condition. Participants were tested in an electrically shielded, sound-attenuated, dark cubicle (inside dimensions: $2 \times 2.2 \times 2$ m). A computer mouse was placed under the participants' dominant hand to collect responses. The stimuli were presented through headphones. The sound consisted of woodblock sounds (duration: 200 ms with 5 ms rise/fall). All background stimuli had a center frequency at 2.45 kHz. Within the AEP session, target stimuli had a center frequency at 2.75 kHz. Within the OEPs session, targets consisted of missing stimuli. All stimuli were presented at a sound pressure level of 65 dB.

2.2. Experimental design

A visual image of the 'learning-oddball' paradigm is presented in Fig. 1. Two sessions, each lasting for about 10 min, were recorded. One session employed deviant stimuli as targets and one session employed omitted stimuli as targets. The presentation order of the sessions was counterbalanced among the participants. In both sessions, targets ($n = 96$) with a 12.5% probability, interspersed within a train of backgrounds (SOA 800 ms), were presented in an eyes closed situation. Within one session, six blocks of 16 consecutive targets were presented as one continuous, ongoing train of stimuli (of 96 targets and 672 background tones). The first eight targets were presented in a random position (preceded by a semi-random (2–6 or 8–12) number of background tones), the following eight targets presented in a fixed position (all preceded by seven background tones). Thus, targets presented in fixed positions became predictable. The program E-Prime was used for presenting the stimuli. The program was set up in such a way that it generated eight strings containing a 'random' target. This was done by presenting a semi-random number of

background stimuli (2–6 or 8–12), followed by one target stimulus. This way, a random target was never preceded by seven background stimuli. However, occasionally two random targets were preceded by the same number of background tones. After generating eight random target strings, eight fixed target strings were generated by presenting seven background stimuli followed by one target stimulus. The program was started separately for each individual participant resulting in different random sequences. The task of the participants was to respond after the first standard tone following a target stimulus. This delayed response task was chosen in order to avoid motor activity closely locked to targets.

EEG recordings. EEG (band-pass: DC – 100 Hz, sampling rate 500 Hz) was recorded with a SYNAMPS amplifier (Neuroscan, Herndon, VA) from 27 Ag/AgCl electrodes (AF3, AF4, F7, F3, Fz, F4, F8, FC5, FC1, FC2, FC6, T7, C3, Cz, C4, T8, CP5, CP1, CP2, CP6, P7, P3, Pz, P4, P8, PO3, PO4) mounted in an elastic cap (EASICAP, FMS, Breitenbrunn, GER) at placements based on the International 10–20 recording system (American Encephalographic Society, 1994) and referenced to linked mastoids and stored on disk for offline processing. Vertical and horizontal eye movements were recorded by two additional bipolar channels placed above and below the right eye and on the outer canthi of each eye. Impedances of all electrodes was kept below 10 kΩ.

2.3. Data processing

First, epochs from −2048 ms to 2048 ms around all presented auditory target stimuli ($n = 96$) and all presented omitted target stimuli ($n = 96$) were off-line down-sampled to 250 Hz, de-trended and baseline corrected over the full 4.096 s length of each epoch. Second, these epochs were then collectively subjected to an independent component analysis, as implemented in EEGLAB (Delorme and Makeig, 2004), running in the MATLAB environment (The Mathworks, Inc., Natick, MA). Variance-components with activity attributable to artifacts, such as eye movement, fronto-temporal muscle activity and mains noise, were removed. We did not employ ICA components beyond the level of artifact reduction for several reasons. Within the current experiment the ICA output does not necessarily add to the clarity of the results. Apart from this, since we ran ICA separately for each individual, there would be a matching problem of ICA's across subjects.

Finally, all individual single-trial ERP responses were de-noised by means of a recently proposed algorithm based on the wavelet transform analysis method (Quian Quiroga and Garcia, 2003). The accuracy of this method in smoothing ERPs has been demonstrated with both simulated data and visual and auditory ERP data (Atienza et al., 2005; Jongsma et al., 2004; Quian Quiroga and Garcia, 2003; Quian Quiroga and van Luijtelaar, 2002; Sambeth et al., 2003; Spencer, 2005; Talnov et al., 2003). De-noising parameters were the same for all participants. Whole waveforms were additionally smoothed using a 3-point moving average across adjacent epochs. The above described data processing was applied to each channel independently. Under the assumption that scalp potentials are coupled to hemodynamic activity, single-trial ERPs can also be used for prediction of regional brain activation in functional magnetic resonance data (Eichele et al., 2005). Since some peaks diminished or appeared rapidly over consecutive targets, peak amplitudes were determined within a fixed latency window based on the grand average responses (of all subjects, for all targets, for AEPs and OEPs separately) and subsequently kept constant (Jongsma et al., 2005).

AEPs elicited by deviant target stimuli consisted, alongside an N1 and P2, of a prominent N2 and P3 component. In addition, a CNV-like component was observed. Mean component amplitudes in fixed latency windows (N2, 180–220 ms; P3, 350–430 ms; CNV, −300 ms to 0 ms) were further analyzed (Jongsma et al., 2005; Koelsch et al., 2004). In line with this, grand average OEPs elicited by omitted target stimuli also consisted of a N2, P3 and CNV-like component. Mean component amplitudes in the same fixed latency windows (N2, 180–220 ms; P3; 350–430 ms; CNV, −300 ms to 0 ms) were further included in analyses (Lang and Kotchoubey, 2000). In addition, since the N2 is considered to be intimately linked to the P3 (Daffner et al., 2000; Nuchpongsai et al., 1999; Naatanen et al., 1981), a P3–N2 component was constructed by subtracting the N2 amplitude from the P3 amplitude. This resulted in a more stable component, especially with regard to the single-trial ERP analyses.

2.4. Statistical analysis

Step 1. See also Fig. 2a. Component amplitudes of de-noised ERPs were determined as the average value within a fixed latency window (N2, 180–220 ms; P3, 350–430 ms; CNV, −300 to 0 ms). For each component (the AEP CNV, N2, P3 and P3–N2 component and the OEP CNV, N2, P3 and P3–N2 component) a two-within ANOVA analysis was performed: condition × electrode site, (condition, two levels: random targets vs fixed targets; electrode site, 27 levels). For EEG channels it is clear that nearby channels are generally more correlated than distant channels, thus leading to heterogeneous covariances. Therefore, the Geisser and Greenhouse correction was applied to the degrees of freedom. Post-hoc analyses applying Bonferroni correction were performed to determine condition effects per electrode site when appropriate. Reaction times of correct responses were analyzed. Correct responses were defined as responses within a time window of −400 ms to +400 ms around the point of optimal response (i.e., the first background stimulus after the target stimulus). Error rates were calculated and the RTs of the correct responses were analyzed with a *t*-test (random targets vs fixed targets).

Step 2. See also Fig. 2b. A priori defined hypotheses were tested by nonlinear regression analysis of the AEP

CNV, N2, P3 and P3–N2 and AEP RTs, as well of the OEP CNV, N2, P3 and P3–N2 component and OEP RTs, using the program GraphPad Prism 4. The over participants averaged RTs were smoothed using a 3-point moving average. For AEP and OEP component amplitudes, *F*-tests for best fit were obtained for all 27 electrode sites comparing:

H_0: a straight line with slope = zero. There is no learning effect.
H_1: a sigmoid-curve. With each cycle, 'learning' occurs more rapidly.

Step 3. See also Fig. 2c. Single-trial component amplitudes were determined at group level ($n = 24$). For the CNV component at Fz (maximal effect) and for the P3–N2 component at Pz (maximal effect). In addition, single-trial RTs were determined at group level ($n = 24$). Thus, each separate cycle ($n = 6$), containing 16 targets, was analyzed, resulting in six sigmoid-curves per session, per component and per RT. In addition, a regression analysis was performed with *F*-tests for best fit on found Tn50s – or the point where 50% of the amplitude modulation was reached.

Thus, regression analysis was applied on the estimated Tn50 values obtained in step 2 of the analysis, using the program: GraphPad Prim 4.03. The linear equations of the H_0 ($Y = \text{Intercept}$, there are no over-cycle effects) and the H_1 hypothesis ($Y = \text{Intercept} + \text{Slope} \times X$, with each cycle, 'learning' occurs more rapidly) were fitted to the data. An *F*-test determined whether the decrease of sum of squares for the H_1 was worth the loss of degrees of freedom. For the fitting and the *F*-tests three procedures were applied on each ERP component: the first most conservative procedure took into account only the number of cycles (i.e., 6) and consequently yielded five (H_0) or four (H_1) degrees of freedom. In the second procedure the significance was tested with 23 vs 22 degrees of freedom, reflecting the number of participants. In the last procedure the total number of measurement (i.e., 146, namely: subjects × cycles) was taken into account, resulting in 143 vs 142 degrees of freedom. An overview of these results together with the raw data in an Excel file are available from the author upon request.

3. Results

3.1. The amount of pattern learning

Fig. 3a shows the grand average ERPs to higher pitch targets, or auditory event-related potentials (AEPs) and to stimulus omissions, or omission event-related potentials (OEPs) at midlines electrode sites (Fz, Cz and Pz) for both random (dotted lines) and regular (solid lines) targets. Though all 27 electrode sites were included in the analyses, only results from midline sites (Fz, Cz and Pz) are depicted in the figures.

We observed a slow negative shift in ERPs elicited by the regular targets – the contingent negative variation (CNV) – starting about 500 ms before target onset. CNV was at a maximum in the central frontal region and showed larger negative amplitudes to regular targets than to random targets.

Random target stimuli elicited an N2, appearing between 180 and 220 ms after stimulus onset, with a maximum amplitude over the central region and a marked P3 component – a positive wave appearing between 350 and 430 ms after target presentation – with a maximum amplitude over the central posterior region of the brain (Picton, 1992; Polich, 1996; Pritchard, 1981; Sutton et al., 1965). A similar P3–N2 complex was also observed when the target consisted of an unexpectedly omitted stimulus (Besson and Faïta, 1995; Jongsma et al., 2004, 2005; Walter et al., 1964). Maximum P3–N2 was expressed at the central posterior region and had lower amplitudes (i.e., closer to baseline) with regular targets than with random targets.

Fig. 3b depicts the means and SEMs of concurrent ERP component amplitudes for midline sites in the form of bar graphs. Component amplitudes to regular targets are depicted as solid bars, and component amplitudes to random targets are depicted as dotted bars. Bar graphs are shown for the AEP session (on the left) and the OEP session (on the right). The *y*-axes show amplitudes (in μV). Bar graphs of the concurrent reaction times (RTs) are shown on the lower right-hand side, with *y*-axes showing time (in ms).

Table 1 summarizes all significant *F* and *p*-values from the ANOVA and *t*-test results for the AEP session (Table 1a) and the OEP session (Table 1b).

With respect to the AEP session, the CNV showed a significant effect of condition ($p < .0001$), electrode site ($p = .002$), and a condition × electrode site interaction effect ($p < .0001$). Post-hoc analyses revealed condition effect at frontal-central sites (AF3, AF4, F2, F3, Fz, F4, FC5, FC1, FC2, FC6, T7, Cz, C4, CP5 and CP1; with Bonferroni correction, all $p < .05$). On the N2 we found no main effects of condition or electrode site, but we did find a condition × electrode site interaction effect ($p = .016$). However, in the post-hoc analyses none of the electrodes showed a condition effect after Bonferroni correction. On the P3 a main condition ($p < .0001$) and electrode site effect ($p = .011$) was observed. The condition × electrode site effect did not reach significance ($p = .34$). The P3–N2 showed an effect of condition ($p < .0001$), electrode site ($p = .004$), and a condition × electrode site interaction effect ($p < .033$). Post-hoc analyses revealed condition effect at parietal sites (CP1, P3, Pz and P4; with Bonferroni correction, all $p < .05$).

With respect to the OEP session, the CNV showed a significant effect of condition ($p < .0001$), electrode site ($p < .001$), and a condition × electrode site interaction effect ($p < .0001$). Post-hoc analyses revealed condition effect at frontal-central sites (AF3, AF4, F3, Fz, F4, FC5, FC1, FC2, FC6, T7, Cz, C4, CP5, CP1, CP2 and CP6; with Bonferroni correction, all $p < .05$). On the N2 we found a main effect of electrode site ($p = .021$). No effect on

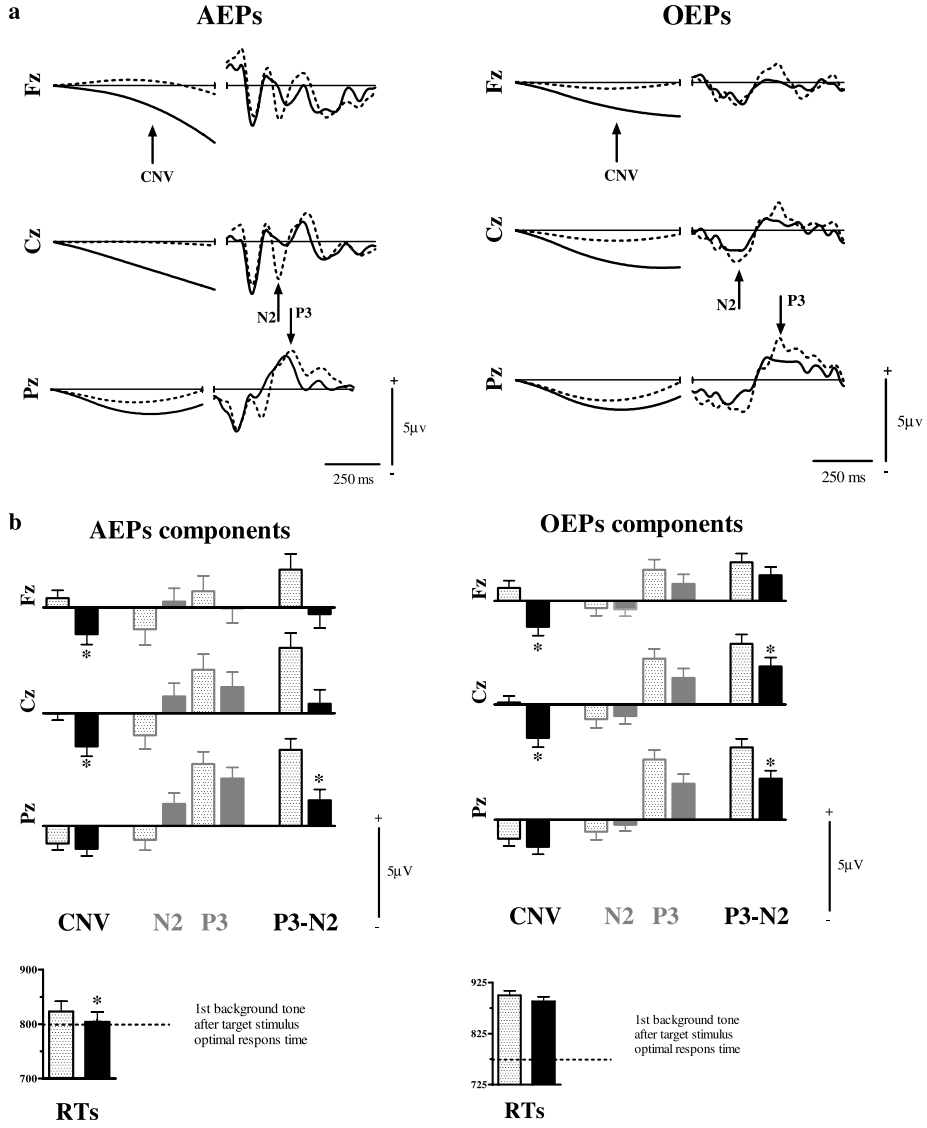

Fig. 3. (a) Shows grand average ERPs at midline sites. On the left side of each electrode panel, the tracings after the first wavelet-denoising solution, extracting the CNVs, are depicted. On the right side, tracings after the second wavelet-denoising solution, extracting the ERP N2, P3 and P3–N2 complex, are depicted. Grand averages of all 24 participants are given for all regular targets (solid lines) and all random targets (dotted lines). Tracings are given for the AEP session (on the left) and the OEP session (on the right). The *x*-axes show time (in ms) and the *y*-axes show amplitudes (in μV). (b) Depicts bar graphs (means and SEMs) of concurrent ERP component amplitudes at midline sites of ERP CNV, N2, P3 and P3–N2 complex. Group averages are given for all regular targets (solid bars) and all random targets (dotted bars). Bar graphs are given for the AEP session (left panel) and the OEP session (right panel). The *y*-axes show amplitudes (in μV). Bar graphs of the concurrent delayed response RTs are depicted at the lower right side with *y*-axes showing time (in ms).

condition, nor a condition × electrode site effect was observed. The P3 showed a main condition ($p < .0001$) and electrode site effects ($p = .013$). The condition × electrode site effect did not reach significance ($p = 0.10$). On the P3–N2 we found a significant effect of condition ($p < .006$) and electrode site ($p < .0001$). As for the P3, the condition × electrode site interaction effect did not reach significance ($p = 0.12$). An explorative post-hoc analysis suggested only condition effect at centro-parietal sites (Cz, CP1, CP2, CP6, P3 and Pz; with Bonferroni correction, all $p < .05$).

The error rates suggest that the task was more difficult within the OEP session than the AEP session (13.05% vs 5.15%). Also, error rates of the responses seemed slightly higher for random targets than regular targets (5.50% vs 4.80% within the AEP session; 13.30% vs 12.80% within the OEPs session). *T*-tests regarding the reaction times showed a significant effects in the AEP session ($p = .021$) and the OEP session ($p = .038$), with faster RTs during regular target sequences.

3.2. The dynamics of pattern learning

Fig. 4 shows component amplitudes and their best-fit curves (either a straight line or a sigmoid-curve) for the CNV, N2, P3 and P3–N2 component amplitudes at midline

Table 1
The amount of pattern learning

AEP	ANOVA results	*F* values	*p*-values
(a) Summary ANOVA's AEP component amplitudes			
CNV	Electrode site effect	$F(2.5, 57.9) = 16.2$	$p = .002$
	Condition effect	$F(1, 23) = 389.9$	$p < .0001$
	Interaction effect	$F(3.09, 71.0) = 4.3$	$p < .0001$
Post-hoc	Bonferroni corrected		
AF3	Condition effect		$p < .05$
AF4			
F2			
F3			
Fz			
F4			
FC5			
FC1			
FC2			
FC6			
T7			
Cz			
C4			
CP5			
CP1			
N2	Electrode site effect	$F(2.1, 48.9) = 26.6$	$p = .07$
	Condition effect	$F(1, 23) = 32.4$	$p = .23$
	Interaction effect	$F(3.16, 72.7) = 3.6$	$p = .016$
Post-hoc	Bonferroni corrected		n.s.
P3	Electrode site effect	$F(2.8, 64.7) = 12.4$	$p < .0001$
	Condition effect	$F(1, 23) = 7.6$	$p = .011$
	Interaction effect	$F(3.0, 68.7) = 11.6$	$p = .34$
P3-N2	Electrode site effect	$F(2.3, 53.8) = 9.8$	$p < .0001$
	Condition effect	$F(1, 23) = 10.6$	$p = .004$
	Interaction effect	$F(2.8, 64.6) = 3.2$	$p = .033$
Post-hoc	Bonferroni corrected		
CP1	Condition effect		$p < .05$
P3			
Pz			
P4			
	t-test		*p*-value
RT	Condition effect		$p = .021$
OEP	ANOVA results	*F* values	*p*-values
(b) Summary ANOVA's OEP component amplitudes			
CNV	Electrode site effect	$F(3.2, 74.4) = 6.32$	$p = .001$
	Condition effect	$F(1, 23) = 20.9$	$p < .0001$
	Interaction effect	$F(3.4, 79.1) = 7.4$	$p < .0001$
Post-hoc	Bonferroni corrected		
AF3	Condition effect		$p < .05$
AF4			
F3			
Fz			
F4			
FC5			
FC1			
FC2			
FC6			
T7			
Cz			
C4			
CP5			
CP1			
CP2			
CP6			
N2	Electrode site effect	$F(3.8, 86.7) = 3.1$	$p = .021$
	Condition effect	$F(1, 23) = 14.1$	$p = .27$
	Interaction effect	$F(2.9, 66.5) = 4.8$	$p = .40$
P3	Electrode site effect	$F(3.8, 88.0) = 12.91$	$p < .0001$
	Condition effect	$F(1, 23) = 7.2$	$p = .013$
	Interaction effect	$F(2.0, 45.5) = 31.0$	$p = .10$
P3-N2	Electrode site effect	$F(3.7, 84.5) = 11.6$	$p < .0001$
	Condition effect	$F(1, 23) = 9.1$	$p = .006$
	Interaction effect	$F(1.8, 41.1) = 52.0$	$p = .115.$
Post-hoc	Bonferroni corrected		
Cz	Condition effect		$p < .05$
CP1			
CP2			
CP6			
P3			
Pz			
	t-test		*p*-value
RT	Condition effect		n.s.

Summarizes *F* and *p* values of 3-within ANOVA results for the AEPs CNV, N2, P3 and P3–N2 amplitudes and the *t*-test result of the reaction times (RTs).

sites – as well as the RTs – for the AEP session (Fig. 4a) and the OEP session (Fig. 4b). Table 2summarizes *F* and *p*-values for the *F*-tests in terms of best fit for all learning curves at all 27 electrode sites. With respect to the AEP CNV, N2, P3, P3–N2 component all components showed 'learning' curves at most electrode sites that described the data significantly better than straight horizontal lines (levels of significance: $^{***}p < .0001$; $^{**}p < .01$; $^{*}p < .05$; n.s. = not significant). Significances for the CNV appeared to be more frontal-central orientated and for the N2, P3 and P3–N2 more central-parietal orientated. The RT data could also be better described by a 'learning' curve than a straight, horizontal line. Similar results were found with respect to the OEPs though the N2 'learning' curves only appeared to reach significance at more laterally orientated temporal-occipital sites.

For the AEP session, the CNV increased in the pre-stimulus period at all frontal central EEG electrode sites (see Table 2). In addition, the N2, P3 and P3–N2 amplitudes rapidly decreased after target presentation became regular (marked with a solid line), resulting in the hypothesized sigmoid learning curve at all central posterior EEG electrode sites (see Table 2). A corresponding effect was seen in the RTs that also decreased after target presentation became regular, though the effect was less clear, and appeared later.

In line, for the OEP session, the CNV increased in the pre-stimulus period at all frontal central EEG electrode sites (see Table 2). In addition, the P3 amplitude rapidly decreased after target presentation became regular (marked

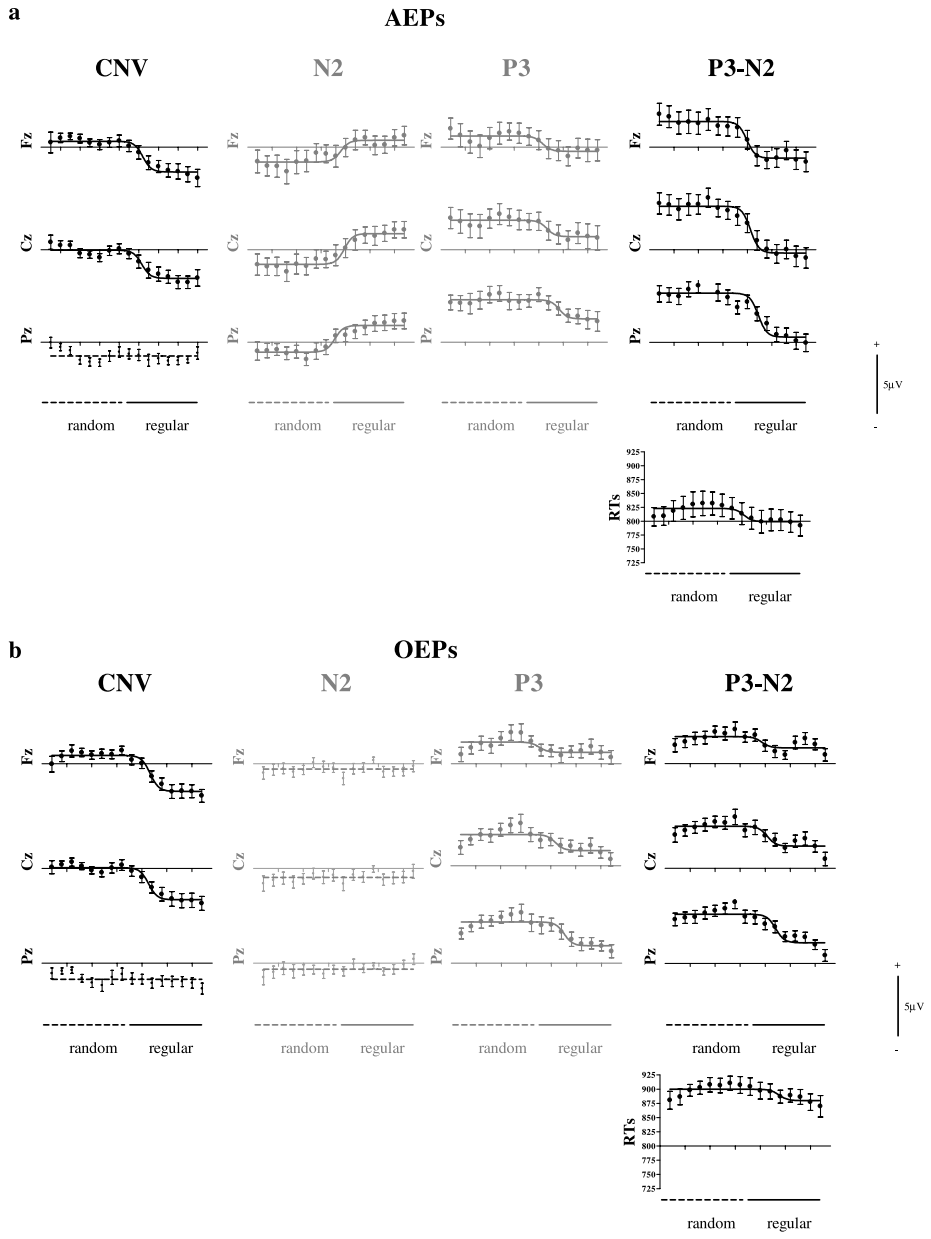

Fig. 4. This figure shows 'learning curves,' or s-curves, at all midline sites for the AEP CNV, N2, P3 and P3–N2 amplitudes and the RTs from the AEP session (a), and the OEP session (b). The *x*-axes show concurrent target position (1–16) with random targets falling on the left side (1–8) and regular targets on the right side. The *y*-axes depict ERP component amplitudes (in μV) and time (in ms) for the RTs. Only when a sigmoid-curve described the data significantly better then a straight line it was plotted with a black solid line. Non-significant sigmoid-curve solutions are depicted with a dotted thin line.

with a solid line), resulting in the hypothesized sigmoid learning curve at all central posterior EEG electrode sites (see Table 2). Although the N2 did not decrease at midline sites, the combined P3–N2 returned stronger and more stable decreases than P3 amplitudes alone. RTs failed to show a significant decrease.

3.3. Higher-order dynamics of pattern learning

Fig. 5 shows the group-averaged single-trial data with the best-fit curves per cycle presented (either a straight horizontal line or a sigmoid-curve) for the CNV at the Fz electrode site (Fig. 5a left panel for AEPs; Fig. 5b left panel for OEPs), and P3–N2 at the Pz electrode site (Fig. 5a middle panel for AEPs, Fig. 5b middle panel for OEPs), along with the RTs (Fig. 5a right panel for AEPs session; Fig. 5b right panel for OEPs session). Table 3 summarizes the significance of *F*-tests for best fit of group-averaged AEPs and OEPs component amplitudes and RTs per trial over six consecutive cycles. With respect to both the AEP and OEP components, the single-trial CNV amplitudes (at Fz) and P3–N2 amplitudes (at Pz) resulted in significant 'learning' curves for all six cycles (all $p < .05$). Moreover, turning point of these 'learning' curves (the Tn50s),

Table 2
The dynamics of pattern learning

Site	CNV	N2	P3	P3–N2	RT
AEP					
(a) Summary of group statistics of fitting 'learning' curves on AEP component amplitudes					
AF3	***	n.s.	n.s.	**	
AF4	***	n.s.	n.s.	***	
F7	***	n.s.	n.s.	n.s.	
F3	***	**	*	***	
Fz	*	***	*	***	
F4	***	***	*	***	
F8	***	n.s.	n.s.	*	
FC5	***	**	*	***	
FC1	***	***	*	***	
FC2	***	***	*	***	
FC6	***	***	n.s.	***	
T7	***	***	n.s.	***	
C3	***	***	*	***	
Cz	***	***	*	***	*
C4	***	***	*	***	
T8	***	***	n.s.	***	
CP5	***	***	**	***	
CP1	***	***	**	***	
CP2	***	***	**	***	
CP6	***	***	*	***	
P7	n.s.	***	***	***	
P3	**	***	***	***	
Pz	n.s.	***	***	***	
P4	*	***	***	***	
P8	n.s.	***	***	***	
PO3	n.s.	***	***	***	
PO4	n.s.	***	***	***	
OEP					
(b) Summary of group statistics of fitting 'learning' curves on OEP component amplitudes					
AF3	***	n.s.	n.s.	n.s.	
AF4	***	n.s.	n.s.	n.s.	
F7	***	n.s.	n.s.	n.s.	
F3	***	n.s.	n.s.	n.s.	
Fz	*	n.s.	*	**	
F4	***	n.s.	*	**	
F8	***	n.s.	n.s.	n.s.	
FC5	***	n.s.	n.s.	*	
FC1	***	n.s.	**	***	
FC2	***	n.s.	**	***	
FC6	***	n.s.	**.	***	
T7	***	**.	n.s.	**	
C3	***	n.s.	***	***	
Cz	***	n.s.	***	***	n.s.
C4	***	n.s.	***	***	
T8	***	***.	n.s.	***	
CP5	***	***	***	***	
CP1	***	n.s.	***	***	
CP2	***	n.s.	***	***	
CP6	***	***	***	***	
P7	n.s.	***	***	***	
P3	***	***	***	***	
Pz	n.s.	n.s.	***	***	
P4	***	*	***	***	
P8	**	n.s.	***	***	
PO3	n.s.	*	***	***	
PO4	n.s.	**	***	***	

F and *p*-values of *F*-tests for best fit of AEPs and OEPs component amplitudes at all electrode sites and RTs from both AEP and OEP session (***$p < .001$; **$p < .01$; *$p < .05$).

appeared to occur earlier with each repetition Thus, additionally, a regression analysis was performed with *F*-tests for best fit on the mean and 95% confidence intervals of these Tn50s – or the point where 50% of the amplitude modulation was reached – from each of these curves, comparing:

H_0: a straight line with slope is equal to zero. There are no over-cycle effects.
H_1: a straight line with slope is not equal to zero. With each cycle, 'learning' occurs more rapidly.

Table 3 (bottom) summarizes the significant results from the *F*-tests for best fit of Tn50s from six consecutive cycles. Tn50s of all 'learning' curves were taken separately for AEP and OEP component amplitudes and RTs per cycle.

Though all separate cycles showed significant learning curves at the single-trial ERP CNV and P3–N2 component amplitudes, some cycles showed decreases even before the introduction of target regularity; possibly due to increased variability of the single-trial data. However, in general, these learning curves showed progressively earlier Tn50s suggesting that the regularity of the pattern was detected more rapidly with each consecutive cycle (see Fig. 5, bottom panels). RTs did not show significant learning curves for all cycles (only for cycles 3 and 4 for AEPs, cycles 2, 3 and 4 for OEPs). Therefore, no *F*-test for straight lines with either slope is equal to zero vs slope is different from zero on the RTs' Tn50s could be performed.

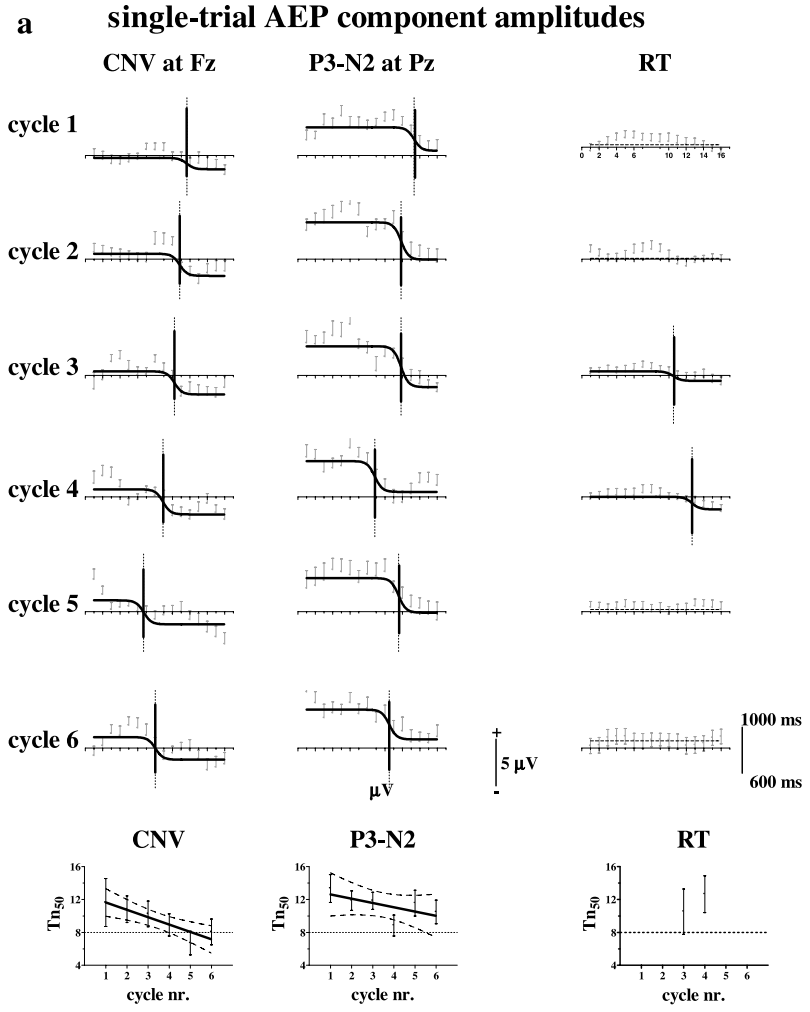

Fig. 5. This figure shows the six sigmoid-curves for the six consecutive cycles, thus showing ERP component amplitudes of all 96 single-trials. The sigmoid-curves for the ERP CNV are derived from the Fz electrode site and the sigmoid-curves for the ERP P3–N2 are derived from the Pz electrode site. Only sigmoid-curves that described the data significantly better then a straight line are depicted in solid black lines. For each 'learning' curve, the Tn50 is marked with a solid vertical line. The *x*-axes plot target position (1–16 for cycle 1; 17–32 for cycle 2; 33–48 for cycle 3; 49–64 for cycle 4; 65–80 for cycle 5; 81–96 for cycle 6). The *y*-axes depict ERP component amplitudes (in µV) and time (in ms) for the RTs. Single-trial 'learning' curves are given for the AEP session (a) and the OEP session (b). In addition, Tn50s (means and 95% confidence intervals) are plotted for the ERP CNV, P3–N2 and the RTs for both the AEP session (a, bottom) and the OEP session (b, bottom). The *x*-axes depict cycle nos. (1–6) and the *y*-axes depict values of the Tn50 (as expressed in target position, 1–16) per cycle. A regression analysis was performed comparing a straight line with slope is equal to zero with a straight line with slope is different from zero.

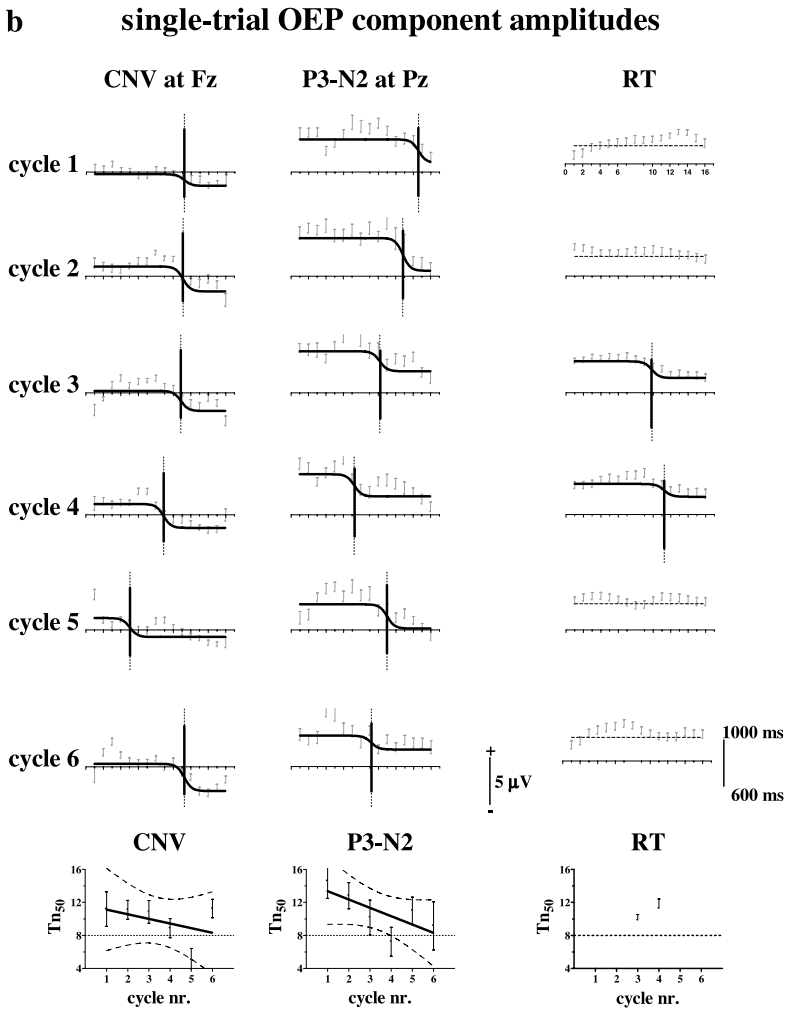

Fig. 5 (*continued*)

4. Discussion

4.1. The amount of pattern learning

We found slightly faster RTs (ca. 20 ms) following regularly presented targets, compared to RTs following randomly presented targets. Other ERP studies found more marked RT effects (ca. 60 ms difference) with pattern learning (Baldwin and Kutas, 1997; Eimer et al., 1996; Rüsseler and Rösler, 2000; Schlaghecken et al., 2000). This is probably due to the fact that in these studies, responses were given immediately following targets (Baldwin and Kutas, 1997; Eimer et al., 1996; Rüsseler and Rösler, 2000; Schlaghecken et al., 2000) whereas in our study participants responded to the background stimulus following 800 ms after target presentation.

In addition, a central anterior distributed CNV was observed in ERPs elicited by the regularly presented targets, but not in ERPs elicited by randomly presented targets. Although such a CNV is commonly elicited in paradigms in which a warning stimulus precedes a target stimulus – thereby making the appearance of the target stimulus expected (Bennett et al., 2004; Birbaumer et al., 1990; Walter et al., 1964) – the P3 and CNV have been strongly associated in the classical ERP literature due to their common relationship to expectation and expectation-related constructs (Donchin, 1981; Korunka, 1993; Sutton et al., 1965) and their common sensitivity to target probability (Korunka, 1993).

In a similar experiment, Eimer and colleagues (1996) observed a slow negative shift preceding targets – the 'Lateralized Readiness Potential' (LRP) – which became more pronounced with learning. They assumed that this component reflected the acquired knowledge, and stated that participants may have learned the stimulus sequence and that expectations were communicated to the motor system at a very early stage of processing, namely, prior to target presentation. However, their participants had to respond directly after a target stimulus was presented, whereas in the current experiment a delayed response was required, thus eliminating the motoric component of response preparation. Because a delayed response task was

Table 3
Higher order dynamics of pattern learning

cycle	CNV	N2	P3	P3–N2	RT
(a) Summary of the Tn50s (turning point) of 'learning' curves per cycle for AEP component amplitudes (mean ± 95% confidence intervals)					
1	11.6 (8.86–14.4)	13.3 (11.3–15.4)	n.s.	13.3 (11.7–14.9)	n.s.
2	10.8 (9.28–12.3)	11.8 (10.7–12.9)	n.s.	11.9 (10.7–13.0)	n.s.
3	10.2 (8.76–11.7)	9.68 (8.61–10.8)	n.s.	11.9 (10.9–12.8)	10.5 (7.93–13.1)
4	8.92 (7.64–10.2)	6.05 (4.06–8.04)	10.1 (8.61–11.6)	8.84 (7.64–10.0)	12.7 (10.5–14.8)
5	6.71 (5.35–8.06)	9.36 (7.16–11.6)	12.2 (10.5–14.0)	11.6 (10.1–13.0)	n.s.
6	8.05 (6.57–9.53)	n.s.	7.96 (6.27–9.65)	10.5 (9.12–11.9)	n.s.
Higher order					
F(Dfn, Dfd) based on no. of cycles	20.5 (1,4) $p = 0.010$	4.82 (1,3) $p = 0.12$ n.s.	–	2.77 (1,4) $p = 0.17$ n.s.	–
F(Dfn, Dfd) based on no. of subjects	18.7;(1,22) $p = 0.0003$	14.3 (1,18) $p = 0.0014$	–	7.01 (1,22) $p = 0.01$	–
F(Dfn, Dfd) based on no. of measurements	18.4 (1,142) $p < 0.0001$	21.4 (1,118) $p < 0.0001$	–	9.84 (1,142) $p = 0.002$	–
(b) Summary of the Tn50s (turning point) of 'learning' curves per cycle for OEP component amplitudes (mean ± 95% confidence intervals)					
1	11.2 (9.22–13.2)	n.s.	n.s.	14.6 (12.6–16.6)	n.s.
2	11.1 (10.0–12.2)	n.s.	12.3 (11.3–13.3)	12.8 (11.3–14.3)	n.s.
3	10.9 (9.56–12.2)	n.s.	10.3 (7.91–12.6)	10.2 (8.18–12.2)	9.84 (8.54–11.2)
4	8.88 (7.77–10.0)	n.s.	13.1 (12.3–13.9)	7.25 (5.59–8.91)	11.3 (9.03–13.5)
5	5.04 (3.74–6.34)	n.s.	12.1 (10.6–13.6)	11.0 (9.42–12.6)	n.s.
6	11.3 (10.2–12.3)	n.s.	9.67 (7.21–12.1)	9.16 (6.40–11.9)	n.s.
Higher order					
F(Dfn, Dfd) based on no. of cycles	0.913 (1,4) $p = 0.39$ n.s	–	0.495 (1,3) $p = 0.53$ n.s.	4.48 (1,4) $p = 0.1$	–
F(Dfn, Dfd) based on no. of subjects	3.74 (1,22) $p = 0.07$	–	1.11 (1,18) $p = 0.30$ n.s.	11.6 (1,22) $p = 0.003$	–
F(Dfn, Dfd) based on no. of measurements	8.96 (1,142) $p = 0.003$	–	1.41 (1,118) $p = 0.24$ n.s.	16.6 (1,142) $p < 0.0001$	–

Summarizes the over participants averaged Tn50s (means and 95% confidence intervals) of learning curves. (Target 9 being the first regular target) for the AEP session (a) and the OEP session (b).

employed in the current experiment, no lateralized readiness potential was elicited by the target stimulus. Instead, regularly presented target stimuli started to function as a kind of warning stimulus, after which a response was then acquired. Interestingly, a CNV-like potential was observed preceding these 'warning' targets. Although conventionally the CNV develops before an expected motor response, it also develops before an expected stimulus that does not require a motor response (Hohnsbeim et al., 1998). Thus, the CNV is assumed to reflect the cognitive preparation of the next trial, or the facilitation of specific brain area, which are relevant for the next trial (Hohnsbeim et al., 1998). The CNV has also been shown to develop during the temporal interval between two events. This wave would reflect anticipatory processing of a temporally expected stimulus. The CNV is thus the main ERP correlate of the estimation or production of a time interval and has been shown to increase during the learning of a temporal interval (McAdam, 1966; Pfeuty et al., 2003). This is in line with our observations, where the temporal interval between regular targets (6.4 s) was learned.

Finally, we found that the central posterior distributed P3–N2 complex was smaller in response to regularly presented targets as compared to randomly presented targets in both the oddball and omission sessions. The CNV was maximal for the 'regular' condition over frontal sites. As expected, we did observe a condition × electrode site interaction effect revealing a CNV condition effect over frontal sites for both the AEP and OEP session. Since the P3–N2 was maximal for the 'random' condition over centro-parietal sites, an interaction effect was also expected. We did observe an interaction effect within the AEP session revealing a P3–N2 condition effect over parietal sites. For the OEP session the interaction effect was not significant. This might be due to the fact that the OEP P3–N2 is a very broad and smeared component that is visible over most electrode sites, with exception of some frontal sites. Compared to the current experiment, Eimer and colleagues (1996) described similar N2 effects due to implicit pattern learning. In addition, others have reported decreased P3 due to learning (Rose et al., 2001), high expectancy (Sutton et al., 1965) and regularity (Lang and Kotchoubey, 2000). Correspondingly, in a previous study we found that the P3–N2 complex rapidly disappeared when omitted target stimuli could be expected (Jongsma et al., 2005).

Both the P3 and CNV appear to be sensitive to (local) probability effects (Bauer et al., 1992; Croft et al., 2003; Fitzgerald and Picton, 1981; Korunka et al., 1993). Therefore, we wanted to explore whether our results could be

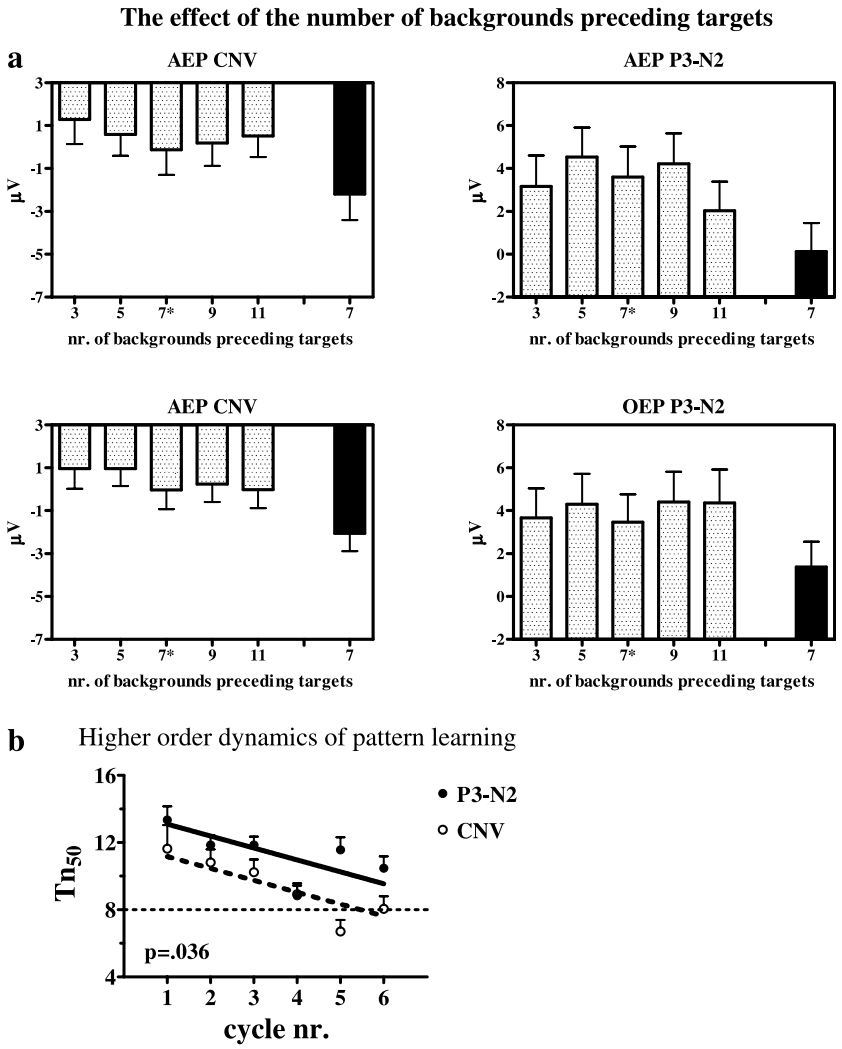

Fig. 6. (a) Shows a bar graph estimating the amplitudes of the ERP CNV (on the left) and the ERP P3–N2 (on the right) for both the AEP session (top) and OEP session (bottom). Component amplitudes to random targets (preceded by 3, 5, 7*(taken as the first target from regular series), 9 or 11 background tones) are depicted in dotted bars, component amplitudes to regular targets (2nd–8th within each regular cycle preceded by seven background tones) are depicted in black bars. (b) Shows the linear regression of the Tn50s for the ERP CNV and P3–N2 as combined from both the AEP and OEP session. The *x*-axes depict cycle nos. (1–6) and the *y*-axes depict values of the Tn50 (as expressed in target position, 1–16) per cycle. As can be seen in the graph, the appearance of the ERP CNV preceded the decay of the ERP P3–N2 for each cycle. An *F*-test comparing the linear regression of the ERP P3–N2 with the linear regression of the CNV gives a significant difference of intercept.

(partly) ascribed to probability effects. Although during the total experiment global probability was kept constant (12.5% for both random and regular targets), local probability varied with respect to only the random targets which could be interspersed with 2–12 background tones. Although not statistically tested, and for explorative purposes only, we estimated probability effects of the CNV and P3–N2 component amplitudes by grouping targets preceded by 3, 5, 7 (though in random series), 9 or 11 background stimuli and compared them to targets preceded by seven background stimuli (from regular series). Fig. 6a depicts these results suggesting that the current findings cannot be ascribed due to (local) probability effects as described by others (Croft et al., 2003; Fitzgerald and Picton, 1981). Thus, when learning a regular sequence, the expectation, or predictability, of regular targets alone results in the increase of the CNV and the decreased of the P3–N2 amplitude (Donchin, 1981; Jentzsch and Sommer, 2001; Jongsma et al., 2005; Polich and Kok, 1995).

Thus, different ERP components may serve as markers for pattern learning. Moreover, these specific components (CNV, P3–N2) mapping pattern learning seem to be modality independent, since they appear in response to both deviant and omitted targets.

4.2. The dynamics of pattern learning

We observed that ERPs in response to randomly presented target stimuli contained a marked P3–N2 complex, possibly reflecting processes related to target evaluation. However, when target presentation became regular, the P3–N2 complex decreased and a marked CNV component

appeared. It is likely, that regular target presentation gives leads to a memory formation of the target-to-target interval. Such a memory formation could give rise to the development of the CNV component occurring ca. 300 ms before target presentation, possibly reflecting processed linked to target anticipation (Nobre, 2001).

Learning curves started at a plateau that remained stable during random target presentations, before falling rapidly following introduction of the regular targets and bottoming out after approx. 4 regularly presented targets. Detecting changes in discrete events requires spanning of the temporal interval between the events. The neural systems involved must create a representation of the event that can be retained for some interval of time (Hughes et al., 2001). For the detection of regularity, at least two consecutive targets with the same number of preceding background tones (7) are needed in order to perceive the regularity. In the current experiment, the time window for temporal integration of the detection of the regularity was thus ca. 13 s. These findings are in line with the instance theory of Logan (2002) – a memory-based theory of learning. Logan (2002) states that the formation of a memory trace for a stimulus, that is predictive for a subsequent stimulus, spans over the whole period collapsing between the stimuli at hand. The process of learning is then accompanied by a shift of attention towards those stimulus features that remain constant.

Interestingly, a previous study measuring ERPs in response to regularly presented targets found that an early (ca. 150 ms after target onset) central anterior distributed component detecting automatic change, the 'Mismatch Negativity' (MMN) disappeared when using short stimulus onset asynchronies (100 ms), but remained intact when targets were presented at regular positions when using longer stimulus onset asynchronies (1300 ms) (Sussman et al., 1998). The authors of this study argued that a slow presentation rate – leading to similar inter-target intervals as in our study (i.e. 6.5 s compared to 6.4 s) – exceeds the limits of the acoustic memory trace underlying this automated MMN. The MMN depends on a short-lived sensory memory, which appears to last about 6 s (Sussman et al., 1998). Therefore, in the current experiment, a longer-lasting auditory memory template must have been formed, spanning at least the full inter-target interval, which probably does not rely on fully automated and involuntary processes.

4.3. Higher-order dynamics of pattern learning

With respect to higher order dynamics of implicit learning, we observed that – within the first presentation cycle – the CNV starts to develop between the 3rd and 4th regularly presented target, and the P3–N2 complex decreases between the 5th and 6th regularly presented target; however, with each repetition of the presentation cycle (cycle length 92 s), both the CNV and P3–N2 effect seems to occur earlier (see also Fig. 6b and Table 3). 'Learning' curves still described the data better than straight, horizontal, lines. Nevertheless, some of these curves returned improbable Tn50s, namely, at points before introduction of the target regularity (e.g., at cycles 4 and 5), probably due to an increase in variability in the single-trial data. The following observations are therefore somewhat speculative.

We observed that the CNV seems to develop prior to the decay of the P3–N2 complex. Thus, after two or three regular targets, a marked CNV develops – apparently expressing target anticipation. Initially, the P3–N2 complex remains intact at the 3rd and 4th regular target presentations. However, when the CNV is fully developed, the P3–N2 complex starts to decrease. It is likely that the CNV early in the regular sequence follows from a 'guess' that some regularity has installed and that it is worth preparing to detect a target. The continuing P3–N2 would reflect evaluation of the situation to confirm the speculation, while later, when the anticipation has been confirmed, the stimulus evaluation decreases. We suggest that the brain seems to be set to finding information in the environment that might lead to target anticipation rather than target evaluation, even without awareness on the part of the participant.

With respect to the delayed response RTs, only significant 'learning' curves were observed for the cycles 3–4 within the auditory session and cycles 3–4 in the omission session. Apparently, delayed response RTs provide a more variable, less robust measure than the ERP components on a single-trial level. Also, in the current experiment, a delayed response task was employed. Participants did not respond directly to the target stimulus, but to the background stimulus following the target. Therefore, effects of target detection would have affected RTs less. This is in Line with Jentzsch and Sommer (2001) who also reported higher variability in RTs than P300 amplitudes. This higher variability might be ascribed to the fact that delayed response RTs are sensitive to more factors – besides the expectancy of the target – for example response strategy and motivational aspects of the participant.

4.4. Conclusions

Our findings imply that dynamic cognitive processes like pattern learning can be studied with the aid of methods such as single-trial ERP measurements. Whereas ERPs have classically been measured within paradigms that avoid systematic trial-to-trial variations (thus allowing averaging procedures), the 'learning-oddball' paradigm described in this study allows us to specifically study systematic trial-to-trial variations. Thus, single-trial ERP research can add to one of the most fascinating and basic subjects of cognitive research, namely learning. Implementing similar single-trial ERP paradigms could also lead to clinically useful tools assessing the ability or speed of pattern learning in different patient groups.

Acknowledgements

This project was supported by The Netherlands Organization for Scientific Research, (NWO) VENI project no. 451-02-026 "It's all in the rhythm" to Marijtje L.A. Jongsma and by a grant from the Research Council of Norway (#155242/300) and Helse-Bergen, Norway (#911101) to Kenneth Hugdahl. All data were collected at the lab facilities of the Department of Biological and Medical Psychology, Division of Cognitive Neuroscience, University of Bergen, Norway, with the help of G. Solhaug, H. Brendalsmo and L. Sørensen. We hereby gratefully acknowledge the reviewer of Clinical Neurophysiology for improving the original manuscript.

References

Aizenstein HJ, Stenger VA, Cochran J, Clark K, Johnson M, Nebes RD, Carter CS. Regional Brain Activation during concurrent implicit and explicit sequence learning. Cereb Cortex 2004;14:199–208.

American Encephalographic Society. Guidelines for standard electrode position nomenclature. J Clin Neurophysiol 1994;11:40–73.

Atienza M, Cantero JL, Quian Quiroga R. Precise timing accounts for posttraining sleep-dependent enhancements of the auditory mismatch negativity. NeuroImage 2005;26:628–34.

Baldwin KB, Kutas M. An ERP analysis of implicit structured sequence learning. Psychophysiology 1997;34:74–86.

Bauer H, Rebert C, Korunka C, Leodolter M. Rare events and the CNV – the oddball CNV. Int J Psychophysiol 1992;13:51–8.

Bennett IJ, Golob EJ, Starr A. Age-related differences in auditory event-related potentials during a cued attention task. Clin Neurophysiol 2004;115:2602–15.

Berns GS, Cohen JD, Mintun MA. Brain regions responsive to novelty in the absence of awareness. Science 1997;276:1272–5.

Besson M, Faïta F. An event-related potential (ERP) study of musical expectancy: Comparisons of musicians with non-musicians. J Exp Psychol Hum Percept Perform 1995;21:1278–96.

Birbaumer N, Elbert T, Canavan AGM, Rockstroh B. Slow potentials of the cerebral cortex and behavior. Physiol Rev 1990;70:1–41.

Bledowski C, Prvulovic D, Hoechstetter K, Scherg M, Wibral M, Goebel R, Linden DE. Localizing P300 generators in visual target and distractor processing: a combined event-related potential and functional magnetic resonance imaging study. J Neurosci 2004;24:9353–60.

Croft RJ, Gonsalvez CJ, Gabriel C, Barry RJ. Target-to-target interval versus probability effects on P300 in one- and two-tone tasks. Psychophysiology 2003;40:322–8.

Daffner KR, Mesulam MM, Scinto LF, Acar D, Calvo V, Faust R, Chabrerie A, Kennedy B, Holcomb P. The central role of the prefrontal cortex in directing attention to novel events. Brain 2000;123:927–39.

Delorme A, Makeig S. EEGLAB: an open source toolbox for analysis of single-trial EEG dynamics including independent component analysis. J Neurosci Methods 2004;134:9–21.

Donchin E. Presidential address, 1980. Surprise!...Surprise? Psychophysiology 1981;18:493–513.

Eichele T, Specht K, Moosmann M, Jongsma ML, Quiroga RQ, Nordby H, Hugdahl K. Assessing the spatiotemporal evolution of neuronal activation with single-trial event-related potentials and functional MRI. Proc Natl Acad Sci USA 2005;102:17798–803.

Eimer M, Goschke T, Schlaghecken F, Stürmer B. Explicit and implicit learning of event sequences: evidence from event-related brain potentials. J Exp Psychol Learn Mem Cog 1996;22:970–87.

Fitzgerald PG, Picton TW. Temporal and sequential probability in Evoked Potential studies. Can J Psychol 1981;35:188–200.

Friston K. A theory of cortical responses. Philos Trans R Soc Lond B Biol Sci 2005;360:815–36.

Gaillard AWK. Problems and paradigms in ERP research. Biol Psychol 1988;26:91–109.

Gonsalvez CJ, Gordon E, Anderson J, Pettigrew G, Barry RJ, Rennie C, Meares R. Numbers of preceding nontargets differentially affect responses to targets in normal volunteers and patients with schizophrenia: a study of event-related potentials. Psychiatr Res 1995;58:69–75.

Gonsalvez CJ, Polich J. P300 amplitude is determined by target-to-target interval. Psychophysiology 2002;39:388–96.

Halgren E, Marinkovic K, Chauvel P. Generators of the late cognitive potentials in auditory and visual oddball tasks. Electroencephalogr Clin Neurophysiol 1998;106:156–64.

Honda M, Deiber MP, Ibáñez V, Pascual-Leone A, Zhuang P, Hallett M. Dynamic cortical involvement in implicit and explicit motor sequence learning. A PET study. Brain 1998;121:2159–217.

Hohnsbeim J, Falkenstein M, Hoormann J. Performance differences in reaction tasks are reflected in event-related brain potentials (ERPs). Ergonomics 1998;41:622–33.

Horovitz SG, Skudlarski P, Gore JC. Correlations and dissociations between BOLD signal and P300 amplitude in an auditory oddball task: a parametric approach to combining fMRI and ERP. Magn Reson Imaging 2002;20:319–25.

Huettel SA, Mack PB, McCarthy G. Perceiving patterns in random series: dynamic processing of sequence in prefrontal cortex. Nature Neurosci 2002;5:485–90.

Hughes HC, Darcey TM, Barkan HI, Williamson PD, Roberts S, Aslin CH. Responses of human association cortex to the omission of an unexpected acoustic event. NeuroImage 2001;13:1073–89.

Jentzsch I, Sommer W. Sequence-sensitive subcomponents of P300: Topographical analyses and dipole source localization. Psychophysiology 2001;38:607–21.

Jongsma MLA, Eichele T, Quian Quiroga R, Jenks KM, Desain P, Honing H, van Rijn CM. The effect of expectancy on omission evoked potentials (OEPs) in musicians and non-musicians. Psychophysiology 2005;42:191–201.

Jongsma MLA, Quian Quiroga R, van Rijn CM. Rhythmic training decreases latency-jitter of omission evoked potentials (OEPs). Neurosci Lett 2004;355:189–92.

Karakas S, Erzengin ÖU, Basar E. The genesis of humane event-related responses explained through the theory of oscillatory neural assemblies. Neurosci Lett 2000;285:45–8.

Katayama J, Polich J. Auditory and visual P300 topography from a 3 stimulus paradigm. Clin Neurophysiol 1999;110:463–8.

Kiss I, Dashieff RM, Lordeon P. A parieto-occipital generator for P300: evidence from human intracranial recordings. Int J Neurosci 1989;49:133–9.

Koelsch S, Kasper E, Sammler D, Schulze K, Gunter T, Friederici AD. Music, language and meaning: brain signatures of semantic processing. Nat Neurosci 2004;7:302–7.

Korunka C, Wenzel T, Bauer H. The 'oddball CNV' as an indicator of different information processing in patients with panic disorders. Int J Psychophysiol 1993;15:207–15.

Lang S, Kotchoubey B. Learning effects on event-related brain potentials. Neuroreport 2000;11:3327–31.

Llinas RR. I of the vortex: from neurons to self. Cambridge: The MIT Press; 2001.

Logan GD. An instance theory of attention and memory. Psychol Rev 2002;109:376–400.

McAdam DW. Slow potentials changes recorded from human brain during learning of a temporal interval. Psychon Sci 1966;6:435–6.

McCarthy G, Wood CC, Williamson PD, Spencer DD. Task-dependent field potentials in human hippocampal formation. J Neurosci 1989;9:4253–68.

Naatanen R, Gaillard AW, Varey CA. Attention effects on auditory EPs as a function of inter-stimulus interval. Biol Psychol 1981;13:173–87.

Nobre AC. Orienting attention to instants in time. Neuropsychologia 2001;39:1317–28.
Nuchpongsai P, Arakaki H, Langman P, Ogura C. N2 and P3b components of the event-related potential in students at risk for psychosis. Psychiatry Res 1999;88:131–41.
Ochoa CJ, Polich J. P300 and blink instructions. Clin Neurophysiol 2000;111:93–8.
Pfeuty M, Ragot R, Pouthas V. Processes involved in tempo perception: A CNV analysis. Psychophysiology 2003;40:69–76.
Picton TW. The P300 wave of the human event-related potential. J Clin Neurophysiol 1992;9:456–79.
Polich J. Meta-analyses of P300 normative aging studies. Psychophysiology 1996;33:334–53.
Polich J, Kok A. Cognitive and biological determinants of P300: an integrative review. Biol Psychol 1995;41:103–46.
Pritchard WS. Psychophysiology of P300. Psychol Bull 1981;89:506–40.
Quian Quiroga R, Garcia H. Single-trial event-related potentials with wavelet denoising. Clin Neurophysiol 2003;114:376–90.
Quian Quiroga R, van Luijtelaar G. Habituation and sensitization in rat auditory evoked potentials: a single-trial analysis with wavelet denoising. Int J Psychophysiol 2002;43:141–53.
Reber AS. Implicit learning of artificial grammars. J Verb Learn Verb Behav 1967;5:855–63.
Reber AS. Implicit learning and tacit knowledge. J Exp Psychol Gen 1989;118:219–35.
Rose M, Verleger R, Wascher E. ERP correlates of associative learning. Psychophysiology 2001;38:440–50.
Rugg MD, Coles MGH. Electrophysiology of Mind. Event related brain potentials and cognition. London: Oxford University Press; 1995.
Rüsseler J, Hennighausen E, Münte TF, Rösler F. Differences in incidental and intentional learning of sensorimotor sequences as revealed by event-related potentials. Cogn Brain Res 2003;15:116–26.
Rüsseler J, Rösler F. Implicit and explicit learning of event sequences: evidence for distinct coding of perceptual and motor representation. Acta Psychol 2000;104:45–67.
Salamon E. Mechanisms of knowledge learning and acquisition. Med Sci Monit 2002;8:RA133–=0?>RA139.
Sambeth A, Maes JHR, van Luijtelaar G, Molenkamp IBS, Jongsma MLA, van Rijn CM. Auditory event-related potentials in humans and rats: effects of task manipulation. Psychophysiology 2003;40:1–9.
Schendan HE, Searl MM, Melrose RJ, Stern CE. An fMRI study of the role of the medial temporal lobe in implicit and explicit sequence learning. Neuron 2003;37:1013–25.
Schlaghecken F, Stürmer B, Eimer M. Chunking processes in the learning of event sequences: Electrophysiological indicators. Mem Cognit 2000;28:821–31.
Seger CA. Implicit learning. Psychol Bull 1994;115:163–96.
Smith ME, Halgren E, Sokolik M, Baudena P, Musolino A, Liegeois-Chauvel C, Chauvel P. The intracranial topography of the P3 event-related potential elicited during auditory oddball. Electroencephalogr Clin Neurophysiol 1990;76:235–48.
Spencer KM. Averaging, Detection, and Classification of single-trial ERPs. In: Handy TC, editor. Event related potentials. A methods handbook. Cambridge: The MIT Press; 2005. p. 209–28.
Squires KC, Wickens C, Squires NK, Donchin E. The effect of stimulus sequence on the waveform of the cortical event-related potential. Science 1976;193:1142–6.
Sussman E, Ritter W, Vaughan Jr HG. Predictability of stimulus deviance and the mismatch negativity. Neuroreport 1998;9:4167–70.
Sutton S, Braren M, Zubin J. Evoked-Potential correlates of stimulus uncertainty. Science 1965;150:1187–8.
Talnov AN, Quian Quiroga R, Meier M, Matsumoto G, Brankack J. Entorhinal inputs to dentate gyrus are activated mainly by conditioned events with long time intervals. Hippocampus 2003;13:755–65.
Tarkka IM, Stokic DS, Basile LF, Papanicolaou AC. Electric source localization of the auditory P300 agrees with magnetic source localization. Electroencephalogr Clin Neurophysiol 1995;96:538–45.
Walter WG, Cooper R, Aldridge VJ, McCallum WC, Winter AL. Contingent Negative Variation: an electric sign of sensorimotor association and expectancy in the human brain. Nature 1964;203:380–4.
Zappoli R. Permanent or transitory effects on neurocognitive components of the CNV complex induced by brain dysfunctions, lesions and ablations in humans. Int J Psychophysiol 2003;48:189–220.

Paper II

Eichele T, Specht K, Moosmann M, Jongsma ML, Quiroga RQ, Nordby H, Hugdahl K. (2005) Assessing the spatiotemporal evolution of neuronal activation with single-trial event-related potentials and functional MRI. *Proceedings of the National Academy of Sciences of the United States of America*. 102(49):17798-803.

Assessing the spatiotemporal evolution of neuronal activation with single-trial event-related potentials and functional MRI

Tom Eichele*†‡, Karsten Specht*†, Matthias Moosmann*§, Marijtje L. A. Jongsma¶, Rodrigo Quian Quiroga‖, Helge Nordby*, and Kenneth Hugdahl*,**

*Department of Biological and Medical Psychology, University of Bergen, 5009 Bergen, Norway; §Berlin Neuroimaging Center–Charité, Campus Mitte, 10117 Berlin, Germany; ¶Nijmegen Institute for Cognition and Information, Department of Biological Psychology, Radboud University of Nijmegen, P.O. Box 9104, 6500 HE, Nijmegen, The Netherlands; ‖Department of Engineering, University of Leicester, LE1 7RH Leicester, United Kingdom; and **Division of Psychiatry, Haukeland University Hospital, 5009 Bergen, Norway

Edited by Marcus E. Raichle, Washington University School of Medicine, St. Louis, MO, and approved October 17, 2005 (received for review June 30, 2005)

The brain acts as an integrated information processing system, which methods in cognitive neuroscience have so far depicted in a fragmented fashion. Here, we propose a simple and robust way to integrate functional MRI (fMRI) with single trial event-related potentials (ERP) to provide a more complete spatiotemporal characterization of evoked responses in the human brain. The idea behind the approach is to find brain regions whose fMRI responses can be predicted by paradigm-induced amplitude modulations of simultaneously acquired single trial ERPs. The method was used to study a variant of a two-stimulus auditory target detection (oddball) paradigm that manipulated predictability through alternations of stimulus sequences with random or regular target-to-target intervals. In addition to electrophysiologic and hemodynamic evoked responses to auditory targets *per se*, single-trial modulations were expressed during the latencies of the P2 (170-ms), N2 (200-ms), and P3 (320-ms) components and predicted spatially separated fMRI activation patterns. These spatiotemporal matches, i.e., the prediction of hemodynamic activation by time-variant information from single trial ERPs, permit inferences about regional responses using fMRI with the temporal resolution provided by electrophysiology.

multimodal imaging | P3 pattern learning | target detection

Functional MRI (fMRI) of the blood oxygenation level-dependent (BOLD) response (BOLD-fMRI) measures local changes in brain hemodynamics associated with a cognitive process noninvasively with a high spatial resolution. However, an unsolved issue in fMRI research is the insufficient temporal resolution of the BOLD response. In contrast to the spatial resolution of BOLD-fMRI, event-related potentials (ERP) access the current induced by synaptic activity instantaneously, with an effective temporal resolution on the order of tens to hundreds of milliseconds in case of long-latency cortical responses. However, the location of underlying generators cannot be inferred with certainty. In combination, these two complementary noninvasive methods would allow for joint high-resolution spatial and temporal mapping of the mental process under investigation and add to a more complete understanding of the neural correlates of perception and cognition (1–3). In humans, this integrated spatial and temporal precision could so far be obtained only in direct intracranial recordings, usually performed in patients receiving brain surgery for treatment of epilepsy (4–7).

There are basically three approaches to multimodal integration: (*i*) through fusion, usually referring to the use of a common forward or generative model that can explain both the electroencephalogram (EEG) and fMRI data (8, 9); (*ii*) through constraints, where spatial information from the fMRI is used for a (spatiotemporal) source reconstruction of the EEG (10–12); and (*iii*) through prediction, where the fMRI signal is modeled as some measure of the EEG convolved with a hemodynamic response function, a principle used in our study.

Invasive recordings in animals have shown that the BOLD response is approximately linearly related to local changes in the underlying neuronal activity. The relationship appears to be stronger for the afferent pre- and postsynaptic processing, which produces the local field potential (LFP), than it is for the output from the neuron, i.e., spike rate or multiunit activity (13–16). The LFP is the basis for the scalp EEG and ERP when coherent at a more macroscopic scale (17), implying that spatiotemporal data integration can be achieved by investigating correlations between BOLD and scalp EEG/ERP. This can be done either continuously over time, as in the study of background rhythms (18–20) and epileptic discharges (21, 22) in the EEG, or in the context of inducing variation in a given cognitive operation (23–25). When a consistent relationship is detected, one can infer that the corresponding fMRI activation either directly represents the electric source or modulates remote generators (18–25). However, the temporal evolution of neuronal activation has not been addressed. To resolve this issue, we used the trial-to-trial variability of single-trial ERPs (26, 27) recorded simultaneously with the fMRI as predictors for hemodynamic responses to a variant of an auditory target detection (oddball) paradigm. In this design, infrequent targets were interspersed with frequent standard stimuli at random or regular intervals in an alternating way (see also Fig. 5, which is published as supporting information on the PNAS web site). Sequences of regularly spaced targets, i.e., patterns embedded in this design, affect the subjective predictability/expectancy (28, 29), and pilot experiments indicated that several components, at different latencies in the ERP, are modulated according to a sigmoid function of the number of times an interval is repeated, and learned. These amplitude modulations (AMs) develop across trials, on a timescale slow enough to be sampled with fMRI, and should be consistently correlated with the BOLD response in discrete brain regions across the observation time, assuming temporally and spatially independent neuronal generators (Fig. 1). fMRI responses that can be predicted by AMs in the ERP can be tied to the processing engaged at the time of the AMs. The approach thus allows inferences about

This work was presented in part in poster form at the Helsinki School in Cognitive Neuroscience, March 2–11, 2005, Lammi, Finland, and at the Annual Meeting of the Organization for Human Brain Mapping, June 12–16, 2005, Toronto, ON, Canada.

Conflict of interest statement: No conflicts declared.

This paper was submitted directly (Track II) to the PNAS office.

Freely available online through the PNAS open access option.

Data deposition: The neuroimaging data have been deposited with the fMRI Data Center, www.fmridc.org (accession no. 2-2005-120AE).

Abbreviations: ERP, event-related potential; fMRI, functional MRI; BOLD, blood oxygenation level-dependent; EEG, electroencephalogram; AM, amplitude modulation; TTI, target-to-target interval.

†T.E. and K.S. equally contributed to this work.

‡To whom correspondence should be addressed. E-mail: tom.eichele@psybp.uib.no.

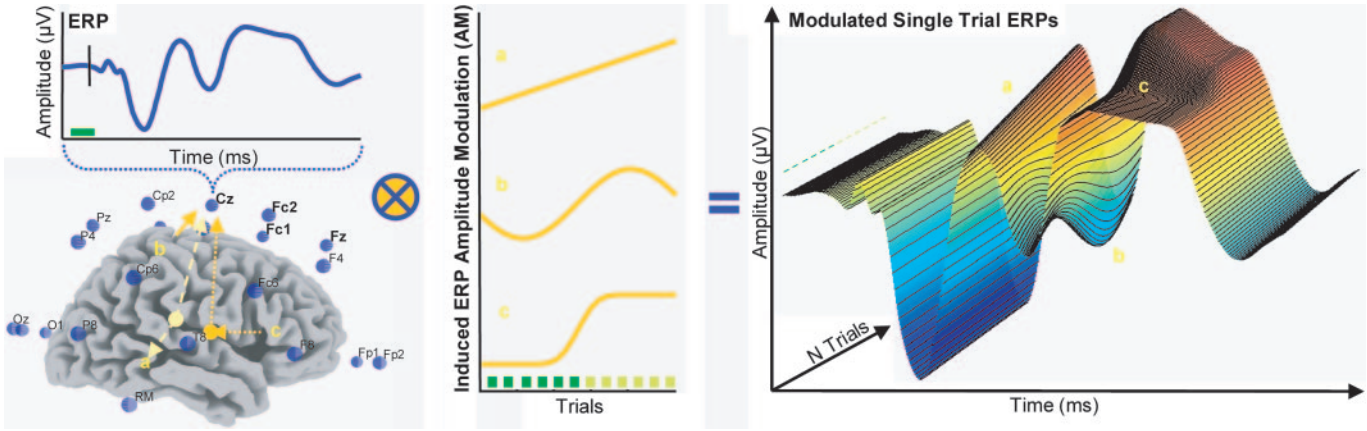

Fig. 1. Illustration of how ERP AM can achieve high temporal resolution in fMRI. A suitable paradigm in a simultaneous ERP-fMRI recording can be used to induce slow and localized AM (a, b, and c) at or below the sampling frequency of the MR data acquisition. In this example, the model AM are generated in separate areas sensitive to the manipulation and are detectable in both ERP and fMRI. Consecutive correlation analysis between the fMRI time series and the multiple ERP time series yields complementary information regarding the spatial location and timing of these processes. Neuroelectric source acitivities need not necessarily propagate to the scalp directly but can modulate or be modulated by remote sources (indicated by arrows).

regional responses using fMRI with the effective temporal resolution afforded by the ERP.

Methods

Subjects. Fifteen healthy right-handed participants (21–28 years, seven female and eight male) took part in the experiment after providing a written statement of informed consent.

Stimuli. The stimuli used in the pattern learning paradigm consisted of 50-ms chords presented continuously during the sparse sampling fMRI acquisition in an eyes-closed condition via headphones (≈80 dB) with an onset asynchrony of 2 s. Infrequent "targets" (500 Hz, 25% probability) were interspersed with frequent "standards" (250 Hz, 75% probability). For a total of 216 targets, alternating sequences of six consecutive targets were presented either with a random target-to-target interval (TTI) ranging from 4 to 22 s or with a regular 8-s TTI (Fig. 5). Each of these 12-target cycles lasted on the average 96 s. When detecting a target, participants were instructed to press a response button in the middle of the interval between the target and the next standard stimulus. The delayed-response mode was chosen to focus on stimulus-related perceptual and cognitive effects associated with predictability. The instruction hampers the expected behavioral effect, i.e., response-time speeding, and thus minimizes the confounding effect of motor-related potentials on the auditory evoked potential. Participants received a training session with random targets and were not informed about the presence of regularity beforehand.

fMRI Data Acquisition and Preprocessing. Imaging was performed on a 1.5-T Siemens (Erlangen, Germany) scanner. Scanning of anatomy was done with a T1-weighted MPRAGE sequence. Thereafter, 300 BOLD-sensitive echo planar images (EPI) were collected in two sessions, with a 10- to 15-min break in between. EPI volumes were anterior–posterior comissure line aligned and consisted of 18 axial slices with 5.5-mm thickness including a 0.5-mm interslice gap [flip angle 90°; echo time 60 ms; field of view 220 × 220 mm; matrix 64 × 64 voxel). We used a sparse-sampling acquisition design (30) with 8 s repetition time (TR) and 2 s acquisition time, leaving a 6 s silent gap. This allowed EEG recording without scanner noise and gradient artifacts. Baseline data were collected at the beginning and end of each session, nullevents were defined as EPI volumes with only standard stimuli during the TR. Preprocessing and statistical analyses were carried out by using SPM2 (Wellcome Department of Imaging Neuroscience, University College London, London) running in MATLAB (Mathworks, Natick, MA). All images were realigned to the first image in the time series to correct for head movement and normalized to the Montreal Neurological Institute reference space. Normalized data were resliced to a voxel size of 3 mm^3, smoothed with an 8-mm full-width half-maximum Gaussian kernel, and high-pass-filtered (256 s).

EEG Data Acquisition and Preprocessing. EEGs were recorded at 5-kHz sampling frequency with a MR-compatible amplifier (Brain Products, Munich) placed inside the MR scanner. Subjects were fitted with an elastic cap (BraincapMR, FMS, Falk Minow Services, Herrsching, Germany) containing 28 Ag/AgCl electrodes (FP1, FP2, F7, F3, Fz, F4, F8, T7, C3, Cz, C4, T8, P7, P3, Pz, P4, P8, O1, OZ, O2, FC5, FC1, FC2, FC6, CP5, CP1, CP2, and CP6). Vertical eye movement was acquired from below the right eye; the electrocardiogram was recorded from the subject's back. Channels were referenced to FCz, with a forehead ground and impedances kept below 5 kΩ. EEGs were downsampled offline to 500 Hz and filtered from 1 to 45 Hz. Target epochs from −312 to 712 ms around stimulus onsets were subjected to independent components analysis (ICA), implemented in EEGLAB (31) (Institute for Neural Computation, University of California, San Diego) running in MATLAB. Components related to pulse and eye-movement artifacts were removed from the data. After recalculation to average reference, single trials were wavelet-denoised (26). Coefficients were selected on the basis of ICA-corrected ERPs and were the same for all participants and electrodes. For targets (9%) that were presented within the echo planar image volume acquisition, the ERP was estimated as the mean of two surrounding targets. The data were then downsampled to 125 Hz, smoothed to account for intra- and intersubject latency variability, and high-pass-filtered across trials (216 s). For all these 8-ms frames from −100 to 600 ms (n = 88) around stimulus onset, separate single-trial amplitude vectors were extracted and entered into the joint ERP-fMRI analysis.

Joint ERP-fMRI Analysis. The fMRI time series were modeled with a design that was deployed sequentially for all frames of the ERP time series and replicated for four frontal-central electrodes (Fz, FC1, FC2, and Cz), i.e., those electrode sites where paradigm-induced amplitude modulations were maximally expressed. For each of these designs, two regressors were formed by convolving stimulus functions with a canonical hemodynamic response function. The first stimulus function encoded a generic obligatory response to target stimuli of constant amplitude, applicable to

regional fMRI responses associated with "exogenous" features of the auditory evoked response and the motor task. The second stimulus function encoded the amplitude of the single-trial ERPs measured at each frame to find brain regions whose responses could be predicted by paradigm-induced amplitude modulations at that time frame/electrode, thus sensitive to predictability/pattern learning. This function was decorrelated (Schmidt–Gram orthogonalization) from the first, ensuring that activation related to the second function was specific to the electrophysiological measure and not to some general feature in the evoked response to targets. The regressors were entered into single-subject fixed-effects regression analyses; on the group level, random effects analyses were performed by entering the contrast images of each subject into one-sample *t* tests. fMRI activation to targets (first regressor) is significant at $P < 0.05$, family-wise error corrected, extent 10 voxel. AM-related activations (second regressor) are significant at $P < 0.001$ on the voxel level, cluster extent threshold $P < 0.01$, unless otherwise stated uncorrected for multiple comparisons. This threshold appears adequate in this experiment, because we were interested in the profile of responses and their colocalization with the auditory evoked responses per se, with maximal sensitivity. To minimize the risk of reporting Type I false-positive activation, we applied a descriptive criterion: results were considered reliable and reported only when same/similar activation patterns are replicated in adjacent time points and in two or more of the electrodes. A schematic of the analysis procedure is given in Fig. 2.

Curve Fitting. To illustrate the principal ERP amplitude modulations, hypotheses were tested by nonlinear regression analysis of N1, P2, N2, and P3 amplitudes in the frontocentral region of interest (i.e., the average of Fz, FC1, FC2, and Cz) and the response times. H0 assumed that the measure is insensitive to patterning, represented by a straight horizontal line; H1 assumed that the measure is sensitive to patterning and decreasing or increasing its amplitude, best described as a sigmoid function.

Results

Upon debriefing, all participants noted that targets had occasionally appeared rhythmically, indicating that they explicitly apprehended regular target sequences in the experiment. However, none of them was able to recollect whether these regular patterns were of constant length, or whether regular patterns alternated with random target sequences in succession, suggesting that the overall order of the experiment remained either unrecognized or was implicitly acquired.

Average ERPs. The sequence of cerebral processes leading to discrimination of a target stimulus in an active oddball condition may be indexed by a number of generic ERP components: N1, P2, mismatch negativity (MMN), N2b, P3a, and P3b (32). The extent to which components are detectable in the waveforms depends on experimental parameters. N1 and P2 typically tend to be enhanced under "attend" compared with "ignore" conditions (33). MMN, being an automatic response to changes in auditory stimulation, may be difficult to estimate because of overlapping components like the N2b, which is elicited by infrequent events in attended input, or when the difference between standard and deviant stimuli is relatively large, as in a standard oddball paradigm (32). N2b is usually followed by P3a, indicating a passive shift of attention, and the P3b (also labeled P3 or P300), which is particularly sensitive to task relevance, target probability, sequence, and TTI (23, 28, 29, 34–36). Fig. 3 displays the grand-average ERPs to standards, regular and random TTI target categories, along with results from a pointwise *t* statistic. After a sequence of midlatency responses and P1 (70–80 ms), a broad centrally distributed N1 (100–120 ms) emerges, followed by a more central-parietal P2 (160–180 ms). The dominant feature in the ERPs to both target categories in comparison with the standard is a frontal-central N2 (200–220 ms), followed by a double-peaked P3 (270–360 ms). The earlier peak at 270 ms is more prominent frontocentrally, the later peak is prominent at parietal sites. TTI regularity in the averaged waveforms most strongly affects N2 and P3 amplitudes but is also seen as a P2 decrement and reduced N1 enhancement.

Curve Fitting. Response times were on average 905 ms (SD 200) and remained unaffected by the presence of patterns ($F = 0.22$, not significant), indicating that participants followed the delayed-response instruction.

N1 amplitudes were also insensitive to regularity ($F = 0.31$, not significant). All three subsequent components were found to be sensitive to patterns, showing amplitude effects that were best fitted with sigmoid curves: P2 ($F = 5.60$, $P < 0.005$), N2 ($F = 15.64$, $P < 0.0001$), and P3 ($F = 29.89$, $P < 0.0001$). The estimated turning points of these functions were all between the second and third target presentation in regular sequences. The effect strength gradually increased across components, indicative of either higher intra- and intersubject consistency at later timepoints or more stable single-trial estimates. Although the global effect could be well approximated with a sigmoid learning curve, the raw data expressed unique shape variations (Fig. 4 *Left*).

fMRI–Target Processing. Areas constantly contributing to target processing in a uniform fashion were found in the superior temporal gyri of both hemispheres extending into the insula and hippocampal formation, the inferior parietal lobe, anterior cingulate gyrus, supplementary motor area, pre- and postcentral gyri (left>right), cuneus, and the middle and superior frontal gyri (right>left), (Fig. 4 and Table 1, which is published as supporting information on the PNAS web site).

AM-Correlated fMRI. The entire spatiotemporal activation results for all four electrodes and timepoints, along with plots of the average scalp topography, waveform, and AM, were compiled into Movies 1 and 2, which are published as supporting information on the PNAS web site.

Here, we focus on the maxima of the three most consistent AM-correlated fMRI activation patterns: P2 (≈170 ms), N2 (≈200 ms), and P3 (≈320 ms).

Inverse relations between BOLD and AM on P2 were seen in posterior cingulate, precuneus, supramarginal gyri, left parietal, and frontal areas (Fig. 4; see also Table 2, which is published as supporting information on the PNAS web site). Inverse relations were also seen for N2, with the most consistent region across electrodes being located in the right medial frontal gyrus. Additional clusters were in the right and left superior frontal gyri, left subcallosal gyrus, left hippocampus, and right amygdala (Fig. 4; see also Table 3, which is published as supporting information on the PNAS web site). Note that these latter results stem from the Cz electrode, where the clusters pass FDR correction, but are also seen at FC1 and FC2 at a lower cluster extent threshold. We observed positive linear relations between BOLD responses and the P3 AM (≈320 ms), mainly in the middle and inferior frontal gyri, inferior parietal lobule, and middle temporal gyri in the right hemisphere. Smaller additional activations were also observed in the right insula, right postcentral gyrus, left supramarginal, and middle frontal gyri (Fig. 4; see also Table 4, which is published as supporting information on the PNAS web site). There was no consistent amplitude modulation of N1 (100 ms), such that it did not differ from the stimulus function and thus did not support a significant regression.

Except for a close spatial relationship between P2- and P3-related regions in the left supramarginal gyrus (mm distance X 0–3, *y*, 9; and *z*, 8), there was no considerable overlap among the AM activations. There was also no direct match between any of the AM- and target/response-related local maxima. Note that the delayed-response instruction used in this experiment effectively pruned the salient speeding of response times induced by target predictability.

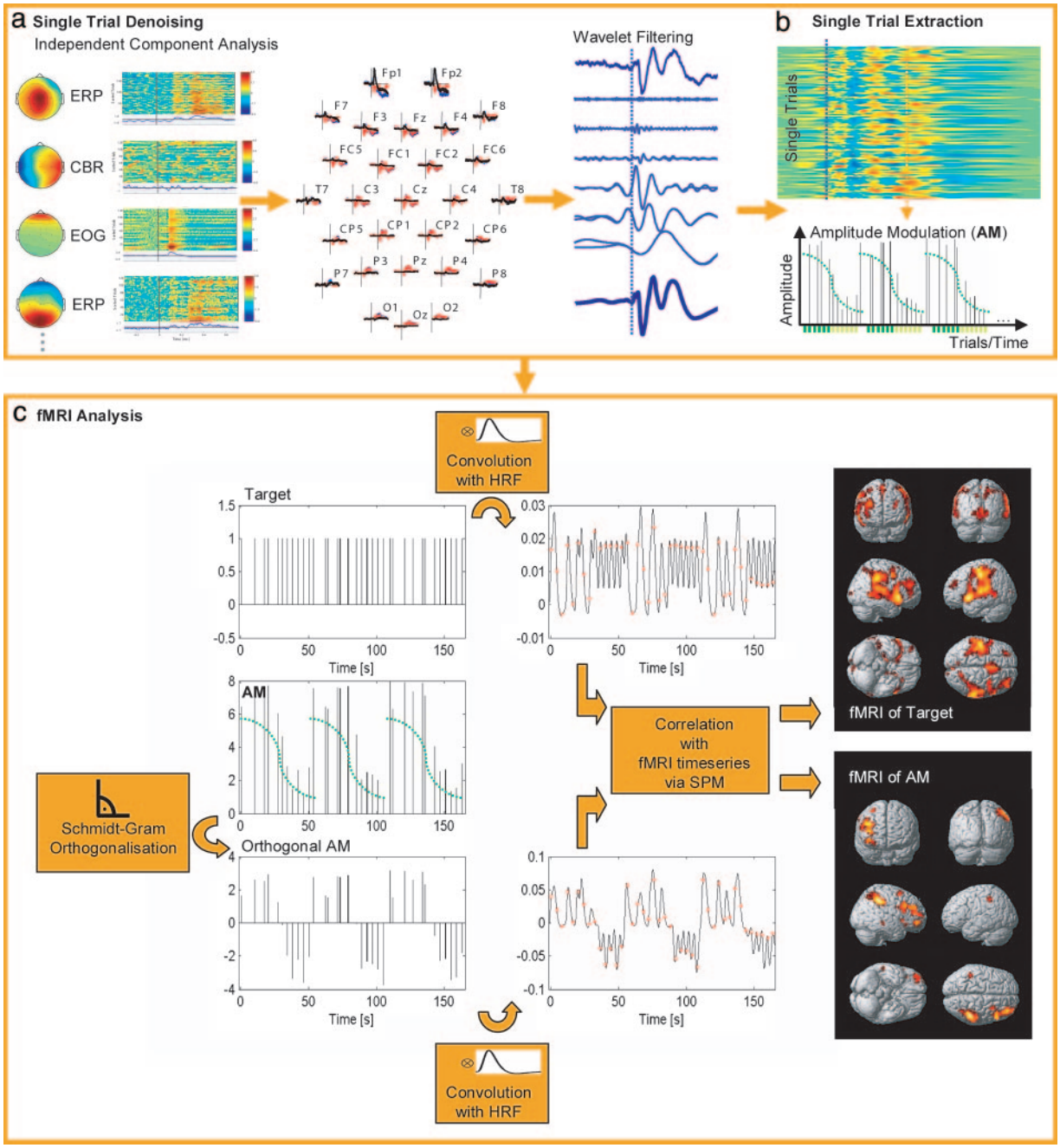

Fig. 2. Flowchart of the single-trial ERP and fMRI analysis. Data are decomposed with independent components analysis (*a*), and artifact topographies (cardioballistic, eye movement) are removed. Effects of component removal on the ERPs are shown in a representative subject (*Upper Center*). Subsequently, wavelet denoising (*b*) is applied to the single trials. AM vectors are derived separately for each time point and electrode. To ensure specificity, shared variance between target presentation and AM is removed by orthogonalization. The regressors are convolved with canonical hemodynamic response functions (HRF) to account for the neurovascular coupling before voxelwise correlations with the fMRI signal (*c*).

Consequently, we did not observe ERP-related fMRI activation in areas in the motor system(s) that were found sensitive to sequence learning elsewhere (37, 38).

Discussion

When studying the neuronal substrates of cognitive processes, the researcher typically considers both their spatial and temporal properties. There is, however, a disparity between the major methods in human cognitive neuroimaging, focusing either on the "where" (e.g., fMRI) or "when" (e.g., ERPs), thus providing only a limited window into the neuronal correlates. We propose here that a key to merging both methods is to exploit the functional resolution, that is, how signatures of an experimental manipulation are correlated. The crucial aspect of this approach for spatiotemporal integration is to make effective use of single-trial variability in the entire ERP time series to predict regional fMRI activations, i.e., using time-variant effects induced by a manipulation as a vehicle to achieve a temporal expansion of the fMRI. The prospect of this conjunction is that it allows application of an electrophysiologically derived temporal order to fMRI activation that aids in determining the hierarchy and "serial" functional connectivity of brain regions associated with

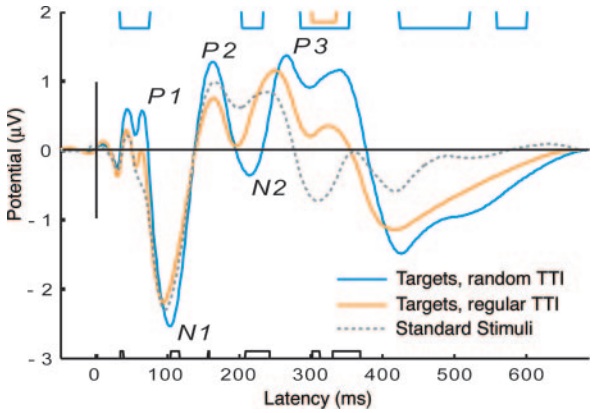

Fig. 3. Grand-average ERP at frontocentral sites. Waveforms are shown from −100 to 600 ms around stimulus onset for all targets at the third to sixth position of all random TTI cycles (blue), all targets at the third to sixth position of all regular TTI cycles (orange), and all standards not immediately before or after a target (gray dotted). Effects of target predictability appear most prominently as amplitude reductions of N2 and P3 and, to a lesser degree, P1, N1, and P2 are also affected. Above the waveform, significant differences ($P < 0.05$) from a pointwise t statistic are plotted as blue rectangles for random target vs. standard comparison and in orange for the regular target vs. standard comparison. Black rectangles below the waveform indicate significant differences between the random and regular target categories.

a process, in this case recognition of temporal patterns in the auditory environment.

Later components in the ERPs are often attributed to "endogenous" or "top-down" processing (32). Recent models of brain function in the context of perceptual inference and learning focus on the hierarchical nature of cortical systems and suggest that these components derive from high levels of processing (ref. 39; for an overview, see ref. 40). We therefore expected that the regionally specific correlates of target predictability would most likely be located outside the sensory regions, in multimodal higher-order cortical areas. Conversely, the fMRI correlates of earlier exogenous components (32), insensitive to the manipulation, would be localized in the vicinity of sensory regions. For this reason, we did not constrain our search for AM-related effects to the main effects of auditory stimulation but used a whole-brain search for the latency-specific correlates. The regional deployment of our activations conformed roughly to our general prediction that later components were coherent with metabolic or synaptic activity in higher cortical areas.

Activation associated with auditory target processing, insensitive to predictability, was seen maximally expressed in the superior temporal gyri and in further areas associated with auditory and visual target detection (12, 41, 42).

Three independent stages separated from peak to peak by 30 ms (P2-N2), 120 ms (N2-P3), and 150 ms (P2-P3) were additionally identified, where the amplitude modulations of single-trial ERP sequences selectively predicted fMRI activation.

The first stage reached maximum intensity during P2 (≈170 ms) after target onset. It is worth noting that the regions mediating the P2 effect overlap with those being associated with "default mode" brain activation (18, 43). P2 hosts processing negativities that indicate matching processes between the sensory input and a neuronal representation of stimuli selected for further processing and as such are markers of sensory memory and selective attention (32). The main sources of these components reside bilaterally in the temporal and frontal lobes (32). It is, however, conceivable that activated brain regions have a modulating effect on these components, allowing for optimization of resource allocation when target occurrence is predictable. This interpretation would also be consistent with the role appointed to the "default mode" (18, 43). In addition, fMRI/positron-emission tomography results of spatial and temporal attention, and sequencing are overlapping with the sites seen here (37, 38). The fMRI activation in the supramarginal and posterior cingulate gyri ≈170 ms matches with the onset latency of a widespread waveform that has been reported from intracranial recordings (5).

The second spatiotemporal stage during the N2 (≈200 ms) was located in the anterior frontomedian cortex and parahippocampal regions. Portions of the N2 reflect the attentive detection of a mismatch between stimulus features and an actively generated memory template. fMRI correlates of this memory process are

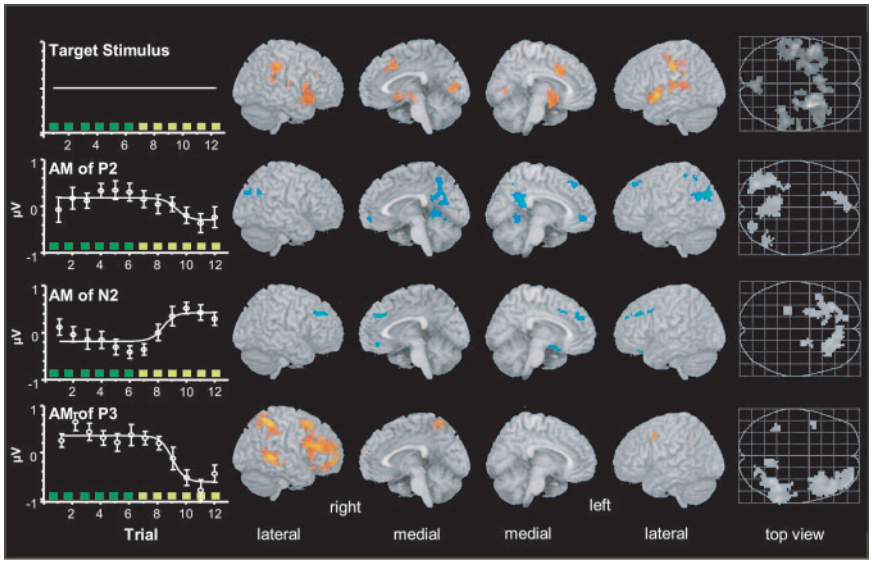

Fig. 4. AM-correlated fMRI results. Render views and maximum-intensity projections of the general target related activation and positive (red) and negative (blue) correlations with the respective AM. Each correlation map shows for each voxel the maximum t value from the four electrodes (FZ, FC1, FC2, and Cz). To the left of each rendering of the AM-correlated fMRI, the average AM (empty circles ± SEM) and the fitted sigmoid curves are shown. Top row, target-related activation, $P < 0.05$ (FWE), cluster size ≥10; second row, P2 (170 ms); third row, N2 (200 ms); and fourth row, P3 (320 ms). All AM-related activations were thresholded at $P < 0.001$ (uncorrected), cluster extent threshold $P < 0.01$.

observed in the same brain regions as activated in the present study (38, 42). Moreover, intracranial recordings in the vicinity of these regions have documented depth N2s in the same peak latency range (6, 7). Further, the scalp N2 to auditory targets is strongly reduced in patients with bilateral hippocampal damage (44), and the sigmoid AM is consistent with recent fMRI findings showing rapid prefrontal and hippocampal habituation to novel events (45).

The overall strongest and most extensive spatiotemporal stage was related to the P3 (≈320 ms) and yielded activations in frontal, temporal, and parietal regions most prominent in the right hemisphere. For all these regions, intracranial recordings have evidenced depth P3s with about the same peak latency (5–7). P3 has been suggested to index a mechanism that is elicited when a memory representation of the recent stimulus context is updated upon detection of deviance from it (36, 46, 47). The effects of a variety of manipulations (e.g., task relevance, information content, probability, and sequence) have been delineated in support of this view (36, 46, 47). fMRI activation in the P3-related regions is seen in a variety of related cognitive operations, including target processing (12, 23, 41, 42, 48), attention, working memory (38, 49) and sequencing (37). Although the rightward lateralization is not strictly predicted from scalp (46, 47) and intracranial measurements (4–7), hemodynamic activity to auditory target/novel stimuli has been shown to be greater in frontal, temporal, and parietal regions of the right hemisphere (42, 50). Also, our data co-localize with fMRI studies reporting right-lateralized attentional mechanisms that would host much of the functionality that is probed by target detection in general (49, 51–53) and, specifically, by manipulating target predictability (54, 55). One should note, however, that a portion of the lateralization might also be attributable to the left-lateralized activation around the central sulcus induced by the motor task, which could have minimized the relative contribution of the predictability effect in adjacent areas to the total variance of the fMRI signal.

The common feature in all three sequential spatiotemporal stages was the sigmoid-shaped response amplitude modulation coherently expressed in the ERP and fMRI, because the target-to-target interval was repeated and became predictable. One classic psychophysiological example for such behavior is the orienting response/reflex, which displays rapid habituation to regularly presented stimuli and dishabituation to deviants from a pattern of preceding stimuli (56, 57). Similarly, this principal mode of responding is overlapping with that of the mismatch negativity (32) and P3 components (36, 42, 46, 58). At the core, all these neuronal processes encompass detection of a salient change in the environment, comparison against a stored representation, and the elicitation of an adequate response. Models accounting for these effects, however, to an extent are conceptually incomplete in the sense that they focus more on why and how the brain responds to unexpected events than on how the representation, i.e., a prediction, is established in the first place. This aspect, however, can be accounted for by linking these orienting response/reflex-type responses with a Bayesian scheme that defines neuronal systems as reciprocally connected hierarchical generative models that construct context-dependent expectancies (39). The amplitude behavior of ERP components (and, correspondingly, the fMRI signal) would here represent the state of prediction error in the model, indicating to which degree "surprise" about the sensory input is suppressed (39): to detect the presence (or absence) of patterns in the environment means to extract contingency rules with highly salient predictive value for the anticipation of future events (39, 55, 59). In this context, our data capture the spatiotemporal dynamics associated with such perceptual inference and learning.

We thank Roger Barndon for his invaluable help with MRI data acquisition, Christine Holen for her help with subject preparation, and Jody C. Culham and Anthony Singhal for helpful comments on an earlier draft. M.M. was supported by the Berlin Neuroimaging Center, Berlin (BMBF). The present study was financially supported by grants from the Research Council of Norway (to K.H.).

1. Dale, A. M. & Halgren, E. (2001) *Curr. Opin. Neurobiol.* **11,** 202–208.
2. Horwitz, B. & Poeppel, D. (2002) *Hum. Brain Mapp.* **17,** 1–3.
3. Hopfinger, J. B., Khoe, W. & Song, A. W. (2005) in *Event Related Potentials, A Methods Handbook.*, ed. Handy, T. C. (MIT Press, Cambridge, MA), pp. 345–380.
4. Halgren, E., Marinkovic, K. & Chauvel, P. (1998) *Electroencephalogr. Clin. Neurophysiol.* **106,** 156–164.
5. Halgren, E., Baudena, P., Clarke, J. M., Heit, G., Liegeois, C., Chauvel, P. & Musolino, A. (1995) *Electroencephalogr. Clin. Neurophysiol.* **94,** 191–220.
6. Halgren, E., Baudena, P., Clarke, J. M., Heit, G., Marinkovic, K., Devaux, B., Vignal, J. P. & Biraben, A. (1995) *Electroencephalogr. Clin. Neurophysiol.* **94,** 229–250.
7. Baudena, P., Halgren, E., Heit, G. & Clarke, J. M. (1995) *Electroencephalogr. Clin. Neurophysiol.* **94,** 251–264.
8. Martinez-Montes, E., Valdes-Sosa, P. A., Miwakeichi, F., Goldman, R. I. & Cohen, M. S. (2004) *NeuroImage* **22,** 1023–1034.
9. Valdes-Sosa, P. A. (2004) *Neuroinformatics* **2,** 239–250.
10. Bonmassar, G., Schwartz, D. P., Liu, A. K., Kwong, K. K., Dale, A. M. & Belliveau, J. W. (2001) *NeuroImage* **13,** 1035–1043.
11. Liu, A. K., Belliveau, J. W. & Dale, A. M. (1998) *Proc. Natl. Acad. Sci. USA* **95,** 8945–8950.
12. Bledowski, C., Prvulovic, D., Hoechstetter, K., Scherg, M., Wibral, M., Goebel, R. & Linden, D. E. (2004) *J. Neurosci.* **24,** 9353–9360.
13. Heeger, D. J. & Ress, D. (2002) *Nat. Rev. Neurosci.* **3,** 142–151.
14. Lauritzen, M. & Gold, L. (2003) *J. Neurosci.* **23,** 3972–3980.
15. Logothetis, N. K., Pauls, J., Augath, M., Trinath, T. & Oeltermann, A. (2001) *Nature* **412,** 150–157.
16. Kim, D. S., Ronen, I., Olman, C., Kim, S. G., Ugurbil, K. & Toth, L. J. (2004) *NeuroImage* **21,** 876–885.
17. Nunez, P. L. (1995) *Neocortical Dynamics and Human EEG Rhythms* (Oxford Univ. Press, New York).
18. Laufs, H., Krakow, K., Sterzer, P., Eger, E., Beyerle, A., Salek-Haddadi, A. & Kleinschmidt, A. (2003) *Proc. Natl. Acad. Sci. USA* **100,** 11053–11058.
19. Moosmann, M., Ritter, P., Krastel, I., Brink, A., Thees, S., Blankenburg, F., Taskin, B., Obrig, H. & Villringer, A. (2003) *NeuroImage* **20,** 145–158.
20. Goldman, R. I., Stern, J. M., Engel, J., Jr., & Cohen, M. S. (2002) *NeuroReport* **13,** 2487–2492.
21. Gotman, J., Benar, C. G. & Dubeau, F. (2004) *J. Clin. Neurophysiol.* **21,** 229–240.
22. Salek-Haddadi, A., Friston, K. J., Lemieux, L. & Fish, D. R. (2003) *Brain Res. Brain Res. Rev.* **43,** 110–133.
23. Horovitz, S. G., Skudlarski, P. & Gore, J. C. (2002) *Magn. Reson. Imaging* **20,** 319–325.
24. Mangun, G. R., Hopfinger, J. B., Kussmaul, C. L., Fletcher, E. & Heinze, H. J. (1997) *Hum. Brain Mapp.* **5,** 273–279.
25. Horovitz, S. G., Rossion, B., Skudlarski, P. & Gore, J. C. (2004) *NeuroImage* **22,** 1587–1595.
26. Quian Quiroga, R. & Garcia, H. (2003) *Clin. Neurophysiol.* **114,** 376–390.
27. Spencer, K. M. (2005) in *Event Related Potentials, A Methods Handbook*, ed. Handy, T. C. (MIT Press, Cambridge, MA), pp. 209–228.
28. Sutton, S., Braren, M., Zubin, J. & John, E. R. (1965) *Science* **150,** 1187–1188.
29. Squires, K. C., Wickens, C., Squires, N. K. & Donchin, E. (1976) *Science* **193,** 1142–1146.
30. Hall, D. A., Haggard, M. P., Akeroyd, M. A., Palmer, A. R., Summerfield, A. Q., Elliott, M. R., Gurney, E. M. & Bowtell, R. W. (1999) *Hum. Brain Mapp.* **7,** 213–223.
31. Delorme, A. & Makeig, S. (2004) *J. Neurosci. Methods* **134,** 9–21.
32. Naatanen, R. (1992) *Attention and Brain Function* (Lawrence Erlbaum, Hillsdale, NJ).
33. Naatanen, R. & Picton, T. (1987) *Psychophysiology* **24,** 375–425.
34. Croft, R. J., Gonsalvez, C. J., Gabriel, C. & Barry, R. J. (2003) *Psychophysiology* **40,** 322–328.
35. Duncan-Johnson, C. C. & Donchin, E. (1977) *Psychophysiology* **14,** 456–467.
36. Donchin, E. & Coles, M. G. H. (1988) *Behav. Brain Sci.* **11,** 357–374.
37. Janata, P. & Grafton, S. T. (2003) *Nat. Neurosci.* **6,** 682–687.
38. Cabeza, R. & Nyberg, L. (2000) *J. Cognit. Neurosci.* **12,** 1–47.
39. Friston, K. (2005) *Philos. Trans R. Soc. London B* **360,** 815–836.
40. Friston, K. J. (2005) *Annu. Rev. Psychol.* **56,** 57–87.
41. Linden, D. E., Prvulovic, D., Formisano, E., Vollinger, M., Zanella, F. E., Goebel, R. & Dierks, T. (1999) *Cereb. Cortex* **9,** 815–823.
42. Kiehl, K. A., Stevens, M. C., Laurens, K. R., Pearlson, G., Calhoun, V. D. & Liddle, P. F. (2005) *NeuroImage* **25,** 899–915.
43. Raichle, M. E., MacLeod, A. M., Snyder, A. Z., Powers, W. J., Gusnard, D. A. & Shulman, G. L. (2001) *Proc. Natl. Acad. Sci. USA* **98,** 676–682.
44. Knight, R. (1996) *Nature* **383,** 256–259.
45. Yamaguchi, S., Hale, L. A., D'Esposito, M. & Knight, R. T. (2004) *J. Neurosci.* **24,** 5356–5363.
46. Polich, J. (2003) in *Detection of Change: Event-Related Potential and fMRI Findings*, ed. Polich, J. (Kluwer, Norwell, MA), pp. 83–99.
47. Picton, T. W. (1992) *J. Clin. Neurophysiol.* **9,** 456–479.
48. Kirino, E., Belger, A., Goldman-Rakic, P. & McCarthy, G. (2000) *J. Neurosci.* **20,** 6612–6618.
49. Coull, J. T. (1998) *Prog. Neurobiol.* **55,** 343–361.
50. Stevens, M. C., Calhoun, V. D. & Kiehl, K. A. (2005) *NeuroImage* **26,** 782–792.
51. Downar, J., Crawley, A. P., Mikulis, D. J. & Davis, K. D. (2000) *Nat. Neurosci.* **3,** 277–283.
52. Corbetta, M. & Shulman, G. L. (2002) *Nat. Rev. Neurosci.* **3,** 201–215.
53. Foucher, J. R., Otzenberger, H. & Gounot, D. (2004) *NeuroImage* **22,** 688–697.
54. Ivry, R. & Knight, R. T. (2002) *Nat. Neurosci.* **5,** 394–396.
55. Huettel, S. A., Mack, P. B. & McCarthy, G. (2002) *Nat. Neurosci.* **5,** 485–490.
56. Sokolov, E. N. (1963) *Perception and the Conditioned Reflex* (Pergamon, Oxford, U.K.).
57. Loveless, N. (1983) in *Orienting and Habituation: Perspectives in Human Research*, ed. Siddle, D. (Wiley, Chichester, U.K.), pp. 71–108.
58. Halgren, E. & Marinkovic, K. (1995) in *Recent Advances in Event-Related Brain Potential Research*, eds. Ogura, C., Koga, Y. & Shimokochi, M. (Elsevier, Amsterdam), pp. 1072–1084.
59. Llinas, R. R. (2001) *I of the Vortex: from Neurons to Self* (MIT Press, Cambridge, MA).

Paper III

Eichele T, Calhoun VD, Specht K, Moosmann M, Jongsma ML, Quiroga RQ, Nordby H, Hugdahl K. (2007) Unmixing concurrent EEG-fMRI with parallel independent component analysis. *International Journal of Psychophysiology,* epub Aug 2

Available online at www.sciencedirect.com
ScienceDirect
ELSEVIER
International Journal of Psychophysiology xx (2007) xxx–xxx
INTERNATIONAL JOURNAL OF PSYCHOPHYSIOLOGY
www.elsevier.com/locate/ijpsycho

Unmixing concurrent EEG-fMRI with parallel independent component analysis

Tom Eichele [a,*,1], Vince D. Calhoun [b,c,d,1], Matthias Moosmann [a], Karsten Specht [a], Marijtje L.A. Jongsma [e], Rodrigo Quian Quiroga [f], Helge Nordby [a], Kenneth Hugdahl [a,g]

[a] *Department of Biological and Medical Psychology, University of Bergen, Jonas Lies Vei 91, 5011 Bergen, Norway*
[b] *The MIND Institute, 1101 Yale Boulevard, N.E, Albuquerque, NM 87131, USA*
[c] *Department of Electrical and Computer Engineering, University of New Mexico, Albuquerque, New Mexico*
[d] *Department of Psychiatry, Yale University School of Medicine, New Haven, Connecticut, United States*
[e] *NICI, Department of Biological Psychology, University of Nijmegen, P.O.Box 9104, 6500 HE University of Nijmegen, The Netherlands*
[f] *Department of Engineering, University Road, Leicester LE1 7RH, United Kingdom*
[g] *Haukeland University Hospital, Bergen, Norway*

Received 17 November 2006; accepted 27 April 2007

Abstract

Concurrent event-related EEG-fMRI recordings pick up volume-conducted and hemodynamically convoluted signals from latent neural sources that are spatially and temporally mixed across the brain, i.e. the observed data in both modalities represent multiple, simultaneously active, regionally overlapping neuronal mass responses. This mixing process decreases the sensitivity of voxel-by-voxel prediction of hemodynamic activation by the EEG when multiple sources contribute to either the predictor and/or the response variables. In order to address this problem, we used independent component analysis (ICA) to recover maps from the fMRI and timecourses from the EEG, and matched these components across the modalities by correlating their trial-to-trial modulation. The analysis was implemented as a group-level ICA that extracts a single set of components from the data and directly allows for population inferences about consistently expressed function-relevant spatiotemporal responses. We illustrate the utility of this method by extracting a previously undetected but relevant EEG-fMRI component from a concurrent auditory target detection experiment.

Keywords: EEG-fMRI; ICA; ERP; Auditory; Change detection

1. Introduction

Processing of simple stimuli and tasks produces spatially and temporally extensive event-related neuronal responses in the brain. For example, auditory target detection induces hemodynamic activation in about fourty cortical, subcortical and cerebellar regions (Kiehl et al., 2005), complementing the results from intracranial recordings (Baudena et al., 1995; Halgren et al., 1995a,b). These neuronal mass responses can be observed across scales and modalities from single unit recordings, intracranial and scalp electrophysiology, as well as metabolic and hemodynamic signals, but no single technique provides a sufficient view of the full temporal, spatial and functional extent of these responses. Visibility can be improved with techniques that integrate data across different neuroimaging modalities (Debener et al., 2006; Hopfinger et al., 2005; Horwitz and Poeppel, 2002; Makeig et al., 2002). In the case of concurrent EEG-fMRI recordings, one can complement the temporal resolution provided by scalp potentials with the spatial precision of fMRI. This can be done for example by finding correlations between single-trial modulation at a selected latency in the event-related EEG and activation in the fMRI volume employing mass univariate voxel-by-voxel analysis

* Corresponding author. Tel.: +47 55 586290/01/02; fax: +47 55 589872.
E-mail addresses: tom.eichele@psybp.uib.no (T. Eichele), vcalhoun@unm.edu (V.D. Calhoun), moosmann@gmail.com (M. Moosmann), karsten.specht@psybp.uib.no (K. Specht), marijej@nici.ru.nl (M.L.A. Jongsma), rodri@vis.caltech.edu (R.Q. Quiroga), nordby@psych.uib.no (H. Nordby), hugdahl@psych.uib.no (K. Hugdahl).
[1] TE and VDC equally contributed to this work.

0167-8760/$ - see front matter © 2007 Elsevier B.V. All rights reserved.
doi:10.1016/j.ijpsycho.2007.04.010

(Bénar et al., 2007; Debener et al., 2005b; Eichele et al., 2005). Implicit in this approach is the critical assumption that the scalp EEG data from a selected channel and latency can predict the fMRI activation in single voxels (Friston et al., 1995; Friston, 2005b). This is imposed by the sampling properties of the recordings, and the way fMRI time-series data are commonly analyzed. While this assumption provides a workable solution to 'integration-by-prediction', it is not necessarily physiologically plausible for many of the samples from both modalities. The reason for this is that a salient event can induce multiple, simultaneously active, regionally overlapping, and functionally separable responses which add to existing neuronal background activity, in other words, event-related processes are spatially and temporally mixed across the brain. The scalp EEG samples a volume-conducted, spatially degraded version of the responses, where the potential at any location and latency can be considered a mixture of multiple independent timecourses that stem from large-scale synchronous field potentials (Makeig et al., 2004a; Onton et al., 2006). Similarly, the neurovascular transformation of the distributed neuronal activity into hemodynamic signals (Lauritzen and Gold, 2003; Logothetis, 2003) affords detection of blood oxygenation level dependent responses (BOLD, Ogawa et al., 1990) that are temporally degraded and spatially mixed across the fMRI volume (Calhoun and Adali, 2006; McKeown et al., 2003).

This physiological spatiotemporal mixing process creates situations in which prediction of fMRI activity by EEG features has to contend with the fact that neither the predictor, nor the response variables are any likely to represent a single source of variability. For example, the point-to-point correlation between the two data mixtures fails when the trial-to-trial modulation in the EEG receives different contributions from several function-relevant spatially separate sources such that no single regional fMRI response represents the predicted signal. Also, this applies to the case where the EEG feature captures a single source, but the fMRI activity at corresponding locations is buried in the spread of other, unrelated sources, leading to underestimation of the spatial extent of the response. Although denoising and inclusion of parametric modulations into the stimulus paradigm (Eichele et al., 2005), and temporal unmixing of the EEG (Debener et al., 2005b) solve parts of the problem and make way for refined spatiotemporal mapping, there is still need for improvement of the analysis tools for integration of concurrent recordings (cf. Debener et al., 2006). One such improvement is to unmix both modalities in parallel at the single-trial level, which follows naturally from the recent work (Calhoun et al., 2006b; Debener et al., 2005b; Eichele et al., 2005) and the reasoning laid out above.

Following the above arguments, we develop an analysis framework for group data that employs Infomax independent component analysis (ICA, Bell and Sejnowski, 1995; Lee et al., 1999; for an overview see Stone, 2002) to recover a set of statistically independent maps from the fMRI (sICA), and independent time-courses from the EEG (tICA) separately, and match these components across modalities by correlating their trial-to-trial modulation. ICA was developed to address linear mixing problems similar to the 'cocktail party problem' in which many people are speaking at once and multiple microphones pick up different mixtures of the speakers' voices (Bell and Sejnowski, 1995). The algorithm used here attempts to separate mixed signals into maximally independent sources by maximization of information transfer between them. ICA has general applicability to normally distributed two-dimensional mixtures, and regarding psychophysiological data it has been used for decomposition of averaged ERPs (Makeig et al., 1997), single trial EEG (Makeig et al., 2004b; Onton et al., 2006), fMRI (Calhoun and Adali, 2006) and EEG-fMRI (Calhoun et al., 2006b; Debener et al., 2005b; Feige et al., 2005). ICA can be used for EEG-fMRI integration assuming that the different recording modalities faithfully sample features from the same set of sources, expressed in the covariation between single trials (Debener et al., 2005b) or subjects (Calhoun et al., 2006b).

Unlike univariate methods such as the general linear model, ICA is not naturally suited to generalize results from a group of subjects. There are two strategies to allow for matching of independent components across individuals: one is to combine individual ICs across subjects with clustering techniques (Esposito et al., 2005; Onton et al., 2006). Another approach is to create aggregate data containing observations from all subjects, estimate a single set of ICs and then back-reconstruct these in the individual data (Calhoun et al., 2001; Schmithorst and Holland, 2004). We adopted the latter strategy for the group EEG temporal ICA analysis, because it directly estimates components that are consistently expressed in the population, involves the least amount of user interaction and is straightforward to combine with the existing framework for group ICA of fMRI data (Calhoun et al., 2001).

In summary, possible ways for EEG-fMRI integration include predicting both modalities, a mass-univariate framework testing all voxel timeseries in the fMRI, as well as channels and timepoints in the EEG employing a pre-defined model function as is commonly done in fMRI timeseries analysis (however, to the best of our knowledge this has not yet been realized). Another option is to predict the fMRI data with the measured EEG single trial amplitudes, assuming that some EEG timepoints and channels represent functional processes in some voxels without much overlap, representing a point-to-point correlation between mixtures (Bénar et al., 2007; Eichele et al., 2005). A third solution is to unmix the EEG and predict the fMRI mixture with the modulation of a temporally independent component (Debener et al., 2005b; Feige et al., 2005). The method developed here un-mixes both modalities separately, and matches temporal ICs in the EEG with spatial ICs in the fMRI.

The utility of this method is demonstrated in previously published data that were collected in an auditory oddball with varying degrees of target predictability. The parametric modulation induced distinct EEG-correlated fMRI activation patterns at the latencies of the P2, N2, and P3 (Eichele et al., 2005; see also Jongsma et al., 2006). We have re-analyzed these data with the open search question whether systematic EEG-fMRI covariation was missed out in our previous analysis and if it could be recovered by parallel ICA. A likely candidate for such a miss is the auditory onset response and the subsequent low-level orienting/change detection processes. Although being

Please cite this article as: Eichele, T. et al. Unmixing concurrent EEG-f MRI with parallel independent component analysis. Int. J. Psychophysiol. (2007), doi:10.1016/j.ijpsycho.2007.04.010

expressed in the N1-ERP (Naatanen and Picton, 1987; Woods, 1995) and in bilateral temporal fMRI activation (Kiehl et al., 2005; Liebenthal et al., 2003; Linden et al., 1999) this process did not support a significant correlation between the modalities (cf. Eichele et al., 2005).

2. Methods

2.1. Subjects

Fifteen healthy, right-handed participants (21–28 years, 7f/8 m) took part in the experiment after providing informed consent.

2.2. Stimuli

Chords of 50 ms duration were presented in an eyes-closed condition via headphones with an onset asynchrony of 2 s. Infrequent targets (500 Hz) were presented at a probability of 0.25 among frequent standards (250 Hz, *P* 0.75). Alternating sequences of six successive targets were presented either with pseudorandom target-to-target interval (TTI) ranging from 4 to 22 s or with a regular 8 s TTI. Each of these 12-target sequences lasted on the average 96 s, and were repeated 18 times (216 targets total). In order to avoid speeded response times to predictable targets, participants were instructed to respond in the middle of the interval between the target and the next standard stimulus. Participants were not informed about the presence of regular patterns beforehand.

2.3. fMRI data acquisition (Fig. 1, B^f)

Imaging was performed on a 1.5T scanner (Siemens, Germany). After scanning of anatomy with a T1-weighted MPRAGE sequence, 300 BOLD sensitive echo planar images (EPI) were collected. EPI volumes were aligned to the anterior-posterior comissura line and consisted of 18 axial slices with 5.5 mm thickness including 0.5 mm interslice gap, flip angle: 90°, excitation time: 60 ms, field of view: 220 × 220 mm, matrix: 64 × 64 voxels. A sparse-sampling acquisition protocol (Hall et al., 1999) with 8 s repetition time and 2 s acquisition time was used. The protocol makes use of the hemodynamic lag between stimulus onset and BOLD peak and allowed for EEG-recording without interfering scanner noise and gradient artefacts during a 6 s silent gap between successive volume acquisitions.

2.4. EEG data acquisition (Fig. 1, B^e)

EEGs were recorded continuously at 5 kHz with an amplifier placed inside the MR-scanner (BrainProducts, Germany). Subjects were fitted with an elastic cap containing 30 Ag/AgCl electrodes (FP1, FP2, F7, F3, Fz, F4, F8, T7, C3, Cz, C4, T8, P7, P3, Pz, P4, P8, O1,OZ, O2, FC5, FC1, FC2, FC6, CP5, CP1, CP2, CP6, EOG, ECG) referenced to FCz, impedances were kept below 5 kΩ.

The analyses reported below were done in Matlab (www.mathworks.com) with the academic freeware toolboxes EEGLAB (http://sccn.ucsd.edu/eeglab), GIFT (http://icatb.sourceforge.org), SPM2 (http://www.fil.ion.ucl.ac.uk/spm), and customized functions. A schematic overview of the analyses is provided in Fig. 1.

2.5. EEG preprocessing (Fig. 1, T^e)

Continuous EEGs were downsampled offline to 500 Hz and filtered from 1–45 Hz (24 db/octave). EEG epochs from −312 to 712 ms (512 points) around standard and target sound onsets were recalculated to average reference and subjected to an individual tICA as implemented in EEGLAB (Delorme and Makeig, 2004). This step was used to identify and remove pulse and eye movement artefacts from the data (cf. Debener et al., 2007; Jung et al., 2000), retaining minimally 20 out of 30 components. Single-trials were then wavelet-denoised (Quian Quiroga and Garcia, 2003), constraining the single trial EEGs to the time-frequency features relevant for the evoked activity.

2.6. fMRI preprocessing (Fig. 1, T^f)

All images were realigned to the first image in the time-series to correct for head movement and then normalized to the Montreal Neurological Institute (MNI) reference space, and were resliced to a voxel size of 3 mm^3 and smoothed with a 8 mm FWHM gaussian kernel. Voxel timecourses were high-pass filtered at 128 s with a 5th order Butterworth digital filter to remove slow drift, normalized to unit variance, and the image volume for the analysis was constrained to voxels with >50% probability of being grey matter. These pre-processing steps are optional, and empirical choices for this particular data set, but are not principally necessary for sICA of fMRI.

2.7. Group spatial ICA of fMRI data (sICA)

An exploratory single-subject spatial ICA was used for inspection of individual components across subjects in our sample, and in order to derive the appropriate number of components to be estimated in the group ICA step using minimum description length criteria (Li et al., in press). The estimated dimensionality of the data across subjects averaged to 24, thus the data from each participant was pre-whitened and reduced (in time) to 24 dimensions via principal component analysis (PCA), retaining between 70–90% of the variance (Fig. 1, R^f). Individual principal components were then concatenated together in a single set (Fig. 1, G^f) in which sICA was performed. In addition to the resulting independent spatial maps, this analysis reconstructs component timecourses by multiplying the dewhitening matrix from the first data reduction by the corresponding partition of the unmixing matrix. These timecourses reflect the trial-to-trial hemodynamic variability of the fMRI experiment and were used for assessment of covariation between components in the two modalities (see tIC-sIC integration). For the fMRI sIC component maps, mean and variance of the voxel weights were calculated, and the variance across subjects was used as an estimate of the population variance. The weights were treated as random variables and

Please cite this article as: Eichele, T. et al. Unmixing concurrent EEG-f MRI with parallel independent component analysis. Int. J. Psychophysiol. (2007), doi:10.1016/j.ijpsycho.2007.04.010

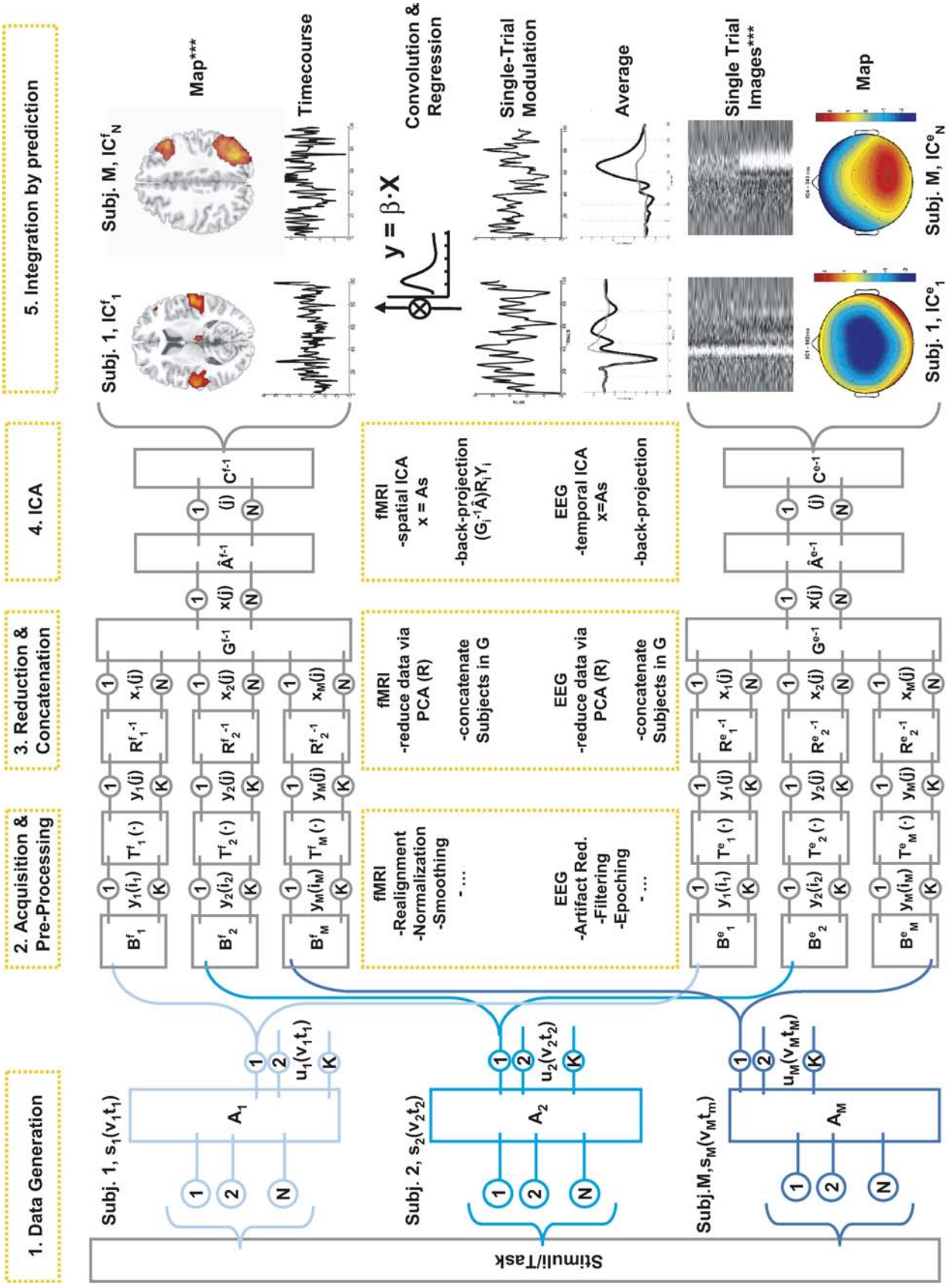

Please cite this article as: Eichele, T. et al. Unmixing concurrent EEG-f MRI with parallel independent component analysis. Int. J. Psychophysiol. (2007), doi:10.1016/j.ijpsycho.2007.04.010

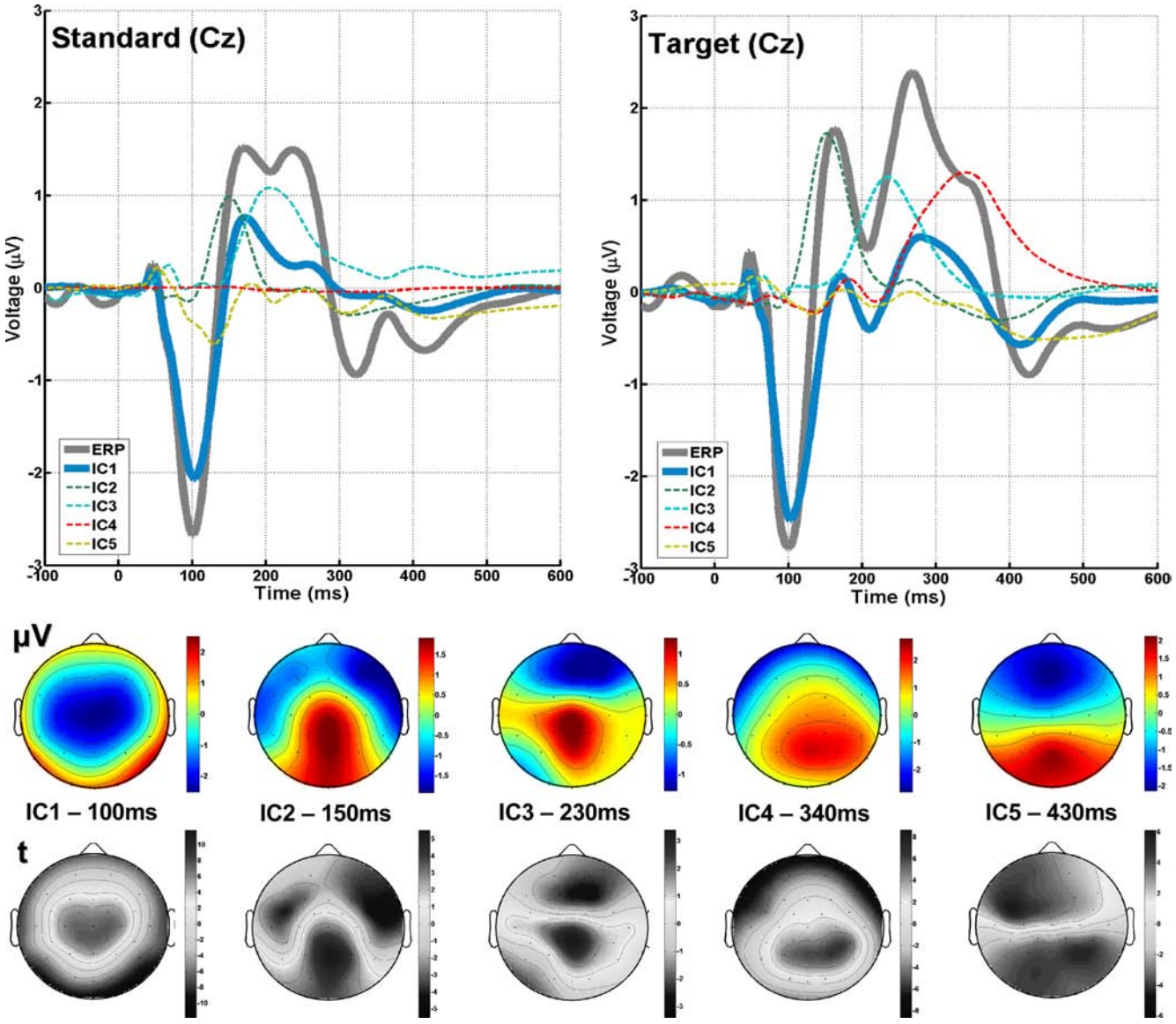

Fig. 2. tIC timecourses and topographies. Top: average ERP and corresponding timecourses of the five independent components or standard (left) and target (right) epochs. Bottom: component topographies, as scalp potential (μV) and *t*-statistic (*t*).

entered into voxel-wise one-sample *t*-tests against the null hypothesis of zero magnitude. Results from these tests were considered significant at 1% false positive discovery rate (FDR, Benjamini and Hochberg, 1995) with a cluster extent threshold of at least 5 voxels.

2.8. Group temporal ICA of EEG data (tICA)

For estimation of the group tICA we adopt the rationale proposed by Calhoun (Calhoun et al., 2001). The analysis framework is divided into the underlying data generation and

Fig. 1. Schematic of parallel group independent component analysis. We assume that an experimental manipulation induces responses in a set of generic event/function-related neuronal sources (*s*) in a consistent manner across the sampled population (Subj. 1-M). The sources are expressed spatially (*v*) and temporally (*t*) and mixed by the unknown mixing system A. Neurovascular coupling transforms the mixed signals (*u*) to hemodynamic (BOLD) responses which are sampled from the entire cerebral volume by the MR scanner (B^f), while passive volume conduction enables recording of the signals as scalp EEG (B^e). At this step the signals are either temporally (in B^f) or spatially (in B^e) degraded, but they sufficiently retain their functional signature, i.e. the trial-to-trial modulation, which affords later matching of components. Modality-specific pre-processing steps (T^f, T^e) are then implemented to allow for later group inferences (e.g. spatial normalisation of individual MR volumes), and to reduce noise (e.g. ICA-based artefact removal from the EEG). Hereafter, the individual data are pre-whitened and reduced to N principal component maps (R^f) or timecourses (R^e). Individual PCs are then concatenated together in aggregate data-sets (G^f, G^e), containing the *N* signal mixtures *x* from all subjects. From the aggregate fMRI data, the mixing matrix $\hat{A}^f$ and the source maps (s) are estimated using spatial ICA, recovering *N* spatially independent components in $\hat{C}^f$. From the aggregate EEG data, the mixing matrix $\hat{A}^e$ and the source timecourses (s) are estimated using temporal ICA, recovering *N* temporally independent components in $\hat{C}^e$. For each modality, individual component maps and timecourses are back-reconstructed by projecting the aggregate components into the individual, pre-processed data. Components are matched across modalities by correlating the trial-to-trial modulations of the fMRI-sICs with those of the EEG tICs. ***: independent.

Please cite this article as: Eichele, T. et al. Unmixing concurrent EEG-f MRI with parallel independent component analysis. Int. J. Psychophysiol. (2007), doi:10.1016/j.ijpsycho.2007.04.010

mixing process, recording, pre-processing, reduction and component estimation, and is illustrated for both modalities in Fig. 1. We assume that the scalp EEG signal is a gaussian mixture containing statistically independent non-gaussian source timeseries $s(t)=[s_1(t), s_2(t), \ldots, s_i(t)]^T$ indicated by $s_i(t)$ at time t for the ith source. The sources have weights that specify the contribution to each timepoint. The weights are multiplied by each source's fixed topography. Secondly, it is assumed that the N sources are linearly mixed so that a given timepoint contains a weighted mixture of the sources. The linear combination of sources is represented by the unknown mixing system A, and yields $u(t)=[u_1(t), u_2(t), \ldots, u_N(t)]^T$, representing N ideal samples of the signals $u_n(t)$ at time t, for the ith source in the brain. The sampling of the electric activity on the scalp with the EEG amplifier results in $y(i)=[y_1(i), y_2(i), \ldots, y_K(i)]^T$ where the EEG is sampled at T timepoints indicated by $i=1, 2, \ldots, T$. A set of possible transformations during preprocessing, such as downsampling and filtering determine the effective sampling such that $y(j)=[y_1(j), y_2(j), \ldots, y_K(j)]^T$.

For each individual separately, the preprocessed single trial data $y(j)$ are pre-whitened and reduced via principal component analysis (Fig. 1, $R^{e}{}_1^{-1} \ldots R^{e}{}_M^{-1}$) containing the major proportion of variance in the N uncorrelated timecourses of $x(j)=[x_1(j), x_2(j), \ldots, x_N(j)]^T$. Then, group data is generated by concatenating individual principal components in the aggregate data set G^e (Fig. 1).The choice of twenty PCs was determined by the

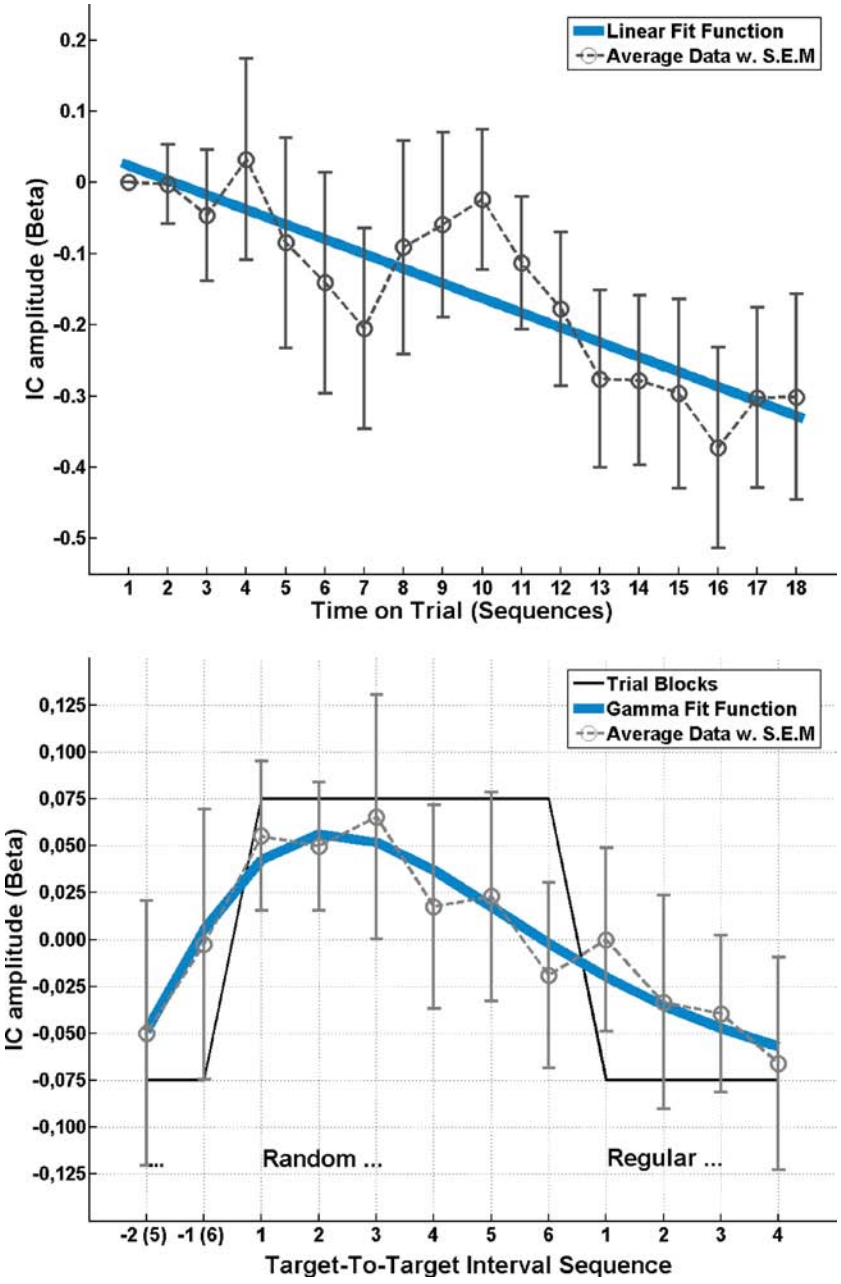

Fig. 3. tIC 1 amplitude effects. Top: slow linear decrement of component activity with time on trial. Bottom: within a sequence indicated by the box-car function (black line) the trial-to-trial dynamics yield a gamma-shaped modulation following the transition between regular and random targets.

Please cite this article as: Eichele, T. et al. Unmixing concurrent EEG-f MRI with parallel independent component analysis. Int. J. Psychophysiol. (2007), doi:10.1016/j.ijpsycho.2007.04.010

dimensionality of the data after artefact removal (see above). TICA was performed in this set, estimating the optimal inverse of the mixing matrix (Fig. 1, A^{e-1}) that led to the observed scalp data and a single set of source timecourses (s). In order to acquire robust task-related components in the data we ran 50 replications entering random subsamples of 100 standard and 100 target epochs from each subject into the group ICA, estimating 20 components, as determined by the remaining dimensionality of the data after individual ICA. Consistently task-related components were identified by means of two criteria: firstly, replicability of the average component timecourses across analyses ($r>0.90$), and secondly, significant differences between standard and target epochs in dependent sample t-tests across timepoints and channels. For the five components (Fig. 2) that met these criteria, the aggregate timecourses from all replications were averaged together and used for a two-step back-reconstruction using multiple regression.

2.9. tIC-sIC integration

The computation of an EEG-tICA on the one end, and an fMRI-sICA on the other end replaces prediction of multiple voxel timeseries using multiple channel/timepoint measures by the condensed result from the two separate decompositions: For the timecourses of the 24 spatially independent components in the fMRI separately, data were modelled with a design that was formed by convolving stimulus functions with a canonical hemodynamic response function. The first stimulus function encoded an invariant evoked response to target stimuli. Five additional functions encoded the detrended single trial weights of the EEG tIC's to find fMRI sIC's with covarying timeseries. The EEG-tIC weight functions were decorrelated (Schmidt-Gram orthogonalization) from the unspecific hemodynamic response to stimulus onsets per se, ensuring specificity of the inferences from the electrophysiological predictors. The predictors were entered into single-subject fixed-effects regression analyses; on group level, random effects analyses were performed by entering the individual β-weights from the regression between each EEG-tIC and fMRI-sIC into one-sample t-tests. The covariation between the trial-to-trial timecourses from the two modalities was considered significant at $p<0.05$.

3. Results

For brevity we focus only on the amplitude effects and fMRI correlates of the first extracted component, which was not detected previously.

3.1. Component backprojection

The first step was to estimate the individual topographies for the components by fitting the tIC timecourses to the individual ERPs from all channels. The goodness-of-fit of this model to the data is expressed in the F-statistic and the percentage-variance-explained (r^2) for each channel. Across subjects, β-weights from each component and each channel were entered into zero-mean t-tests, providing random-effects statistics of the topographies (Fig. 2). The backprojection for single subject averages attained fit statistics with r^2 ranging from 0.10 ($F_{1,506}=11.28$) to 0.99 ($F>10^3$), averaging to 0.75±0.15 ($F_{1,506}=541\pm623$) across subjects and channels, indicating an overall good prediction of the model with five tICs, considering that low r^2-values were found mainly in channels with polarity reversal. The t-tests of the component β-weights for each channel across subjects ranged from $t_{df14}=-7.55$ to 7.04 for tIC1, IC2: t_{df14} −4.22 to 5.41, tIC3: t_{df14} −2.43 to 2.78, tIC4: t_{df14} −5.70 to 6.25, tIC5: t_{df14}−4.26 to 5.97 (all $p<0.05$) replicating the component amplitude topographies (Fig. 2).

In the second step, tIC amplitudes in all single trials were estimated by forming a design matrix containing predictors from all tIC timecourses concatenated across channels which was fitted to the raw spatiotemporal data of each trial, thus estimating five β-weights with the corresponding F-statistic and r^2. Separately for the tICs, one-sample t-tests were conducted on the β-weights within-subject-across-trials and between-subjects-within-trials. Both types of tests yield information regarding the goodness of the aggregate components in predicting individual trials as opposed to representing average phenomena that are essentially not well represented in single trials. Another purpose of this particular back-reconstruction was to condense topography and timecourse of a component to a single value for each trial, to be used later as a predictor for fMRI activity. This is an appropriate data reduction since the underlying sources are assumed to be spatially fixed, which means that testing of electrodes separately can be omitted. Additionally, we can constrain sources to be uniformly amplitude modulated in each trial, thus omitting testing of multiple latencies. The statistics for the available 3240 single trials resulted in a range of r^2 from 0.003 to 0.60, with a mean of 0.15±0.10 ($F=588\pm519$). As a more informative test of the components contributions to the single trials, the t-statistic of the β-weights within-subjects (across trials) indicated consistent scaling in the majority of components and subjects. tIC1 was found significant in 15/15 participants (pp) at $t_{(df215)}>2.35$ ($p<0.01$) with an average (t_{avg}) at $t_{(df215)}=14.49\pm8.39$ (±SD), minimum (min): 3.66, maximum (max): 38.55; tIC2: 14/15 pp, t_{avg} 8.62±6.64, min −2.17 max 24.61; tIC3: 9/15 pp,

Table 1
fMRI regional activation in the EEG-correlated spatial component

Region	BA	x	y	z	peak voxel (t)
Subcallosal gyrus, R	25	2	18	−11	−7.33
Anterior cingulate gyrus, R	32	4	18	32	6.52
Transverse temporal gyrus, L	41	−56	−19	12	6.61
Superior temporal gyrus, R	41	57	−24	12	6.52
Superior temporal gyrus, R	22	60	−13	6	9.47
Superior temporal gyrus, L	22	−56	−13	1	7.33
STG/temporal pole, L	38	−58	14	−11	8.22
STG/temporal pole, R	38	62	11	−6	7.87
Brainstem, R	–	3	−22	−9	−11.35
Brainstem, L	–	−3	−11	−10	−6.34

The table summarizes the Talairach coordinates (x, y, z in mm) and Brodmann area labels for clusters of significant activity ($p<0.01$, FDR corr.).

Please cite this article as: Eichele, T. et al. Unmixing concurrent EEG-f MRI with parallel independent component analysis. Int. J. Psychophysiol. (2007), doi:10.1016/j.ijpsycho.2007.04.010

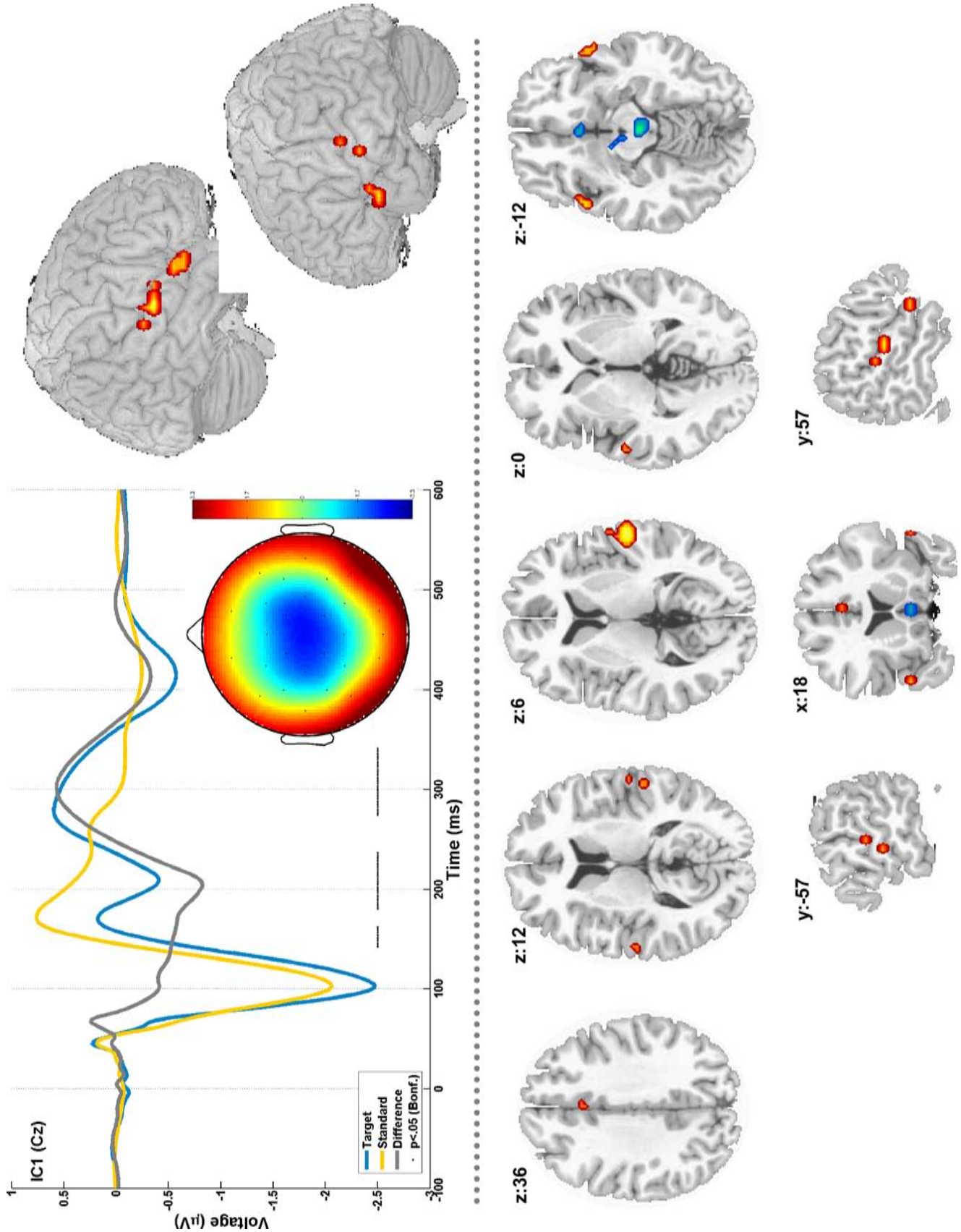

Please cite this article as: Eichele, T. et al. Unmixing concurrent EEG-f MRI with parallel independent component analysis. Int. J. Psychophysiol. (2007), doi:10.1016/j.ijpsycho.2007.04.010

t_{avg} 6.72±7.42, min −2.16 max 20.90; tIC4: 14/15 pp, t_{avg} 13.91±7.08, min −0.67 max 30.08, tIC5: 14/15 pp, t_{avg} 11.10±6.99, min 0.81 max 28.42. Similarly, at a threshold of $t_{(df14)} \geq 2.63$ ($p<0.01$), the majority of the weight estimates were robust across subjects for the target epochs across the observation time. Here, tIC1 was present in 172 out of 216 epochs (79.6%) with an averaged $t_{(df14)}$ 3.63±1.29, tIC2 amplitudes were more variable with only 76 (35.2%) trials, t_{avg} 2.30±1.05; similarly tIC3 with 45 trials (20.8%) t_{avg} 1.76±1.01; tIC4: 165 trials (76.4%) t_{avg} 3.48±1.44; tIC5: 123 trials (57.0%) t_{avg} 2.81±1.17.

3.2. tIC1 amplitude effects

In order to assess slow drifts evolving with the total time-on-trial regardless of the local manipulation of predictability, the twelve targets within one sequence were blocked and averaged together, yielding one observation for each of the 18 sequence repetitions in each participant, with the first point serving as baseline. The group averaged measure was used to derive a best-fit function (with as little parameters as possible). In this case, a simple linear trend $f(x)=s\,x+c$ across repetitions, with a slope (s) of −0.021 and offset c 0.045 provided a reasonable fit ($r^2=0.76$). This function was then used as a predictor of the single subject data, yielding sufficient individual statistics in 6/15 participants ($r^2 \geq 0.2$, $F_{1,16} \geq 4$, $p \leq 0.06$), and the β-weights being significantly larger than zero ($t_{df14}=4.10$, $p<0.001$). Amplitude modulation of tIC1 in response to switching between random and regular TTI was assessed by averaging the 18 repetitions from each of the six random and six regular sequence positions across the observation time together, after removing the mean from each sequence repetition to account for the trend (see above). Inspection of the group averaged response suggested a transient amplitude increment induced by the shift from predictable to unpredictable intervals with a subsequent decline across the remainder of the sequence, while there was no discernible response to the shift from unpredictable to predictable context. This shape was best modelled ($r^2=0.91$) with a gamma distribution function $y=f(x|a,b)=\frac{1}{b^a\Gamma(a)}x^{a-1}e^{\frac{x}{b}}$, with the parameters shape $a=2.9$ and scale $b=1.7$. This function was then used as a predictor of the single subject data, yielding sufficient positive correlation with the average-based model in 5/15 participants ($r^2 \geq 0.27$, $F_{1,10} \geq 3.68$, $p \leq 0.08$), however, a right-tailed t-test on the β-weights failed the significance threshold by a small margin ($t_{df14}=1.60$, $p=0.07$). Assuming that the degree of individual variability regarding shape and scale of the gamma function accounted for the failure of the test at small sample size, we conducted a complementary analysis with individual best-fit estimates (maximum positive correlation) from a range of ±0.5 around the group-estimates for a and b. With these parameters left to vary, statistics improved to 8/15 participants ($r^2 \geq 0.31$, $F_{1,10} \geq 4.55$, $p \leq 0.06$) reaching significance in the t-test ($t_{df14}=3.06$, $p<0.01$) (see Fig. 3).

3.3. fMRI correlates

The trial-to-trial amplitude dynamic of tIC1 predicted selectively the timecourse of one sIC fMRI map ($t_{df14}=2.49$, $p=0.02$), that is, no other EEG tIC correlated significantly with this sIC, neither did tIC1 covary with any other of the 24 fMRI sICs. The respective maps' timecourse additionally displayed a strong covariation with the generic evoked response predictor ($t_{df14}=11.15$, $p<0.001$). Local maxima of the FDR corrected t-statistic sIC map (Table 1) were located in the posterior superior temporal gyri and temporal poles bilaterally, the anterior cingulate gyrus, the subcallosal gyrus, the global maximum was situated in an area in the right brainstem framed by the landmarks central gray dorsally and red nucleus ventrally. Additionally, a smaller set of voxels was found in the vicinity of the left mamillary body (Fig. 4, Table 1).

4. Discussion

We have presented a method for parallel spatial and temporal independent component analysis for concurrent multi-subject single-trial EEG-fMRI recordings that addresses the mixing problem in both modalities (Fig. 1). The data are integrated via correlation of the trial-to-trial modulation of the recovered fMRI maps with EEG time-courses. The method afforded identification of an additional spatiotemporal process corresponding to the auditory onset response and subsequent low-level orienting/change detection (Fig. 4). The discussion details the area of application for this method, and provides an account for the potential functional role of the reported component.

4.1. Area of application

The observation that a simple cognitive task such as target detection in an auditory oddball experiment induces spatially and temporally widespread neuronal responses (Baudena et al., 1995; Calhoun et al., 2006b; Eichele et al., 2005; Halgren et al., 1995a,b; Kiehl et al., 2005) pertains to distributed network responses more than to compartmentalized effects (Fox et al., 2005; Halgren and Marinkovic, 1995; Nunez, 2000). We see a major utility for parallel ICA in this context as it provides the means to disentangle and visualize these networks both in their spatial and temporal form (Calhoun and Adali, 2006; Debener et al., 2006; Makeig et al., 2004a; McKeown et al., 2003; Onton et al., 2006).

However, some limitations apply: Infomax assumes sources to have non-normal, either super-or subgaussian distributions

Fig. 4. EEG-fMRI component. The figure shows the timecourse and topography for EEG-tIC1 for standard and target epochs as well as the difference wave between them. The difference wave was subjected to pointwise one-sample t-tests, black dots indicate timeframes with significant difference from zero at $p<.05$, Bonferroni corrected for 512 tests ($t>6.93$). The bilateral temporal activation in the correlated fMRI component is shown as a surface rendering (top right). Additional slices in the lower half illustrate the overall spatial pattern (see also Table 1). The fMRI maps are thresholded at 1% false discovery rate, cluster extent 5 voxels. Positive correlation is plotted in red, inverse correlation in blue.

Please cite this article as: Eichele, T. et al. Unmixing concurrent EEG-f MRI with parallel independent component analysis. Int. J. Psychophysiol. (2007), doi:10.1016/j.ijpsycho.2007.04.010

(Bell and Sejnowski, 1995; Lee et al., 1999), and this seems to hold for a great variety of physiological signals as well as technical artefacts. However, if sources (or noise) are gaussian, ICA will split these up into spurious non-gaussian components. In practice this occurs mostly for heavily noisy data, and where more sources than present in the data are extracted.

Generally, the utility of blind methods such as ICA lies in data-driven assessment of data where specific hypotheses regarding spatial and temporal relationships are lacking, or are ill-specified. In other words, in situations in which a traditional inference test, and its implementation in the statistical parametric mapping framework (Friston, 2003; Friston et al., 1995) is not justifiable, or is too insensitive due to ensuing conservative significance thresholds. Concurrent EEG-fMRI data adds another complexity in that one deals with two multivariate spaces, and necessary specifications would not only encompass the regions in which fMRI activation is expected, but also the particular samples from which to derive the predictor from the EEG. Reversely, and somewhat more critically from our perspective, one should also be able to justify which locations and latencies *not* to test. The two complementary blind decompositions avoid this issue since all available EEG data is used in the estimation and the back-reconstruction to produce maximally condensed predictors, i.e. the trial-to-trial modulation applies uniformly to the entire timecourse and topography of a component, reducing multiple comparisons considerably. Similarly, the separate spatial ICA of the fMRI data involves data reduction since the voxel-wise analysis is replaced by testing of the fMRI component timecourses (here: 24), while the statistical significance of the maps is tested in a separate random-effects analysis, applying appropriate correction using false discovery rate (FDR, Benjamini and Hochberg, 1995). Thus, finding IC-pairs across response modalities identifies coherent neuronal sources that jointly express scalp electrophysiologic and hemodynamic features. However, the current statistic trades in the 'localizing power' afforded by the mass-univariate testing (Friston, 2003; Kiebel and Friston, 2004), i.e. the possibility of drawing inferences on the effect sizes in particular voxels in the fMRI and timepoints/channels in the EEG. A hybrid approach might be plausible for applications in which one would use parallel ICA for hypothesis generation and employ the components as spatial and temporal filters for region of interest definition prior to mass univariate testing.

Here, we opted for a group ICA implementation because it provides a straight-forward and stringent solution for multi-subject component estimation and directly affords population inferences (Calhoun et al., 2001; Schmithorst and Holland, 2004). Group ICA works well for sources that are spatially and temporally coherent across subjects, and will readily detect such sources when present in about 10% of the sampled population (Schmithorst and Holland, 2004). For the sICA on preprocessed fMRI data this means that regional BOLD responses that overlap across subjects can yield group-relevant components, which is the same criterion that applies to group (2nd-level) statistics of fMRI contrast images or simple averaging. Processes that occur in a spatially variable form over time in the recording of a single subject, or that are principally spatially heterogeneous across subjects can not be captured by this implementation. Correspondingly, the group tICA on EEG single trial time domain data is preferentially suited to detect of components that represent or contribute to event-related potentials visible in averaged data. Processes that are not time/phase-locked within and across subjects, such as background rhythms and induced activity are not well visible. However, the choice of input data to parallel ICA is arbitrary such that time domain data can be replaced with e.g. power-spectra or time-frequency data where the fMRI correlates of EEG rhythms or event-related synchronization and desynchronization are subject to study. In this respect, an useful extension of the current framework would be incorporation of multiple EEG and MRI features from single trial data (Calhoun et al., 2006a).

The prerequisites outlined above do not apply to ICA on individual data, which renders this approach principally a more versatile tool to identify components. Individual ICA results can be combined across subjects by means of subsequent component clustering (Esposito et al., 2005; Onton et al., 2006). This allows for group inferences and retains more relevant information about inter-individual variability and its impact on the EEG-fMRI relationship (cf. Goncalves et al., 2006) than does our analysis, such that one should consider either option in light of the purpose of the experiment at hand. Currently, however, the available techniques are implemented and tested mostly for clustering within a modality, how well clusters can be matched across modalities by their trial-to-trial modulation or other features should be further investigated. Adequate algorithms that jointly cluster the maps and timecourses from both EEG and fMRI will yet have to be evaluated. Another consideration is that clustering techniques impose additional assumptions about between-subject correspondence and do not per se provide a turnkey solution, such that proper handling of these techniques would usually require expert user interaction.

4.2. tIC function

tIC1 had a central topography dominated by a large negativity at 100 ms (N1), followed by smaller P2 and N2 deflections and a P3 at 270 ms. The difference wave between standards and targets yields a biphasic pattern with a sustained negativity from 100–200 ms, followed by a P3 (Figs. 2, 4). Altogether, this suggests that tIC1 encompasses the N1 onset response per se, N1-enhancement and a subsequent N2b-P3a (Naatanen and Picton, 1987; Naatanen, 1992) as one coherent process. Given the current experimental parameters, the 'N1-enhancement' seen here may contain contributions from genuine sources of mismatch negativity (MMN), attentive processing negativity (PN/Nd) and 'fresh afferents' of the N1 alike (Naatanen and Picton, 1987; Naatanen, 1992). The N2b-P3a portion of the waveform following the N1/MMN is seen with attention-switching at large or task-relevant stimulus contrasts (Naatanen, 1992; Schroger, 1997).

The single trial amplitude estimates of tIC1 selectively covaried with an fMRI map that comprised a set of fronto-

Please cite this article as: Eichele, T. et al. Unmixing concurrent EEG-f MRI with parallel independent component analysis. Int. J. Psychophysiol. (2007), doi:10.1016/j.ijpsycho.2007.04.010

temporal and mesencephalic regional responses (Fig. 4). Activations were present for local maxima in the superior temporal gyri with a rightward dominance, the temporal poles and the anterior cingulate gyrus. This partition of the map encompasses the assumed sources of the scalp N1/MMN (Naatanen and Picton, 1987; Picton et al., 1999; Picton et al., 2000; Woods, 1995), and correspondingly the brain areas that previous imaging experiments have implicated in automatic auditory deviance detection, stimulus discrimination, sensory memory as well as novelty (surprise) related functions (Liebenthal et al., 2003; Molholm et al., 2005; Rinne et al., 2005; Sabri et al., 2006). The occurrence of deactivations observed in the subcallosal gyrus and the maps' global maximum in the vicinity of the midbrain reticular formation was surprising. However, seeing these areas apparently interacting in anti-correlated fashion with auditory function is plausible, since both have been found to be sensitive to novelty/predictability contrasts with more salient stimuli and tasks (Berns et al., 2001; Bunzeck and Duzel, 2006).

Two modulatory effects were present in tIC1: one effect was a linear amplitude decrement evolving slowly with time on task, and the other was a local within-sequence gamma-shaped modulation (Fig. 3). The slow linear decrement is well in line with reports describing long-term habituation for N1, MMN as well as P3a across the observation time (Debener et al., 2005a; Friedman et al., 2001; Loveless, 1983; McGee et al., 2001; Sambeth et al., 2004; Woods and Elmasian, 1986). This might correspond to a slow adaptive process related to repetitions of stimulus sequences (Jongsma et al., 2006) or the overall decline in arousal/vigilance across trials. Although tIC1 responded with amplitude increment at the transition from regular to random intervals, the corresponding transition from random to regular (i.e. the beginning of a pattern) did not elicit a response. Hence, instead of sigmoid learning curves that characterized the behaviour of later components (Eichele et al., 2005; Jongsma et al., 2006), a gamma-shaped function provided the best fit. Two explanations for this phenomenon can be offered: firstly, tIC1 may respond directly only to an increase in surprise. This means that the weight change elicited by the comparison between actual input and the learning history represented in the amplitude of tIC1 would only reflect increments of 'surprise' with the appearance of a target at an unpredicted interval at the regular-random transition, but not a constant error or the onset of the regular pattern. The second explanation relates to the time-span for which tIC1 can retain information and incorporate it into the learning history. Assuming a memory trace length at or below 10 s (Winkler et al., 2001), it would be plausible that tIC1 cannot retain enough interval repetitions to recognize the emergence of a pattern. For both accounts it is plausible to assume that the modulation is not self-sustaining. It should receive additional backward input from higher levels of processing which would exert an inhibitory influence on tIC1 when intervals are predictable, while the response to the more surprising transition from predictable to unpredictable intervals represents a salient bottom-up signal (Friston, 2005a; Schroger, 1997). Altogether, this indicates that the component is to some extent modulated by target predictability, specifically by increments of surprise/prediction error. This effect needs further examination in 'attended' as well as 'unattended' settings with variations of stimulus onset asynchrony, rules, and the physical deviant/target features (Baldeweg, 2006; Haenschel et al., 2005; Sussman et al., 1998; Ulanovsky et al., 2004).

In conclusion, we believe that parallel ICA is a useful addition to the selection of analysis methods for concurrent EEG-fMRI, it can serve either as a primary tool for inferences about the unmixed sources, or can be employed for data mining, hypothesis generation and model specification/diagnostics.

Acknowledgment

The present study was financially supported with grants from the Research Council of Norway to Kenneth Hugdahl and by the National Institutes of Health, under grants 1 R01 EB 000840 and 1 R01 EB 005846 to Vince Calhoun.

References

Baldeweg, T., 2006. Repetition effects to sounds: evidence for predictive coding in the auditory system. Trends Cogn. Sci. 10 (3), 93–94.

Baudena, P., Halgren, E., Heit, G., Clarke, J.M., 1995. Intracerebral potentials to rare target and distractor auditory and visual stimuli. III. Frontal cortex. Electroencephalogr. Clin. Neurophysiol. 94 (4), 251–264.

Bell, A.J., Sejnowski, T.J., 1995. An information-maximization approach to blind separation and blind deconvolution. Neural Comput. 7 (6), 1129–1159.

Bénar, C.G., Schön, D., Grimault, S., Nazarian, B., Burle, B., Roth, M., Badier, J.M., Marquis, P., Liegeois-Chauvel, C., Anton, J.L., 2007. Single-trial analysis of oddball event-related potentials in simultaneous EEG-fMRI. Hum. Brain. Mapp. 28 (7), 602–613.

Benjamini, Y., Hochberg, Y., 1995. Controlling the false discovery rate: a practical and powerful approach to multiple testing. J. R. Stat. Soc. Methodol. 57, 289–300.

Berns, G.S., McClure, S.M., Pagnoni, G., Montague, P.R., 2001. Predictability modulates human brain response to reward. J. Neurosci. 21 (8), 2793–2798.

Bunzeck, N., Duzel, E., 2006. Absolute coding of stimulus novelty in the human substantia nigra/VTA. Neuron 51 (3), 369–379.

Calhoun, V., Adali, T., 2006. Unmixing fMRI with independent component analysis. IEEE Eng. Med. Biol. Mag. 25 (2), 79–90.

Calhoun, V.D., Adali, T., Pearlson, G.D., Pekar, J.J., 2001. A method for making group inferences from functional MRI data using independent component analysis. Hum. Brain Mapp. 14 (3), 140–151.

Calhoun, V., Adali, T., Liu, J., 2006a. A feature-based approach to combine functional MRI, structural MRI, and EEG brain imaging data. Paper presented at the EMBS, New York, NY.

Calhoun, V.D., Adali, T., Pearlson, G.D., Kiehl, K.A., 2006b. Neuronal chronometry of target detection: fusion of hemodynamic and event-related potential data. NeuroImage 30 (2), 544–553.

Debener, S., Makeig, S., Delorme, A., Engel, A.K., 2005a. What is novel in the novelty oddball paradigm? Functional significance of the novelty P3 event-related potential as revealed by independent component analysis. Brain Res. Cogn. Brain Res. 22 (3), 309–321.

Debener, S., Ullsperger, M., Siegel, M., Fiehler, K., von Cramon, D.Y., Engel, A.K., 2005b. Trial-by-trial coupling of concurrent electroencephalogram and functional magnetic resonance imaging identifies the dynamics of performance monitoring. J. Neurosci. 25 (50), 11730–11737.

Debener, S., Ullsperger, M., Siegel, M., Engel, A.K., 2006. Single-trial EEG-fMRI reveals the dynamics of cognitive function. Trends Cogn. Sci. 10 (12), 558–563.

Debener, S., Strobel, A., Sorger, B., Peters, J., Kranczioch, C., Engel, A.K., Goebel, R., 2007. Improved quality of auditory event-related potentials recorded simultaneously with 3-T fMRI: removal of the ballistocardiogram artefact. NeuroImage 34 (2), 587–597.

Please cite this article as: Eichele, T. et al. Unmixing concurrent EEG-f MRI with parallel independent component analysis. Int. J. Psychophysiol. (2007), doi:10.1016/j.ijpsycho.2007.04.010

Delorme, A., Makeig, S., 2004. EEGLAB: an open source toolbox for analysis of single-trial EEG dynamics including independent component analysis. J. Neurosci. Methods 134 (1), 9–21.

Eichele, T., Specht, K., Moosmann, M., Jongsma, M.L., Quiroga, R.Q., Nordby, H., Hugdahl, K., 2005. Assessing the spatiotemporal evolution of neuronal activation with single-trial event-related potentials and functional MRI. Proc. Natl. Acad. Sci. U. S. A. 102 (49), 17798–17803.

Esposito, F., Scarabino, T., Hyvarinen, A., Himberg, J., Formisano, E., Comani, S., Tedeschi, G., Goebel, R., Seifritz, E., Di Salle, F., 2005. Independent component analysis of fMRI group studies by self-organizing clustering. NeuroImage 25 (1), 193–205.

Feige, B., Scheffler, K., Esposito, F., Di Salle, F., Hennig, J., Seifritz, E., 2005. Cortical and subcortical correlates of electroencephalographic alpha rhythm modulation. J. Neurophysiol. 93 (5), 2864–2872.

Fox, M.D., Snyder, A.Z., Vincent, J.L., Corbetta, M., Van Essen, D.C., Raichle, M.E., 2005. The human brain is intrinsically organized into dynamic, anticorrelated functional networks. Proc. Natl. Acad. Sci. U. S. A. 102 (27), 9673–9678.

Friedman, D., Cycowicz, Y.M., Gaeta, H., 2001. The novelty P3: an event-related brain potential (ERP) sign of the brain's evaluation of novelty. Neurosci. Biobehav. Rev. 25 (4), 355–373.

Friston, K., 2003. Human Brain Function, 2nd ed. Elsevier.

Friston, K., 2005a. A theory of cortical responses. Philos. Trans. R. Soc. Lond., B Biol. Sci. 360 (1456), 815–836.

Friston, K.J., 2005b. Models of brain function in neuroimaging. Annu. Rev. Psychol. 56, 57–87.

Friston, K.J., Holmes, A.P., Poline, J.B., Grasby, P.J., Williams, S.C., Frackowiak, R.S., Turner, R., 1995. Analysis of fMRI time-series revisited. NeuroImage 2 (1), 45–53.

Goncalves, S.I., de Munck, J.C., Pouwels, P.J., Schoonhoven, R., Kuijer, J.P., Maurits, N.M., Hoogduin, J.M., Van Someren, E.J., Heethaar, R.M., Lopes da Silva, F.H., 2006. Correlating the alpha rhythm to BOLD using simultaneous EEG/fMRI: inter-subject variability. NeuroImage 30 (1), 203–213.

Haenschel, C., Vernon, D.J., Dwivedi, P., Gruzelier, J.H., Baldeweg, T., 2005. Event-related brain potential correlates of human auditory sensory memory-trace formation. J. Neurosci. 25 (45), 10494–10501.

Halgren, E., Marinkovic, K., 1995. General principles for the physiology of cognition as suggested by intracranial ERPs. In: Ogura, C., Koga, Y., Shimokochi, M. (Eds.), Recent Advances in Event-Related Brain Potential Research. Elsevier, Amsterdam, pp. 1072–1084.

Halgren, E., Baudena, P., Clarke, J.M., Heit, G., Liegeois, C., Chauvel, P., Musolino, A., 1995a. Intracerebral potentials to rare target and distractor auditory and visual stimuli. I. Superior temporal plane and parietal lobe. Electroencephalogr. Clin. Neurophysiol. 94 (3), 191–220.

Halgren, E., Baudena, P., Clarke, J.M., Heit, G., Marinkovic, K., Devaux, B., Vignal, J.P., Biraben, A., 1995b. Intracerebral potentials to rare target and distractor auditory and visual stimuli. II. Medial, lateral and posterior temporal lobe. Electroencephalogr. Clin. Neurophysiol. 94 (4), 229–250.

Hall, D.A., Haggard, M.P., Akeroyd, M.A., Palmer, A.R., Summerfield, A.Q., Elliott, M.R., Gurney, E.M., Bowtell, R.W., 1999. "Sparse" temporal sampling in auditory fMRI. Hum. Brain Mapp. 7 (3), 213–223.

Hopfinger, J.B., Khoe, W., Song, A.W., 2005. Combining electrophysiology with structural and functional neuroimaging: ERPs, PET, MRI, and fMRI. In: Handy, T.C. (Ed.), Event Related Potentials. A Methods Handbook. The MIT Press, Cambridge, pp. 345–380.

Horwitz, B., Poeppel, D., 2002. How can EEG/MEG and fMRI/PET data be combined? Hum. Brain Mapp. 17 (1), 1–3.

Jongsma, M.L., Eichele, T., Van Rijn, C.M., Coenen, A.M., Hugdahl, K., Nordby, H., Quiroga, R.Q., 2006. Tracking pattern learning with single-trial event-related potentials. Clin. Neurophysiol. 117 (9), 1957–1973.

Jung, T.P., Makeig, S., Humphries, C., Lee, T.W., McKeown, M.J., Iragui, V., Sejnowski, T.J., 2000. Removing electroencephalographic artifacts by blind source separation. Psychophysiology 37 (2), 163–178.

Kiebel, S.J., Friston, K.J., 2004. Statistical parametric mapping for event-related potentials: I. Generic considerations. NeuroImage 22 (2), 492–502.

Kiehl, K.A., Stevens, M.C., Laurens, K.R., Pearlson, G., Calhoun, V.D., Liddle, P.F., 2005. An adaptive reflexive processing model of neurocognitive function: supporting evidence from a large scale (n = 100) fMRI study of an auditory oddball task. NeuroImage 25 (3), 899–915.

Lauritzen, M., Gold, L., 2003. Brain function and neurophysiological correlates of signals used in functional neuroimaging. J. Neurosci. 23 (10), 3972–3980.

Lee, T., Girolami, M., Sejnowski, T., 1999. Independent component analysis using an extended infomax algorithm for mixed subgaussian and supergaussian sources. Neural Comput. 11, 417–441.

Li, Y.O., Adali, T., Calhoun, V.D., in press. Estimating the number of independent components for functional magnetic resonance imaging data. Hum. Brain. Mapp. Feb 1; [Epub ahead of print], doi:10.1002/hbm.20359.

Liebenthal, E., Ellingson, M.L., Spanaki, M.V., Prieto, T.E., Ropella, K.M., Binder, J.R., 2003. Simultaneous ERP and fMRI of the auditory cortex in a passive oddball paradigm. NeuroImage 19, 1395–1404.

Linden, D.E., Prvulovic, D., Formisano, E., Vollinger, M., Zanella, F.E., Goebel, R., Dierks, T., 1999. The functional neuroanatomy of target detection: an fMRI study of visual and auditory oddball tasks. Cereb. Cortex 9 (8), 815–823.

Logothetis, N.K., 2003. The underpinnings of the BOLD functional magnetic resonance imaging signal. J. Neurosci. 23 (10), 3963–3971.

Loveless, N., 1983. The orienting response and evoked potentials in man. In: Siddle, D. (Ed.), Orienting and Habituation: Perspectives in Human Research. Wiley, Chichester, pp. 71–108.

Makeig, S., Jung, T.P., Bell, A.J., Ghahremani, D., Sejnowski, T.J., 1997. Blind separation of auditory event-related brain responses into independent components. Proc. Natl. Acad. Sci. U. S. A. 94 (20), 10979–10984.

Makeig, S., Jung, T.-P., Sejnowski, T.J., 2002. Having your voxels and timing them too? In: Sommer, F., Wichert, A. (Eds.), Exploratory Analysis and Data Modeling in Functional Neuroimaging. The MIT Press, Cambridge.

Makeig, S., Debener, S., Onton, J., Delorme, A., 2004a. Mining event-related brain dynamics. Trends Cogn. Sci. 8 (5), 204–210.

Makeig, S., Delorme, A., Westerfield, M., Jung, T.P., Townsend, J., Courchesne, E., Sejnowski, T.J., 2004b. Electroencephalographic brain dynamics following manually responded visual targets. PLoS Biol. 2 (6), e176.

McGee, T.J., King, C., Tremblay, K., Nicol, T.G., Cunningham, J., Kraus, N., 2001. Long-term habituation of the speech-elicited mismatch negativity. Psychophysiology 38 (4), 653–658.

McKeown, M.J., Hansen, L.K., Sejnowski, T.J., 2003. Independent component analysis of functional MRI: what is signal and what is noise? Curr. Opin. Neurobiol. 13 (5), 620–629.

Molholm, S., Martinez, A., Ritter, W., Javitt, D.C., Foxe, J.J., 2005. The neural circuitry of pre-attentive auditory change-detection: an fMRI study of pitch and duration mismatch negativity generators. Cereb. Cortex 15 (5), 545–551.

Nunez, P.L., 2000. Toward a quantitative description of large-scale dynamic neocortical dynamic function and EEG. Behav. Brain Sci. 23, 371–437.

Naatanen, R., 1992. Attention and Brain Function. Lawrence Erlbaum Associates, Hillsdale.

Naatanen, R., Picton, T., 1987. The N1 wave of the human electric and magnetic response to sound: a review and an analysis of the component structure. Psychophysiology 24 (4), 375–425.

Ogawa, S., Lee, T.M., Kay, A.R., Tank, D.W., 1990. Brain magnetic resonance imaging with contrast dependent on blood oxygenation. Proc. Natl. Acad. Sci. U. S. A. 87 (24), 9868–9872.

Onton, J., Westerfield, M., Townsend, J., Makeig, S., 2006. Imaging human EEG dynamics using independent component analysis. Neurosci. Biobehav. Rev. 30 (6), 808–822.

Picton, T.W., Alain, C., Woods, D.L., John, M.S., Scherg, M., Valdes-Sosa, P., Bosch-Bayard, J., Trujillo, N.J., 1999. Intracerebral sources of human auditory-evoked potentials. Audiol. Neuro-otol. 4 (2), 64–79.

Picton, T.W., Alain, C., Otten, L., Ritter, W., Achim, A., 2000. Mismatch negativity: different water in the same river. Audiol. Neuro-otol. 5 (3-4), 111–139.

Quian Quiroga, R., Garcia, H., 2003. Single-trial event-related potentials with wavelet denoising. Clin. Neurophysiol. 114 (2), 376–390.

Rinne, T., Degerman, A., Alho, K., 2005. Superior temporal and inferior frontal cortices are activated by infrequent sound duration decrements: an fMRI study. NeuroImage 26 (1), 66–72.

Sabri, M., Liebenthal, E., Waldron, E.J., Medler, D.A., Binder, J.R., 2006. Attentional modulation in the detection of irrelevant deviance: a simultaneous ERP/fMRI study. J. Cogn. Neurosci. 18 (5), 689–700.

Sambeth, A., Maes, J.H., Quian Quiroga, R., Van Rijn, C.M., Coenen, A.M., 2004. Enhanced re-habituation of the orienting response of the human event-related potential. Neurosci. Lett. 356 (2), 103–106.

Please cite this article as: Eichele, T. et al. Unmixing concurrent EEG-f MRI with parallel independent component analysis. Int. J. Psychophysiol. (2007), doi:10.1016/j.ijpsycho.2007.04.010

Schmithorst, V.J., Holland, S.K., 2004. Comparison of three methods for generating group statistical inferences from independent component analysis of functional magnetic resonance imaging data. J. Magn. Reson. Imaging 19 (3), 365–368.

Schroger, E., 1997. On the detection of auditory deviations: a pre-attentive activation model. Psychophysiology 34 (3), 245–257.

Stone, J.V., 2002. Independent component analysis: an introduction. Trends Cogn. Sci. 6 (2), 59–64.

Sussman, E., Ritter, W., Vaughan Jr., H.G., 1998. Predictability of stimulus deviance and the mismatch negativity. NeuroReport 9 (18), 4167–4170.

Ulanovsky, N., Las, L., Farkas, D., Nelken, I., 2004. Multiple time scales of adaptation in auditory cortex neurons. J. Neurosci. 24 (46), 10440–10453.

Winkler, I., Schroger, E., Cowan, N., 2001. The role of large-scale memory organization in the mismatch negativity event-related brain potential. J. Cogn. Neurosci. 13 (1), 59–71.

Woods, D.L., 1995. The component structure of the N1 wave of the human auditory evoked potential. Electroencephalogr. Clin. Neurophysiol. Suppl 44, 102–109.

Woods, D.L., Elmasian, R., 1986. The habituation of event-related potentials to speech sounds and tones. Electroencephalogr. Clin. Neurophysiol. 65 (6), 447–459.

Please cite this article as: Eichele, T. et al. Unmixing concurrent EEG-f MRI with parallel independent component analysis. Int. J. Psychophysiol. (2007), doi:10.1016/j.ijpsycho.2007.04.010

Doctoral Theses at The Faculty of Psychology, University of Bergen

1980	Allen, H.M., Dr. philos.	Parent-offspring interactions in willow grouse (Lagopus L. Lagopus).
1981	Myhrer, T., Dr. philos.	Behavioral Studies after selective disruption of hippocampal inputs in albino rats.
1982	Svebak, S., Dr. philos.	The significance of motivation for task-induced tonic physiological changes.
1983	Myhre, G., Dr. philos.	The Biopsychology of behavior in captive Willow ptarmigan.
	Eide, R., Dr. philos.	PSYCHOSOCIAL FACTORS AND INDICES OF HEALTH RISKS. The relationship of psychosocial conditions to subjective complaints, arterial blood pressure, serum cholesterol, serum triglycerides and urinary catecholamines in middle aged populations in Western Norway.
	Værnes, R.J., Dr. philos.	Neuropsychological effects of diving.
1984	Kolstad, A., Dr. philos.	Til diskusjonen om sammenhengen mellom sosiale forhold og psykiske strukturer. En epidemiologisk undersøkelse blant barn og unge.
	Løberg, T., Dr. philos.	Neuropsychological assessment in alcohol dependence.
1985	Hellesnes, T., Dr. philos.	Læring og problemløsning. En studie av den perseptuelle analysens betydning for verbal læring.
	Håland, W., Dr. philos.	Psykoterapi: relasjon, utviklingsprosess og effekt.
1986	Hagtvet, K.A., Dr. philos.	The construct of test anxiety: Conceptual and methodological issues.
	Jellestad, F.K., Dr. philos.	Effects of neuron specific amygdala lesions on fear-motivated behavior in rats.
1987	Aarø, L.E., Dr. philos.	Health behaviour and sosioeconomic Status. A survey among the adult population in Norway.
	Underlid, K., Dr. philos.	Arbeidsløyse i psykososialt perspektiv.
	Laberg, J.C., Dr. philos.	Expectancy and classical conditioning in alcoholics' craving.
	Vollmer, F.C., Dr. philos.	Essays on explanation in psychology.
	Ellertsen, B., Dr. philos.	Migraine and tension headache: Psychophysiology, personality and therapy.
1988	Kaufmann, A., Dr. philos.	Antisosial atferd hos ungdom. En studie av psykologiske determinanter.

	Mykletun, R.J., Dr. philos.	Teacher stress: personality, work-load and health.
	Havik, O.E., Dr. philos.	After the myocardial infarction: A medical and psychological study with special emphasis on perceived illness.
1989	Bråten, S., Dr. philos.	Menneskedyaden. En teoretisk tese om sinnets dialogiske natur med informasjons- og utviklingspsykologiske implikasjoner sammenholdt med utvalgte spedbarnsstudier.
	Wold, B., Dr. psychol.	Lifestyles and physical activity. A theoretical and empirical analysis of socialization among children and adolescents.
1990	Flaten, M.A., Dr. psychol.	The role of habituation and learning in reflex modification.
1991	Alsaker, F.D., Dr. philos.	Global negative self-evaluations in early adolescence.
	Kraft, P., Dr. philos.	AIDS prevention in Norway. Empirical studies on diffusion of knowledge, public opinion, and sexual behaviour.
	Endresen, I.M., Dr. philos.	Psychoimmuniological stress markers in working life.
	Faleide, A.O., Dr. philos.	Asthma and allergy in childhood. Psychosocial and psychotherapeutic problems.
1992	Dalen, K., Dr. philos.	Hemispheric asymmetry and the Dual-Task Paradigm: An experimental approach.
	Bø, I.B., Dr. philos.	Ungdoms sosiale økologi. En undersøkelse av 14-16 åringers sosiale nettverk.
	Nivison, M.E., Dr. philos.	The relationship between noise as an experimental and environmental stressor, physiological changes and psychological factors.
	Torgersen, A.M., Dr. philos.	Genetic and environmental influence on temperamental behaviour. A longitudinal study of twins from infancy to adolescence.
1993	Larsen, S., Dr. philos.	Cultural background and problem drinking.
	Nordhus, I.H., Dr. philos.	Family caregiving. A community psychological study with special emphasis on clinical interventions.
	Thuen, F., Dr. psychol.	Accident-related behaviour among children and young adolescents: Prediction and prevention.
	Solheim, R., Dr. philos.	Spesifikke lærevansker. Diskrepanskriteriet anvendt i seleksjonsmetodikk.
	Johnsen, B.H., Dr. psychol.	Brain assymetry and facial emotional expressions: Conditioning experiments.
1994	Tønnessen, F.E., Dr. philos.	The etiology of Dyslexia.
	Kvale, G., Dr. psychol.	Psychological factors in anticipatory nausea and vomiting in cancer chemotherapy.
	Asbjørnsen, A.E., Dr. psychol.	Structural and dynamic factors in dichotic listening: An interactional model.

	Bru, E., Dr. philos.	The role of psychological factors in neck, shoulder and low back pain among female hospitale staff.
	Braathen, E.T., Dr. psychol.	Prediction of exellence and discontinuation in different types of sport: The significance of motivation and EMG.
	Johannessen, B.F., Dr. philos.	Det flytende kjønnet. Om lederskap, politikk og identitet.
1995	Sam, D.L., Dr. psychol.	Acculturation of young immigrants in Norway: A psychological and socio-cultural adaptation.
	Bjaalid, I.-K., Dr. philos	Component processes in word recognition.
	Martinsen, Ø., Dr. philos.	Cognitive style and insight.
	Nordby, H., Dr. philos.	Processing of auditory deviant events: Mismatch negativity of event-related brain potentials.
	Raaheim, A., Dr. philos.	Health perception and health behaviour, theoretical considerations, empirical studies, and practical implications.
	Seltzer, W.J., Dr.philos.	Studies of Psychocultural Approach to Families in Therapy.
	Brun, W., Dr.philos.	Subjective conceptions of uncertainty and risk.
	Aas, H.N., Dr. psychol.	Alcohol expectancies and socialization: Adolescents learning to drink.
	Bjørkly, S., Dr. psychol.	Diagnosis and prediction of intra-institutional aggressive behaviour in psychotic patients
1996	Anderssen, N., Dr. psychol.	Physical activity of young people in a health perspective: Stability, change and social influences.
	Sandal, Gro Mjeldheim, Dr. psychol.	Coping in extreme environments: The role of personality.
	Strumse, Einar, Dr. philos.	The psychology of aesthetics: explaining visual preferences for agrarian landscapes in Western Norway.
	Hestad, Knut, Dr. philos.	Neuropsychological deficits in HIV-1 infection.
	Lugoe, L.Wycliffe, Dr. philos.	Prediction of Tanzanian students' HIV risk and preventive behaviours
	Sandvik, B. Gunnhild, Dr. philos.	Fra distriktsjordmor til institusjonsjordmor. Fremveksten av en profesjon og en profesjonsutdanning
	Lie, Gro Therese, Dr. psychol.	The disease that dares not speak its name: Studies on factors of importance for coping with HIV/AIDS in Northern Tanzania
	Øygard, Lisbet, Dr. philos.	Health behaviors among young adults. A psychological and sociological approach
	Stormark, Kjell Morten, Dr. psychol.	Emotional modulation of selective attention: Experimental and clinical evidence.
	Einarsen, Ståle, Dr. psychol.	Bullying and harassment at work: epidemiological and psychosocial aspects.

1997	Knivsberg, Ann-Mari, Dr. philos.	Behavioural abnormalities and childhood psychopathology: Urinary peptide patterns as a potential tool in diagnosis and remediation.
	Eide, Arne H., Dr. philos.	Adolescent drug use in Zimbabwe. Cultural orientation in a global-local perspective and use of psychoactive substances among secondary school students.
	Sørensen, Marit, Dr. philos.	The psychology of initiating and maintaining exercise and diet behaviour.
	Skjæveland, Oddvar, Dr. psychol.	Relationships between spatial-physical neighborhood attributes and social relations among neighbors.
	Zewdie, Teka, Dr. philos.	Mother-child relational patterns in Ethiopia. Issues of developmental theories and intervention programs.
	Wilhelmsen, Britt Unni, Dr. philos.	Development and evaluation of two educational programmes designed to prevent alcohol use among adolescents.
	Manger, Terje, Dr. philos.	Gender differences in mathematical achievement among Norwegian elementary school students.
1998		
V	Lindstrøm, Torill Christine, Dr. philos.	«Good Grief»: Adapting to Bereavement.
	Skogstad, Anders, Dr. philos.	Effects of leadership behaviour on job satisfaction, health and efficiency.
	Haldorsen, Ellen M. Håland, Dr. psychol.	Return to work in low back pain patients.
	Besemer, Susan P., Dr. philos.	Creative Product Analysis: The Search for a Valid Model for Understanding Creativity in Products.
H	Winje, Dagfinn, Dr. psychol.	Psychological adjustment after severe trauma. A longitudinal study of adults' and children's posttraumatic reactions and coping after the bus accident in Måbødalen, Norway 1988.
	Vosburg, Suzanne K., Dr. philos.	The effects of mood on creative problem solving.
	Eriksen, Hege R., Dr. philos.	Stress and coping: Does it really matter for subjective health complaints?
	Jakobsen, Reidar, Dr. psychol.	Empiriske studier av kunnskap og holdninger om hiv/aids og den normative seksuelle utvikling i ungdomsårene.
1999		
V	Mikkelsen, Aslaug, Dr. philos.	Effects of learning opportunities and learning climate on occupational health.
	Samdal, Oddrun, Dr. philos.	The school environment as a risk or resource for students' health-related behaviours and subjective well-being.
	Friestad, Christine, Dr. philos.	Social psychological approaches to smoking.
	Ekeland, Tor-Johan, Dr. philos.	Meining som medisin. Ein analyse av placebofenomenet og implikasjoner for terapi og terapeutiske teoriar.
H	Saban, Sara, Dr. psychol.	Brain Asymmetry and Attention: Classical Conditioning Experiments.

	Carlsten, Carl Thomas, Dr. philos.	God lesing – God læring. En aksjonsrettet studie av undervisning i fagtekstlesing.
	Dundas, Ingrid, Dr. psychol.	Functional and dysfunctional closeness. Family interaction and children's adjustment.
	Engen, Liv, Dr. philos.	Kartlegging av leseferdighet på småskoletrinnet og vurdering av faktorer som kan være av betydning for optimal leseutvikling.
2000		
V	Hovland, Ole Johan, Dr. philos.	Transforming a self-preserving "alarm" reaction into a self-defeating emotional response: Toward an integrative approach to anxiety as a human phenomenon.
	Lillejord, Sølvi, Dr. philos.	Handlingsrasjonalitet og spesialundervisning. En analyse av aktørperspektiver.
	Sandell, Ove, Dr. philos.	Den varme kunnskapen.
	Oftedal, Marit Petersen, Dr. philos.	Diagnostisering av ordavkodingsvansker: En prosessanalytisk tilnærmingsmåte.
H	Sandbak, Tone, Dr. psychol.	Alcohol consumption and preference in the rat: The significance of individual differences and relationships to stress pathology
	Eid, Jarle, Dr. psychol.	Early predictors of PTSD symptom reporting; The significance of contextual and individual factors.
2001		
V	Skinstad, Anne Helene, Dr. philos.	Substance dependence and borderline personality disorders.
	Binder, Per-Einar, Dr. psychol.	Individet og den meningsbærende andre. En teoretisk undersøkelse av de mellommenneskelige forutsetningene for psykisk liv og utvikling med utgangspunkt i Donald Winnicotts teori.
	Roald, Ingvild K., Dr. philos.	Building of concepts. A study of Physics concepts of Norwegian deaf students.
H	Fekadu, Zelalem W., Dr. philos.	Pridicting contraceptive use and intention among a sample of adolescent girls. An application of the theory of planned behaviour in Ethiopian context.
	Melesse, Fantu, Dr. philos.	The more intelligent and sensitive child (MISC) mediational intervention in an Ethiopian context: An evaluation study.
	Råheim, Målfrid, Dr. philos.	Kvinners kroppserfaring og livssammenheng. En fenomenologisk – hermeneutisk studie av friske kvinner og kvinner med kroniske muskelsmerter.
	Engelsen, Birthe Kari, Dr. psychol.	Measurement of the eating problem construct.
	Lau, Bjørn, Dr. philos.	Weight and eating concerns in adolescence.
2002		
V	Ihlebæk, Camilla, Dr. philos.	Epidemiological studies of subjective health complaints.
	Rosén, Gunnar O. R., Dr. philos.	The phantom limb experience. Models for understanding and treatment of pain with hypnosis.

	Høines, Marit Johnsen, Dr. philos.	Fleksible språkrom. Matematikklæring som tekstutvikling.
	Anthun, Roald Andor, Dr. philos.	School psychology service quality. Consumer appraisal, quality dimensions, and collaborative improvement potential
	Pallesen, Ståle, Dr. psychol.	Insomnia in the elderly. Epidemiology, psychological characteristics and treatment.
	Midthassel, Unni Vere, Dr. philos.	Teacher involvement in school development activity. A study of teachers in Norwegian compulsory schools
	Kallestad, Jan Helge, Dr. philos.	Teachers, schools and implementation of the Olweus Bullying Prevention Program.
H	Ofte, Sonja Helgesen, Dr. psychol.	Right-left discrimination in adults and children.
	Netland, Marit, Dr. psychol.	Exposure to political violence. The need to estimate our estimations.
	Diseth, Åge, Dr. psychol.	Approaches to learning: Validity and prediction of academic performance.
	Bjuland, Raymond, Dr. philos.	Problem solving in geometry. Reasoning processes of student teachers working in small groups: A dialogical approach.
2003		
V	Arefjord, Kjersti, Dr. psychol.	After the myocardial infarction – the wives' view. Short- and long-term adjustment in wives of myocardial infarction patients.
	Ingjaldsson, Jón Þorvaldur, Dr. psychol.	Unconscious Processes and Vagal Activity in Alcohol Dependency.
	Holden, Børge, Dr. philos.	Følger av atferdsanalytiske forklaringer for atferdsanalysens tilnærming til utforming av behandling.
	Holsen, Ingrid, Dr. philos.	Depressed mood from adolescence to 'emerging adulthood'. Course and longitudinal influences of body image and parent-adolescent relationship.
	Hammar, Åsa Karin, Dr. psychol.	Major depression and cognitive dysfunction- An experimental study of the cognitive effort hypothesis.
	Sprugevica, Ieva, Dr. philos.	The impact of enabling skills on early reading acquisition.
	Gabrielsen, Egil, Dr. philos.	LESE FOR LIVET. Lesekompetansen i den norske voksenbefolkningen sett i lys av visjonen om en enhetsskole.
H	Hansen, Anita Lill, Dr. psychol.	The influence of heart rate variability in the regulation of attentional and memory processes.
	Dyregrov, Kari, Dr. philos.	The loss of child by suicide, SIDS, and accidents: Consequences, needs and provisions of help.
2004		
V	Torsheim, Torbjørn, Dr. psychol.	Student role strain and subjective health complaints: Individual, contextual, and longitudinal perspectives.
	Haugland, Bente Storm Mowatt Dr. psychol.	Parental alcohol abuse. Family functioning and child adjustment.

	Milde, Anne Marita, Dr. psychol.	Ulcerative colitis and the role of stress. Animal studies of psychobiological factors in relationship to experimentally induced colitis.
	Stornes, Tor, Dr. philos.	Socio-moral behaviour in sport. An investigation of perceptions of sportspersonship in handball related to important factors of socio-moral influence.
	Mæhle, Magne, Dr. philos.	Re-inventing the child in family therapy: An investigation of the relevance and applicability of theory and research in child development for family therapy involving children.
	Kobbeltvedt, Therese, Dr. psychol.	Risk and feelings: A field approach.
H	Thomsen, Tormod, Dr. psychol.	Localization of attention in the brain.
	Løberg, Else-Marie, Dr. psychol.	Functional laterality and attention modulation in schizophrenia: Effects of clinical variables.
	Kyrkjebø, Jane Mikkelsen, Dr. philos.	Learning to improve: Integrating continuous quality improvement learning into nursing education.
	Laumann, Karin, Dr. psychol.	Restorative and stress-reducing effects of natural environments: Experiencal, behavioural and cardiovascular indices.
	Holgersen, Helge, PhD	Mellom oss - Essay i relasjonell psykoanalyse.
2005		
V	Hetland, Hilde, Dr. psychol.	Leading to the extraordinary? Antecedents and outcomes of transformational leadership.
	Iversen, Anette Christine, Dr. philos.	Social differences in health behaviour: the motivational role of perceived control and coping.
H	Mathisen, Gro Ellen, PhD	Climates for creativity and innovation: Definitions, measurement, predictors and consequences.
	Sævi, Tone, Dr. philos.	Seeing disability pedagogically – The lived experience of disability in the pedagogical encounter.
	Wiium, Nora, PhD	Intrapersonal factors, family and school norms: combined and interactive influence on adolescent smoking behaviour.
	Kanagaratnam, Pushpa, PhD	Subjective and objective correlates of Posttraumatic Stress in immigrants/refugees exposed to political violence.
	Larsen, Torill M. B. , PhD	Evaluating principals` and teachers` implementation of Second Step. A case study of four Norwegian primary schools.
	Bancila, Delia, PhD	Psychosocial stress and distress among Romanian adolescents and adults.
2006		
V	Hillestad, Torgeir Martin, Dr. philos.	Normalitet og avvik. Forutsetninger for et objektivt psykopatologisk avviksbegrep. En psykologisk, sosial, erkjennelsesteoretisk og teorihistorisk framstilling.
	Nordanger, Dag Øystein, Dr. psychol.	Psychosocial discourses and responses to political violence in post-war Tigray, Ethiopia.

	Rimol, Lars Morten, PhD	Behavioral and fMRI studies of auditory laterality and speech sound processing.
	Krumsvik, Rune Johan, Dr. philos.	ICT in the school. ICT-initiated school development in lower secondary school.
	Norman, Elisabeth, Dr. psychol.	Gut feelings and unconscious thought: An exploration of fringe consiousness in implicit cognition.
	Israel, K Pravin, Dr. psychol.	Parent involvement in the mental health care of children and adolescents. Emperical studies from clinical care setting.
	Glasø, Lars, PhD	Affects and emotional regulation in leader-subordinate relationships.
	Knutsen, Ketil, Dr. philos.	HISTORIER UNGDOM LEVER – En studie av hvordan ungdommer bruker historie for å gjøre livet meningsfullt.
	Matthiesen, Stig Berge, PhD	Bullying at work. Antecedents and outcomes.
H	Gramstad, Arne, PhD	Neuropsychological assessment of cognitive and emotional functioning in patients with epilepsy.
	Bendixen, Mons, PhD	Antisocial behaviour in early adolescence: Methodological and substantive issues.
	Mrumbi, Khalifa Maulid, PhD	Parental illness and loss to HIV/AIDS as experienced by AIDS orphans aged between 12-17 years from Temeke District, Dar es Salaam, Tanzania: A study of the children's psychosocial health and coping responses.
	Hetland, Jørn, Dr. psychol.	The nature of subjective health complaints in adolescence: Dimensionality, stability, and psychosocial predictors
	Kakoko, Deodatus Conatus Vitalis, PhD	Voluntary HIV counselling and testing service uptake among primary school teachers in Mwanza, Tanzania: assessment of socio-demographic, psychosocial and socio-cognitive aspects
	Mykletun, Arnstein, Dr. psychol.	Mortality and work-related disability as long-term consequences of anxiety and depression: Historical cohort designs based on the HUNT-2 study
	Sivertsen, Børge, PhD	Insomnia in older adults. Consequences, assessment and treatment.
2007		
V	Singhammer, John, Dr. philos.	Social conditions from before birth to early adulthood – the influence on health and health behaviour
	Janvin, Carmen Ani Cristea, PhD	Cognitive impairment in patients with Parkinson's disease: profiles and implications for prognosis
	Braarud, Hanne Cecilie, Dr.psychol.	Infant regulation of distress: A longitudinal study of transactions between mothers and infants
	Tveito, Torill Helene, PhD	Sick Leave and Subjective Health Complaints
	Magnussen, Liv Heide, PhD	Returning disability pensioners with back pain to work

	Elin Marie Thuen, Dr.philos.	Learning environment, students' coping styles and emotional and behavioural problems. A study of Norwegian secondary school students.
	Ole Asbjørn Solberg, PhD	Peacekeeping warriors – A longitudinal study of Norwegian peacekeepers in Kosovo
H	Gunn Elisabeth Søreide, Dr.philos.	Narrative construction of teacher identity
	Erling Svensen, PhD	WORK & HEALTH. Cognitive Activation Theory of Stress applied in an organisational setting.
	Simon Nygaard Øverland, PhD	Mental health and impairment in disability benefits. Studies applying linkages between health surveys and administrative registries.